

Fracture Mechanics

Robert Khan

First Edition, 2012

ISBN 978-81-323-4368-4

© All rights reserved.

Published by:

White Word Publications

4735/22 Prakashdeep Bldg,

Ansari Road, Darya Ganj,

Delhi - 110002

Email: info@wtbooks.com

Table of Contents

Chapter 1 - Fracture Mechanics

Chapter 2 - Fatigue (Material)

Chapter 3 - Fractography

Chapter 4 - Focal Mechanism

Chapter 5 - Fracture Toughness

Chapter 6 - Fracture

Chapter 7 - Structural Fracture Mechanics

Chapter 8 - Peridynamics

Chapter 9 - Strength of Materials

Chapter 10 - Stress (Mechanics)

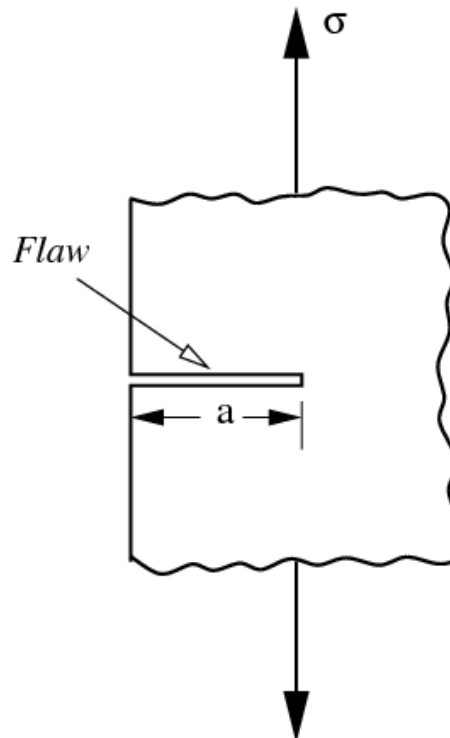
Chapter 11 - Deformation (Engineering)

Chapter 1

Fracture Mechanics

Fracture mechanics is the field of mechanics concerned with the study of the propagation of cracks in materials. It uses methods of analytical solid mechanics to calculate the driving force on a crack and those of experimental solid mechanics to characterize the material's resistance to fracture.

In modern materials science, fracture mechanics is an important tool in improving the mechanical performance of materials and components. It applies the physics of stress and strain, in particular the theories of elasticity and plasticity, to the microscopic crystallographic defects found in real materials in order to predict the macroscopic mechanical failure of bodies. Fractography is widely used with fracture mechanics to understand the causes of failures and also verify the theoretical failure predictions with real life failures.



An edge crack (flaw) of length a in a material.

Linear elastic fracture mechanics

Griffith's criterion

Fracture mechanics was developed during World War I by English aeronautical engineer, A. A. Griffith, to explain the failure of brittle materials. Griffith's work was motivated by two contradictory facts:

- The stress needed to fracture bulk glass is around 100 MPa (15,000 psi).
- The theoretical stress needed for breaking atomic bonds is approximately 10,000 MPa (1,500,000 psi).

A theory was needed to reconcile these conflicting observations. Also, experiments on glass fibers that Griffith himself conducted suggested that the fracture stress increases as the fiber diameter decreases. Hence the uniaxial tensile strength, which had been used extensively to predict material failure before Griffith, could not be a specimen-independent material property. Griffith suggested that the low fracture strength observed in experiments, as well as the size-dependence of strength, was due to the presence of microscopic flaws in the bulk material.

To verify the flaw hypothesis, Griffith introduced an artificial flaw in his experimental specimens. The artificial flaw was in the form of a surface crack which was much larger than other flaws in a specimen. The experiments showed that the product of the square root of the flaw length (a) and the stress at fracture (σ_f) was nearly constant, which is expressed by the equation:

$$\sigma_f \sqrt{a} \approx C$$

An explanation of this relation in terms of linear elasticity theory is problematic. Linear elasticity theory predicts that stress (and hence the strain) at the tip of a sharp flaw in a linear elastic material is infinite. To avoid that problem, Griffith developed a thermodynamic approach to explain the relation that he observed.

The growth of a crack requires the creation of two new surfaces and hence an increase in the surface energy. Griffith found an expression for the constant C in terms of the surface energy of the crack by solving the elasticity problem of a finite crack in an elastic plate. Briefly, the approach was:

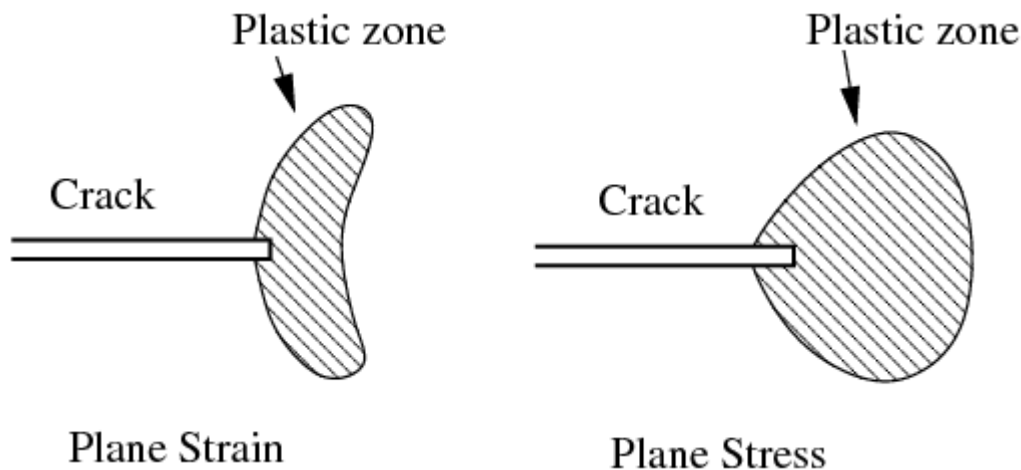
- Compute the potential energy stored in a perfect specimen under an uniaxial tensile load.
- Fix the boundary so that the applied load does no work and then introduce a crack into the specimen. The crack relaxes the stress and hence reduces the elastic energy near the crack faces. On the other hand, the crack increases the total surface energy of the specimen.
- Compute the change in the free energy (surface energy – elastic energy) as a function of the crack length. Failure occurs when the free energy attains a peak

value at a critical crack length, beyond which the free energy decreases by increasing the crack length, i.e. by causing fracture. Using this procedure, Griffith found that

$$C = \sqrt{\frac{2E\gamma}{\pi}}$$

where E is the Young's modulus of the material and γ is the surface energy density of the material. Assuming $E = 62 \text{ GPa}$ and $\gamma = 1 \text{ J/m}^2$ gives excellent agreement of Griffith's predicted fracture stress with experimental results for glass.

Irwin's modification



The plastic zone around a crack tip in a ductile material.

Griffith's work was largely ignored by the engineering community until the early 1950s. The reasons for this appear to be (a) in the actual structural materials the level of energy needed to cause fracture is orders of magnitude higher than the corresponding surface energy, and (b) in structural materials there are always some inelastic deformations around the crack front that would make the assumption of linear elastic medium with infinite stresses at the crack tip highly unrealistic. F. Erdogan (2000)

Griffith's theory provides excellent agreement with experimental data for brittle materials such as glass. For ductile materials such as steel, though the relation $\sigma_y \sqrt{a} = C$ still holds, the surface energy (γ) predicted by Griffith's theory is usually unrealistically high. A group working under G. R. Irwin at the U.S. Naval Research Laboratory (NRL) during World War II realized that plasticity must play a significant role in the fracture of ductile materials.

In ductile materials (and even in materials that appear to be brittle), a plastic zone develops at the tip of the crack. As the applied load increases, the plastic zone increases in size until the crack grows and the material behind the crack tip unloads. The plastic

loading and unloading cycle near the crack tip leads to the dissipation of energy as heat. Hence, a dissipative term has to be added to the energy balance relation devised by Griffith for brittle materials. In physical terms, additional energy is needed for crack growth in ductile materials when compared to brittle materials.

Irwin's strategy was to partition the energy into two parts:

- the stored elastic strain energy which is released as a crack grows. This is the thermodynamic driving force for fracture.
- the dissipated energy which includes plastic dissipation and the surface energy (and any other dissipative forces that may be at work). The dissipated energy provides the thermodynamic resistance to fracture. Then the total energy dissipated is

$$G = 2\gamma + G_p$$

where γ is the surface energy and G_p is the plastic dissipation (and dissipation from other sources) per unit area of crack growth.

The modified version of Griffith's energy criterion can then be written as

$$\sigma_f \sqrt{a} = \sqrt{\frac{E G}{\pi}}$$

For brittle materials such as glass, the surface energy term dominates and $G \approx 2\gamma = 2 \text{ J/m}^2$. For ductile materials such as steel, the plastic dissipation term dominates and $G \approx G_p = 1000 \text{ J/m}^2$. For polymers close to the glass transition temperature, we have intermediate values of $G \approx 2 - 1000 \text{ J/m}^2$.

Stress intensity factor

Another significant achievement of Irwin and his colleagues was to find a method of calculating the amount of energy available for fracture in terms of the asymptotic stress and displacement fields around a crack front in a linear elastic solid. This asymptotic expression for the stress field around a crack tip is

$$\sigma_{ij} \approx \left(\frac{K}{\sqrt{2\pi r}} \right) f_{ij}(\theta)$$

where σ_{ij} are the Cauchy stresses, r is the distance from the crack tip, θ is the angle with respect to the plane of the crack, and f_{ij} are functions that are independent of the crack geometry and loading conditions. Irwin called the quantity K the *stress intensity factor*.

Since the quantity f_{ij} is dimensionless, the stress intensity factor can be expressed in units of $\text{MPa}\cdot\sqrt{\text{m}}$.

When a rigid line inclusion is considered, a similar asymptotic expression for the stress fields is obtained.

Strain energy release

Irwin was the first to observe that if the size of the plastic zone around a crack is small compared to the size of the crack, the energy required to grow the crack will not be critically dependent on the state of stress at the crack tip. In other words, a purely elastic solution may be used to calculate the amount of energy available for fracture.

The energy release rate for crack growth or *strain energy release rate* may then be calculated as the change in elastic strain energy per unit area of crack growth, i.e.,

$$G := - \left[\frac{\partial U}{\partial a} \right]_P = - \left[\frac{\partial U}{\partial a} \right]_u$$

where U is the elastic energy of the system and a is the crack length. Either the load P or the displacement u can be kept fixed while evaluating the above expressions.

Irwin showed that for a mode I crack (opening mode) the strain energy release rate and the stress intensity factor are related by:

$$G = G_I = \begin{cases} \frac{K_I^2}{E} & \text{plane stress} \\ \frac{(1 - \nu^2) K_I^2}{E} & \text{plane strain} \end{cases}$$

where E is the Young's modulus, ν is Poisson's ratio, and K_I is the stress intensity factor in mode I. Irwin also showed that the strain energy release rate of a planar crack in a linear elastic body can be expressed in terms of the mode I, mode II (sliding mode), and mode III (tearing mode) stress intensity factors for the most general loading conditions.

Next, Irwin adopted the additional assumption that the size and shape of the energy dissipation zone remains approximately constant during brittle fracture. This assumption suggests that the energy needed to create a unit fracture surface is a constant that depends only on the material. This new material property was given the name *fracture toughness* and designated G_{Ic} . Today, it is the critical stress intensity factor K_{Ic} which is accepted as the defining property in linear elastic fracture mechanics.

Limitations



The S.S. *Schenectady* split apart by brittle fracture while in harbor (1944)

But a problem arose for the NRL researchers because naval materials, e.g., ship-plate steel, are not perfectly elastic but undergo significant plastic deformation at the tip of a crack. One basic assumption in Irwin's linear elastic fracture mechanics is that the size of the plastic zone is small compared to the crack length. However, this assumption is quite restrictive for certain types of failure in structural steels though such steels can be prone to brittle fracture, which has led to a number of catastrophic failures.

Linear-elastic fracture mechanics is of limited practical use for structural steels for another more practical reason. Fracture toughness testing is very expensive and engineers believe that sufficient information for selection of steels can be obtained from the simpler and cheaper Charpy impact test.

Nonlinear elasticity and plasticity



Vertical stabilizer, which separated from American Airlines Flight 587, leading to a fatal crash

Most engineering materials show some nonlinear elastic and inelastic behavior under operating conditions that involve large loads. In such materials the assumptions of linear elastic fracture mechanics may not hold, that is,

- the plastic zone at a crack tip may have a size of the same order of magnitude as the crack size
- the size and shape of the plastic zone may change as the applied load is increased and also as the crack length increases.

Therefore a more general theory of crack growth is needed for elastic-plastic materials that can account for:

- the local conditions for initial crack growth which include the nucleation, growth, and coalescence of voids or decohesion at a crack tip.
- a global energy balance criterion for further crack growth and unstable fracture.

R-curve

An early attempt in the direction of elastic-plastic fracture mechanics was Irwin's **crack extension resistance curve** or **R-curve**. This curve acknowledges the fact that the resistance to fracture increases with growing crack size in elastic-plastic materials. The

R-curve is a plot of the total energy dissipation rate as a function of the crack size and can be used to examine the processes of slow stable crack growth and unstable fracture. However, the R-curve was not widely used in applications until the early 1970s. The main reasons appear to be that the R-curve depends on the geometry of the specimen and the crack driving force may be difficult to calculate.

J-integral

In the mid-1960s James R. Rice (then at Brown University) and G. P. Cherepanov independently developed a new toughness measure to describe the case where there is sufficient crack-tip deformation that the part no longer obeys the linear-elastic approximation. Rice's analysis, which assumes non-linear elastic (or monotonic deformation-theory plastic) deformation ahead of the crack tip, is designated the J integral. This analysis is limited to situations where plastic deformation at the crack tip does not extend to the furthest edge of the loaded part. It also demands that the assumed non-linear elastic behavior of the material is a reasonable approximation in shape and magnitude to the real material's load response.

Fully plastic failure

If the material is so tough that the yielded region ahead of the crack extends to the far edge of the specimen before fracture, the crack is no longer an effective stress concentrator. Instead, the presence of the crack merely serves to reduce the load-bearing area. In this regime the failure stress is conventionally assumed to be the average of the yield and ultimate strengths of the material.

Engineering applications

The following information is needed for a fracture mechanics prediction of failure:

- Applied load
- Residual stress
- Size and shape of the part
- Size, shape, location, and orientation of the crack

Usually not all of this information is available and conservative assumptions have to be made.

Occasionally post-mortem fracture-mechanics analyses are carried out. In the absence of an extreme overload, the causes are either insufficient toughness (K_{Ic}) or an excessively large crack that was not detected during routine inspection.

Short summary

Arising from the manufacturing process, interior and surface flaws are found in all metal structures. Not all such flaws are unstable under service conditions. Fracture mechanics is

the analysis of flaws to discover those that are safe (that is, do not grow) and those that are liable to propagate as cracks and so cause failure of the flawed structure. Ensuring safe operation of structure despite these inherent flaws is achieved through damage tolerance analysis. Fracture mechanics as a subject for critical study has barely been around for a century and thus is relatively new. There is a high demand for engineers with fracture mechanics expertise—particularly in this day and age where engineering failure is considered 'shocking' amongst the general public.

Appendix: mathematical relations

Griffith's criterion

For the simple case of a thin rectangular plate with a crack perpendicular to the load Griffith's theory becomes:

$$G = \frac{\pi\sigma^2 a}{E} \quad (1.1)$$

where G is the strain energy release rate, σ is the applied stress, a is half the crack length, and E is the Young's modulus. The strain energy release rate can otherwise be understood as: *the rate at which energy is absorbed by growth of the crack.*

However, we also have that:

$$G_c = \frac{\pi\sigma_f^2 a}{E} \quad (1.2)$$

If $G \geq G_c$, this is the criterion for which the crack will begin to propagate.

Irwin's modifications

Eventually a modification of Griffith's solids theory emerged from this work; a term called stress intensity replaced strain energy release rate and a term called fracture toughness replaced surface weakness energy. Both of these terms are simply related to the energy terms that Griffith used:

$$K_I = \sigma\sqrt{\pi a} \quad (2.1)$$

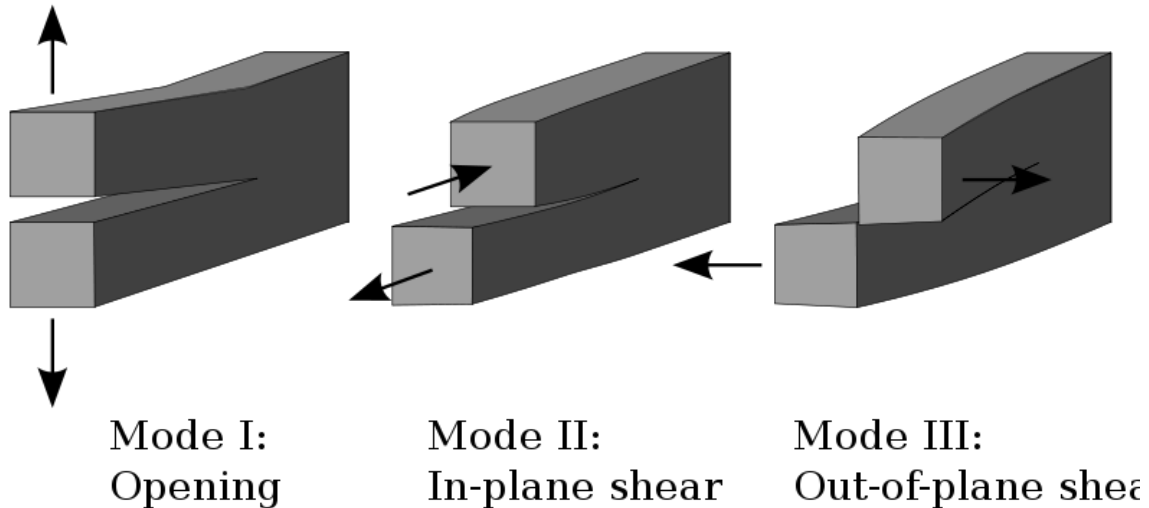
and

$$K_c = \sqrt{EG_c} \text{ (for plane stress)} \quad (2.2)$$

$$K_c = \sqrt{\frac{EG_c}{1-\nu^2}} \text{ (for plane strain)} \quad (2.3)$$

where K_I is the stress intensity, K_c the fracture toughness, and ν is Poisson's ratio. It is important to recognize the fact that fracture parameter K_c has different values when measured under plane stress and plane strain

Fracture occurs when $K_I \geq K_c$. For the special case of plane strain deformation, K_c becomes K_{Ic} and is considered a material property. The subscript I arises because of the different ways of loading a material to enable a crack to propagate. It refers to so-called "mode I" loading as opposed to mode II or III:



The three fracture modes.

There are three ways of applying a force to enable a crack to propagate:

- **Mode I crack** – Opening mode (a tensile stress normal to the plane of the crack)
- **Mode II crack** – Sliding mode (a shear stress acting parallel to the plane of the crack and perpendicular to the crack front)
- **Mode III crack** – Tearing mode (a shear stress acting parallel to the plane of the crack and parallel to the crack front)

We must note that the expression for K_I in equation 2.1 will be different for geometries other than the center-cracked infinite plate, as discussed in stress intensity. Consequently, it is necessary to introduce a dimensionless correction factor, Y , in order to characterize the geometry. We thus have:

$$K_I = Y \sigma \sqrt{\pi a} \quad (2.4)$$

where Y is a function of the crack length and width of sheet given by:

$$Y\left(\frac{a}{W}\right) = \sqrt{\sec\left(\frac{\pi a}{W}\right)} \quad (2.5)$$

for a sheet of finite width W containing a through-thickness crack of length $2a$, or

$$Y\left(\frac{a}{W}\right) = 1.12 - \frac{0.41}{\sqrt{\pi}} \frac{a}{W} + \frac{18.7}{\sqrt{\pi}} \left(\frac{a}{W}\right)^2 - \dots \quad (2.6)$$

for a sheet of finite width W containing a through-thickness edge crack of length a

Elasticity and plasticity

Since engineers became accustomed to using K_{Ic} to characterise fracture toughness, a relation has been used to reduce J_{Ic} to it:

$$K_{Ic} = \sqrt{E^* J_{Ic}} \quad \text{where } E^* = E \text{ for plane stress and } E^* = \frac{E}{1 - \nu^2} \text{ for plane strain} \quad (3.1)$$

The remainder of the mathematics employed in this approach is interesting, but is probably better summarised in external pages due to its complex nature.

Chapter 2

Fatigue (Material)

In materials science, **fatigue** is the progressive and localized structural damage that occurs when a material is subjected to cyclic loading. The nominal maximum stress values are less than the ultimate tensile stress limit, and may be below the yield stress limit of the material.

Fatigue occurs when a material is subjected to repeated loading and unloading. If the loads are above a certain threshold, microscopic cracks will begin to form at the surface. Eventually a crack will reach a critical size, and the structure will suddenly fracture. The shape of the structure will significantly affect the fatigue life; square holes or sharp corners will lead to elevated local stresses where fatigue cracks can initiate. Round holes and smooth transitions or fillets are therefore important to increase the fatigue strength of the structure.

Fatigue life

ASTM defines *fatigue life*, N_f , as the number of stress cycles of a specified character that a specimen sustains before failure of a specified nature occurs.

One method to predict fatigue life of materials is the Uniform Material Law (UML). UML was developed for fatigue life prediction of aluminum and titanium alloys by the end of 20th century and extended to high-strength steels.

Characteristics of fatigue



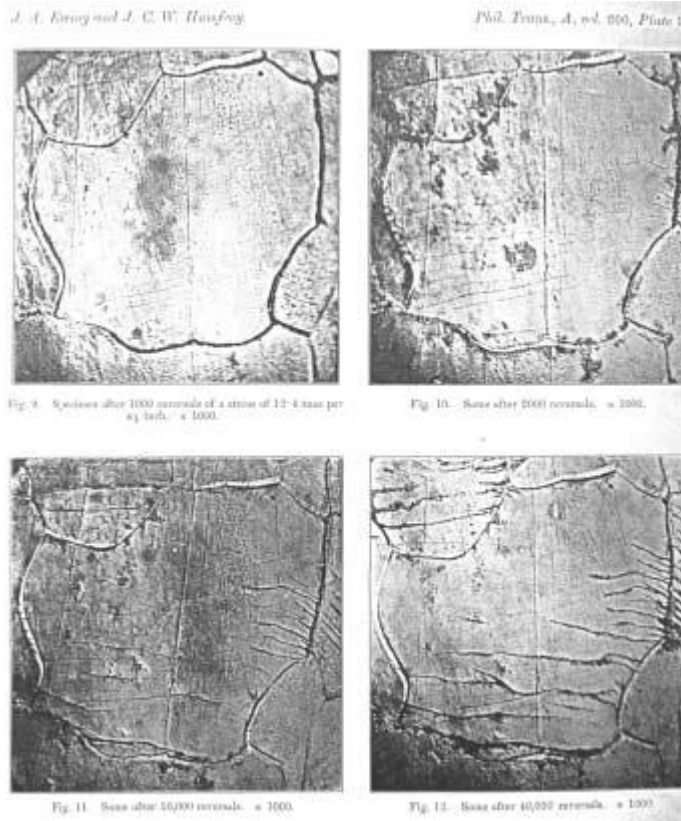
Fracture of an aluminium crank arm. Dark area of striations: slow crack growth. Bright granular area: sudden fracture.

- In metals and alloys, the process starts with dislocation movements, eventually forming persistent slip bands that nucleate short cracks.
- Fatigue is a stochastic process, often showing considerable scatter even in controlled environments.
- The greater the applied stress range, the shorter the life.
- Fatigue life scatter tends to increase for longer fatigue lives.
- Damage is cumulative. Materials do not recover when rested.
- Fatigue life is influenced by a variety of factors, such as temperature, surface finish, microstructure, presence of oxidizing or inert chemicals, residual stresses, contact (fretting), etc.
- Some materials (e.g., some steel and titanium alloys) exhibit a theoretical fatigue limit below which continued loading does not lead to structural failure.

- In recent years, researchers (see, for example, the work of Bathias, Murakami, and Stanzl-Tscheegg) have found that failures occur below the theoretical fatigue limit at very high fatigue lives (10^9 to 10^{10} cycles). An ultrasonic resonance technique is used in these experiments with frequencies around 10–20 kHz.
- High cycle fatigue strength (about 10^3 to 10^8 cycles) can be described by stress-based parameters. A load-controlled servo-hydraulic test rig is commonly used in these tests, with frequencies of around 20–50 Hz. Other sorts of machines—like resonant magnetic machines—can also be used, achieving frequencies up to 250 Hz.
- Low cycle fatigue (typically less than 10^3 cycles) is associated with widespread plasticity in metals; thus, a strain-based parameter should be used for fatigue life prediction in metals and alloys. Testing is conducted with constant strain amplitudes typically at 0.01–5 Hz.

Timeline of early fatigue research history

- 1837: Wilhelm Albert publishes the first article on fatigue. He devised a test machine for conveyor chains used in the Clausthal mines.
- 1839: Jean-Victor Poncelet describes metals as being *tired* in his lectures at the military school at Metz.
- 1842: William John Macquorn Rankine recognises the importance of stress concentrations in his investigation of railroad axle failures. The Versailles train crash was caused by axle fatigue.
- 1843: Joseph Glynn reports on fatigue of axle on locomotive tender. He identifies the keyway as the crack origin.
- 1848: Railway Inspectorate report one of the first tyre failures, probably from a rivet hole in tread of railway carriage wheel. It was likely a fatigue failure.
- 1849: Eaton Hodgkinson is granted a *small sum of money* to report to the UK Parliament on his work in *ascertaining by direct experiment, the effects of continued changes of load upon iron structures and to what extent they could be loaded without danger to their ultimate security*.
- 1854: Braithwaite reports on common service fatigue failures and coins the term *fatigue*.
- 1860: Systematic fatigue testing undertaken by Sir William Fairbairn and August Wöhler.
- 1870: Wöhler summarises his work on railroad axles. He concludes that cyclic stress range is more important than peak stress and introduces the concept of *endurance limit*.



Micrographs showing how surface fatigue cracks grow as material is further cycled.
From Ewing & Humfrey (1903)

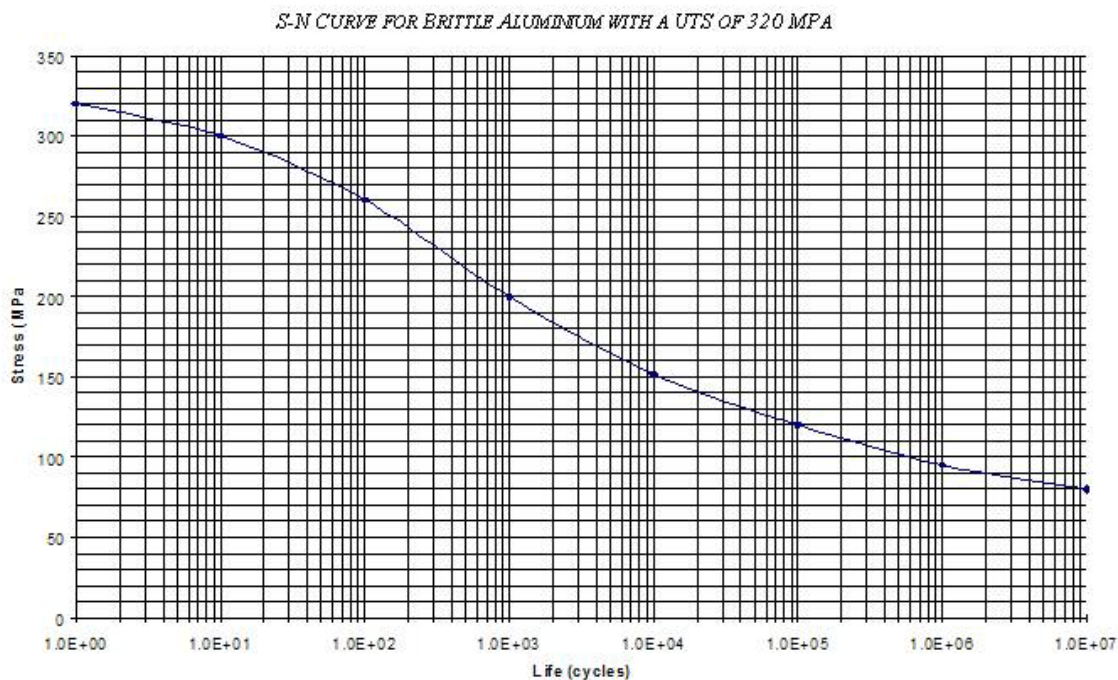
- 1903: Sir James Alfred Ewing demonstrates the origin of fatigue failure in microscopic cracks.
- 1910: O. H. Basquin proposes a log-log relationship for SN curves, using Wöhler's test data.
- 1945: A. M. Miner popularises A. Palmgren's (1924) linear damage hypothesis as a practical design tool.
- 1954: L. F. Coffin and S. S. Manson explain fatigue crack-growth in terms of plastic strain in the tip of cracks.
- 1961: P. C. Paris proposes methods for predicting the rate of growth of individual fatigue cracks in the face of initial scepticism and popular defence of Miner's phenomenological approach.
- 1968: Tatsuo Endo and M. Matsuishi devise the rainflow-counting algorithm and enable the reliable application of Miner's rule to random loadings.
- 1970: W. Elber elucidates the mechanisms and importance of crack closure in slowing the growth of a fatigue crack due to the wedging effect of plastic deformation left behind the tip of the crack.

High-cycle fatigue

Historically, most attention has focused on situations that require more than 10^4 cycles to failure where stress is low and deformation primarily elastic.

The S-N curve

In high-cycle fatigue situations, materials performance is commonly characterised by an *S-N curve*, also known as a *Wöhler curve*. This is a graph of the magnitude of a cyclic stress (*S*) against the logarithmic scale of cycles to failure (*N*).



S-N curves are derived from tests on samples of the material to be characterised (often called *coupons*) where a regular sinusoidal stress is applied by a testing machine which also counts the number of cycles to failure. This process is sometimes known as *coupon testing*. Each coupon test generates a point on the plot though in some cases there is a *runout* where the time to failure exceeds that available for the test. Analysis of fatigue data requires techniques from statistics, especially survival analysis and linear regression.

Probabilistic nature of fatigue

As coupons sampled from a homogeneous frame will manifest variation in their number of cycles to failure, the S-N curve should more properly be an *S-N-P curve* capturing the probability of failure after a given number of cycles of a certain stress. Probability distributions that are common in data analysis and in design against fatigue include the

lognormal distribution, extreme value distribution, Birnbaum–Saunders distribution, and Weibull distribution.

Complex loadings



Spectrum loading

In practice, a mechanical part is exposed to a complex, often random, sequence of loads, large and small. In order to assess the safe life of such a part:

1. Reduce the complex loading to a series of simple cyclic loadings using a technique such as rainflow analysis;
2. Create a histogram of cyclic stress from the rainflow analysis to form a fatigue damage spectrum;
3. For each stress level, calculate the degree of cumulative damage incurred from the S-N curve; and
4. Combine the individual contributions using an algorithm such as *Miner's rule*.

Miner's rule

In 1945, M. A. Miner popularised a rule that had first been proposed by A. Palmgren in 1924. The rule, variously called *Miner's rule* or the *Palmgren-Miner linear damage hypothesis*, states that where there are k different stress magnitudes in a spectrum, S_i ($1 \leq i \leq k$), each contributing $n_i(S_i)$ cycles, then if $N_i(S_i)$ is the number of cycles to failure of a constant stress reversal S_i , failure occurs when:

$$\sum_{i=1}^k \frac{n_i}{N_i} = C$$

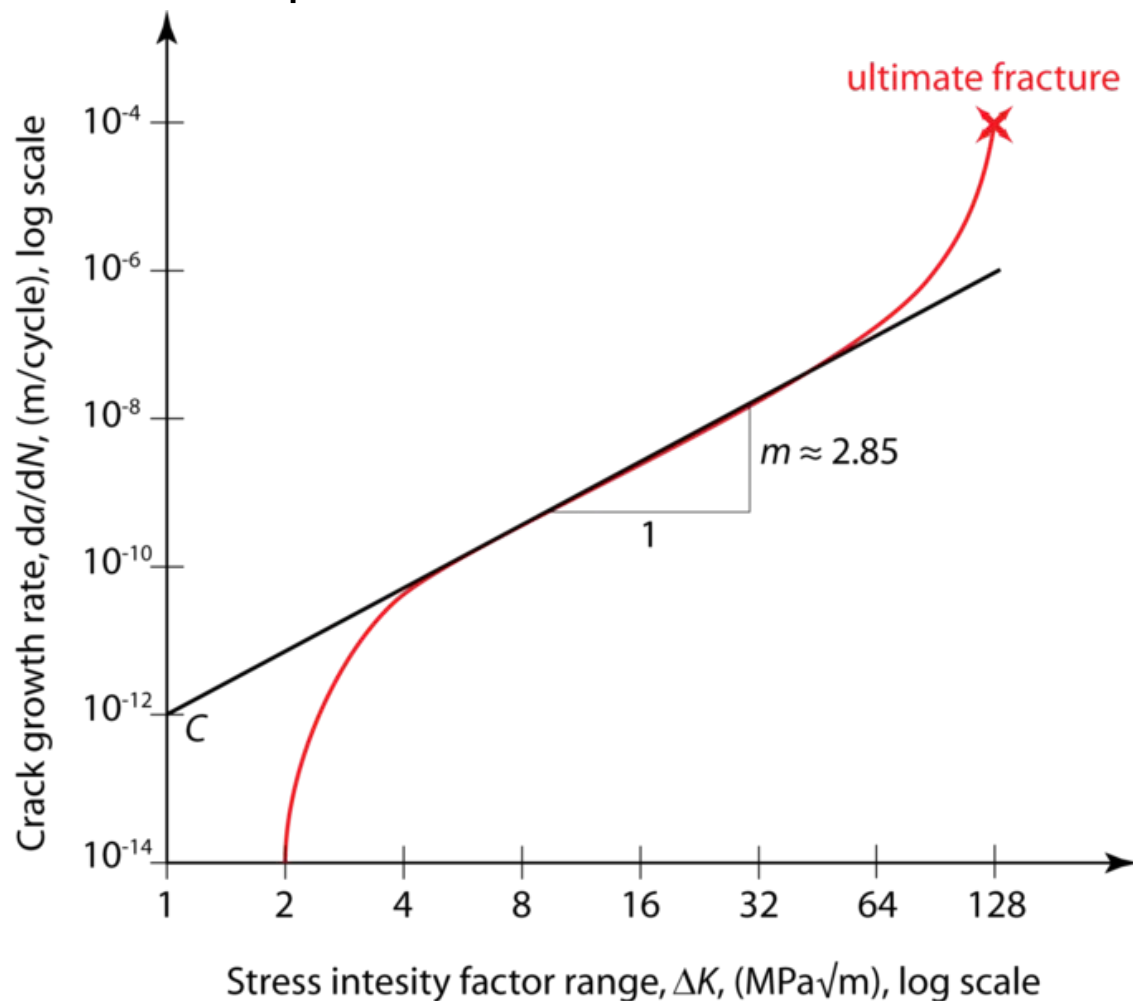
C is experimentally found to be between 0.7 and 2.2. Usually for design purposes, C is assumed to be 1.

This can be thought of as assessing what proportion of life is consumed by stress reversal at each magnitude then forming a linear combination of their aggregate.

Though Miner's rule is a useful approximation in many circumstances, it has several major limitations:

1. It fails to recognise the probabilistic nature of fatigue and there is no simple way to relate life predicted by the rule with the characteristics of a probability distribution. Industry analysts often use design curves, adjusted to account for scatter, to calculate $N_f(S_i)$.
2. There is sometimes an effect in the order in which the reversals occur. In some circumstances, cycles of low stress followed by high stress cause more damage than would be predicted by the rule. It does not consider the effect of overload or high stress which may result in a compressive residual stress. High stress followed by low stress may have less damage due to the presence of compressive residual stress.

Paris' Relationship



Typical fatigue crack growth rate graph.

In Fracture mechanics, Anderson, Gomez and Paris derived relationships for the stage II crack growth with cycles N , in terms of the cyclical component ΔK of the Stress Intensity Factor K

$$\frac{da}{dN} = C(\Delta K)^m$$

where a is the crack length and m is typically in the range 3 to 5 (for metals).

This relationship was later modified (by Forman, 1967) to make better allowance for the mean stress, by introducing a factor depending on $(1-R)$ where $R = \text{min stress}/\text{max stress}$, in the denominator.

Low-cycle fatigue

Where the stress is high enough for plastic deformation to occur, the account in terms of stress is less useful and the strain in the material offers a simpler description. Low-cycle fatigue is usually characterised by the *Coffin-Manson relation* (published independently by L. F. Coffin in 1954 and S. S. Manson 1953):

$$\frac{\Delta\epsilon_p}{2} = \epsilon'_f(2N)^c$$

-where:

- $\Delta\epsilon_p/2$ is the plastic strain amplitude;
- ϵ'_f is an empirical constant known as the *fatigue ductility coefficient*, the failure strain for a single reversal;
- $2N$ is the number of reversals to failure (N cycles);
- c is an empirical constant known as the *fatigue ductility exponent*, commonly ranging from -0.5 to -0.7 for metals in time independent fatigue. Slopes can be considerably steeper in the presence of creep or environmental interactions.

A similar relationship for materials such as Zirconium, used in the nuclear industry.

Fatigue and fracture mechanics

The account above is purely empirical and, though it allows life prediction and design assurance, life improvement or design optimisation can be enhanced using fracture mechanics. It can be developed in four stages.

1. Crack nucleation;
2. Stage I crack-growth;
3. Stage II crack-growth; and
4. Ultimate ductile failure.

Factors that affect fatigue-life

- **Cyclic stress state:** Depending on the complexity of the geometry and the loading, one or more properties of the stress state need to be considered, such as stress amplitude, mean stress, biaxiality, in-phase or out-of-phase shear stress, and load sequence,
- **Geometry:** Notches and variation in cross section throughout a part lead to stress concentrations where fatigue cracks initiate.
- **Surface quality.** Surface roughness cause microscopic stress concentrations that lower the fatigue strength. Compressive residual stresses can be introduced in the surface by e.g. shot peening to increase fatigue life. Such techniques for producing surface stress are often referred to as *peening*, whatever the mechanism used to produce the stress. Low Plasticity Burnishing, Laser peening, and ultrasonic impact treatment can also produce this surface compressive stress and can increase the fatigue life of the component. This improvement is normally observed only for high-cycle fatigue.
- **Material Type:** Fatigue life, as well as the behavior during cyclic loading, varies widely for different materials, e.g. composites and polymers differ markedly from metals.
- **Residual stresses:** Welding, cutting, casting, and other manufacturing processes involving heat or deformation can produce high levels of tensile residual stress, which decreases the fatigue strength.
- **Size and distribution of internal defects:** Casting defects such as gas porosity, non-metallic inclusions and shrinkage voids can significantly reduce fatigue strength.
- **Direction of loading:** For non-isotropic materials, fatigue strength depends on the **direction of the principal stress**.
- **Grain size:** For most metals, smaller grains yield longer fatigue lives, however, the presence of surface defects or scratches will have a greater influence than in a coarse grained alloy.
- **Environment:** Environmental conditions can cause erosion, corrosion, or gas-phase embrittlement, which all affect fatigue life. Corrosion fatigue is a problem encountered in many aggressive environments.
- **Temperature:** Extreme high or low temperatures can decrease fatigue strength.

Design against fatigue

Dependable design against fatigue-failure requires thorough education and supervised experience in structural engineering, mechanical engineering, or materials science. There

are three principal approaches to life assurance for mechanical parts that display increasing degrees of sophistication:

1. Design to keep stress below threshold of fatigue limit (infinite lifetime concept);
2. Design (conservatively) for a fixed life after which the user is instructed to replace the part with a new one (a so-called *lifer* part, finite lifetime concept, or "safe-life" design practice);
3. Instruct the user to inspect the part periodically for cracks and to replace the part once a crack exceeds a critical length. This approach usually uses the technologies of nondestructive testing and requires an accurate prediction of the rate of crack-growth between inspections. This is often referred to as damage tolerant design or "retirement-for-cause".

Stopping fatigue

Fatigue cracks that have begun to propagate can sometimes be stopped by drilling holes, called *drill stops*, in the path of the fatigue crack. This is not recommended as a general practice because the hole represents a stress concentration factor which depends on the size of the hole and geometry. There is thus the possibility of a new crack starting in the side of the hole. It is always far better to replace the cracked part entirely.

Material change

Changes in the materials used in parts can also improve fatigue life. For example, parts can be made from better fatigue rated metals. Complete replacement and redesign of parts can also reduce if not eliminate fatigue problems. Thus helicopter rotor blades and propellers in metal are being replaced by composite equivalents. They are not only lighter, but also much more resistant to fatigue. They are more expensive, but the extra cost is amply repaid by their greater integrity, since loss of a rotor blade usually leads to total loss of the aircraft. A similar argument has been made for replacement of metal fuselages, wings and tails of aircraft.

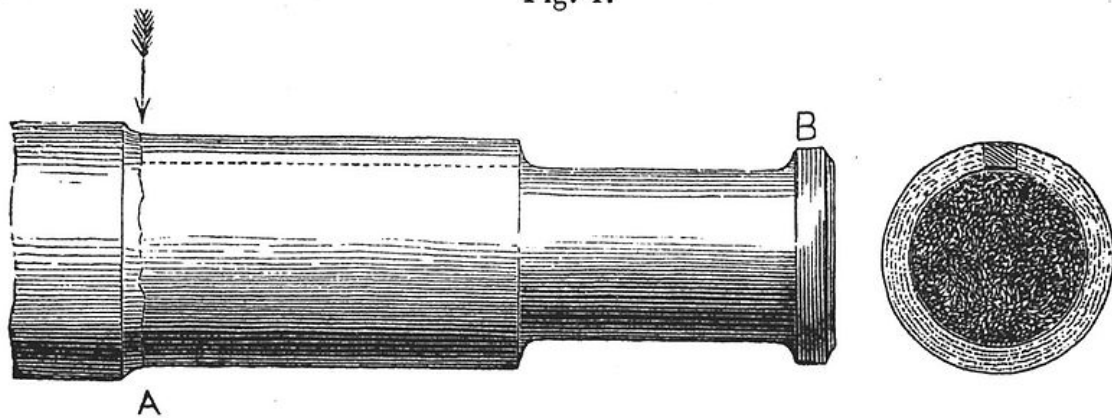
Infamous fatigue failures

Versailles train crash



Versailles train disaster

Fig. 1.



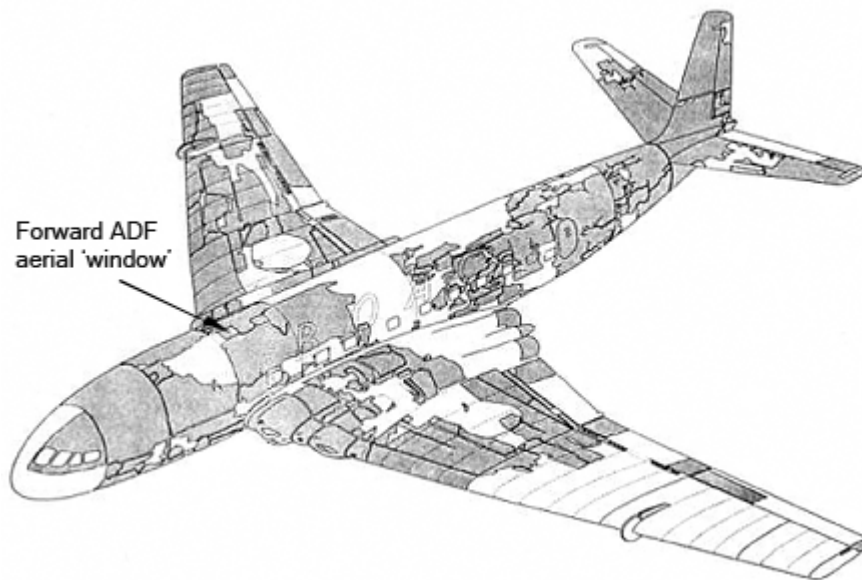
Drawing of a fatigue failure in an axle by Joseph Glynn, 1843.

Following the King's fete celebrations at the Palace of Versailles, a train returning to Paris crashed in May 1842 at Meudon after the leading locomotive broke an axle. The carriages behind piled into the wrecked engines and caught fire. At least 55 passengers were killed trapped in the carriages, including the explorer Jules Dumont d'Urville. This accident is known in France as the "Catastrophe ferroviaire de Meudon". The accident

was witnessed by the British locomotive engineer Joseph Locke and widely reported in Britain. It was discussed extensively by engineers, who sought an explanation.

The derailment had been the result of a broken locomotive axle. Rankine's investigation of broken axles in Britain highlighted the importance of stress concentration, and the mechanism of crack growth with repeated loading. His and other papers suggesting a crack growth mechanism through repeated stressing, however, were ignored, and fatigue failures occurred at an ever increasing rate on the expanding railway system. Other spurious theories seemed to be more acceptable, such as the idea that the metal had somehow "crystallized". The notion was based on the crystalline appearance of the fast fracture region of the crack surface, but ignored the fact that the metal was already highly crystalline.

de Havilland Comet



The recovered (shaded) parts of the wreckage of *G-ALYP* and the site (arrowed) of the failure

Two de Havilland Comet passenger jets broke up in mid-air and crashed within a few months of each other in 1954. As a result systematic tests were conducted on a fuselage immersed and pressurised in a water tank. After the equivalent of 3,000 flights investigators at the Royal Aircraft Establishment (RAE) were able to conclude that the crash had been due to failure of the pressure cabin at the forward Automatic Direction Finder window in the roof. This 'window' was in fact one of two apertures for the aerials of an electronic navigation system in which opaque fibreglass panels took the place of the window 'glass'. The failure was a result of metal fatigue caused by the repeated pressurisation and de-pressurisation of the aircraft cabin. Another fact was that the supports around the windows were riveted, not bonded, as the original specifications for the aircraft had called for. The problem was exacerbated by the punch rivet construction

technique employed. Unlike drill riveting, the imperfect nature of the hole created by punch riveting caused manufacturing defect cracks which may have caused the start of fatigue cracks around the rivet.

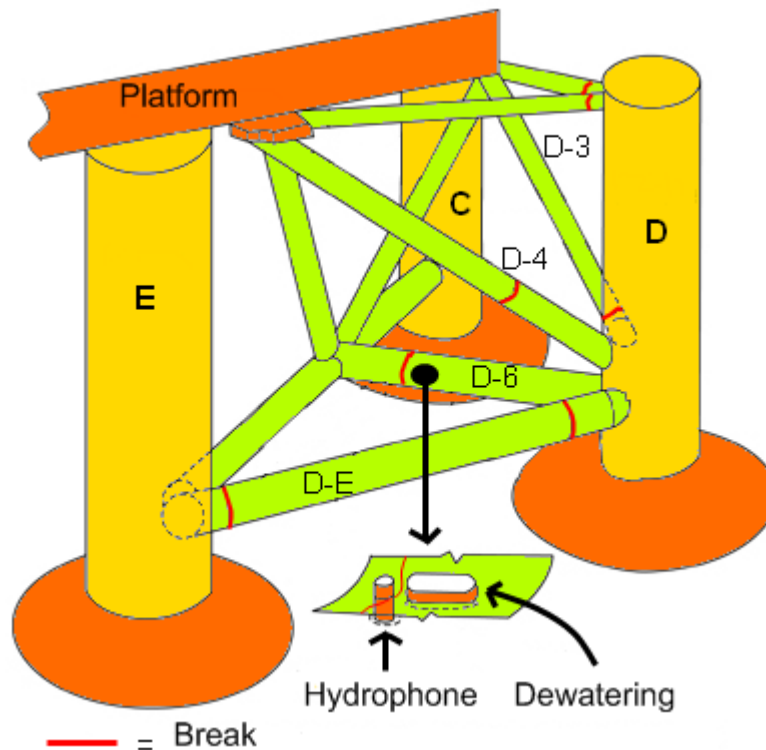


The fuselage fragment of *G-ALYP* on display in the Science Museum in London

The Comet's pressure cabin had been designed to a safety factor comfortably in excess of that required by British Civil Airworthiness Requirements (2.5 times the cabin proof pressure as opposed to the requirement of 1.33 times and an ultimate load of 2.0 times the cabin pressure) and the accident caused a revision in the estimates of the safe loading strength requirements of airliner pressure cabins.

In addition, it was discovered that the stresses around pressure cabin apertures were considerably higher than had been anticipated, especially around sharp-cornered cut-outs, such as windows. As a result, all future jet airliners would feature windows with rounded corners, the curve eliminating a stress concentration. This was a noticeable distinguishing feature of all later models of the Comet. Investigators from the RAE told a public inquiry that the sharp corners near the Comets' window openings acted as initiation sites for cracks. The skin of the aircraft was also too thin, and cracks from manufacturing stresses were present at the corners.

Alexander L. Kielland oil platform capsized



Fractures on the right side of the Alexander L. Kielland rig

The *Alexander L. Kielland* was a Norwegian semi-submersible drilling rig that capsized whilst working in the Ekofisk oil field in March 1980 killing 123 people. The capsizing was the worst disaster in Norwegian waters since World War II. The rig, located approximately 320 km east from Dundee, Scotland, was owned by the Stavanger Drilling Company of Norway and was on hire to the U.S. company Phillips Petroleum at the time of the disaster. In driving rain and mist, early in the evening of 27 March 1980 more than 200 men were off duty in the accommodation on the *Alexander L. Kielland*. The wind was gusting to 40 knots with waves up to 12 m high. The rig had just been winched away from the *Edda* production platform. Minutes before 18:30 those on board felt a 'sharp crack' followed by 'some kind of trembling'. Suddenly the rig heeled over 30° and then stabilised. Five of the six anchor cables had broken, the one remaining cable preventing the rig from capsizing. The list continued to increase and at 18.53 the remaining anchor cable snapped and the rig turned upside down.

A year later in March 1981, the investigative report concluded that the rig collapsed owing to a fatigue crack in one of its six bracings (bracing D-6), which connected the collapsed D-leg to the rest of the rig. This was traced to a small 6 mm fillet weld which joined a non-load-bearing flange plate to this D-6 bracing. This flange plate held a sonar device used during drilling operations. The poor profile of the fillet weld contributed to a reduction in its fatigue strength. Further, the investigation found considerable amounts of lamellar tearing in the flange plate and cold cracks in the butt weld. Cold cracks in the

welds, increased stress concentrations due to the weakened flange plate, the poor weld profile, and cyclical stresses (which would be common in the North Sea), seemed to collectively play a role in the rig's collapse.

Others

- The 1919 Boston Molasses Disaster has been attributed to a fatigue failure.
- The 1957 "Mt. Pinatubo", presidential plane of Philippine President Ramon Magsaysay, crashed due to engine failure caused by metal fatigue.
- The 1968 Los Angeles Airways Flight 417 lost one of its main rotor blades due to fatigue failure.
- The 1985 Japan Airlines Flight 123 crashed after the aircraft lost its vertical stabilizer due to faulty repairs on the rear bulkhead.
- The 1988 Aloha Airlines Flight 243 suffered an explosive decompression due to fatigue failure.
- The 1989 United Airlines Flight 232 lost its tail engine due to fatigue failure.
- The 1992 El Al Flight 1862 lost both engines on its right-wing due to fatigue failure with the #3 Engine.
- The 1998 Eschede train disaster was caused by fatigue failure of a single composite wheel.
- The 2002 China Airlines Flight 611 had disintegrated in-flight due to fatigue failure.
- The 2005 Chalk's Ocean Airways Flight 101 lost its right wing due to fatigue failure brought about by inadequate maintenance practices.

Chapter 3

Fractography

Fractography is the study of fracture surfaces of materials. Fractographic methods are routinely used to determine the cause of failure in engineering structures, especially in product failure and the practice of forensic engineering or failure analysis. In material science research, fractography is used to develop and evaluate theoretical models of crack growth behavior.

One of the aims of fractographic examination is to determine the cause of failure by studying the characteristics of a fracture surface. Different types of crack growth (e.g. fatigue, stress corrosion cracking, hydrogen embrittlement) produce characteristic features on the surface, which can be used to help identify the failure mode. The overall pattern of cracking can be more important than a single crack, however, especially in the case of brittle materials like ceramics and glasses.

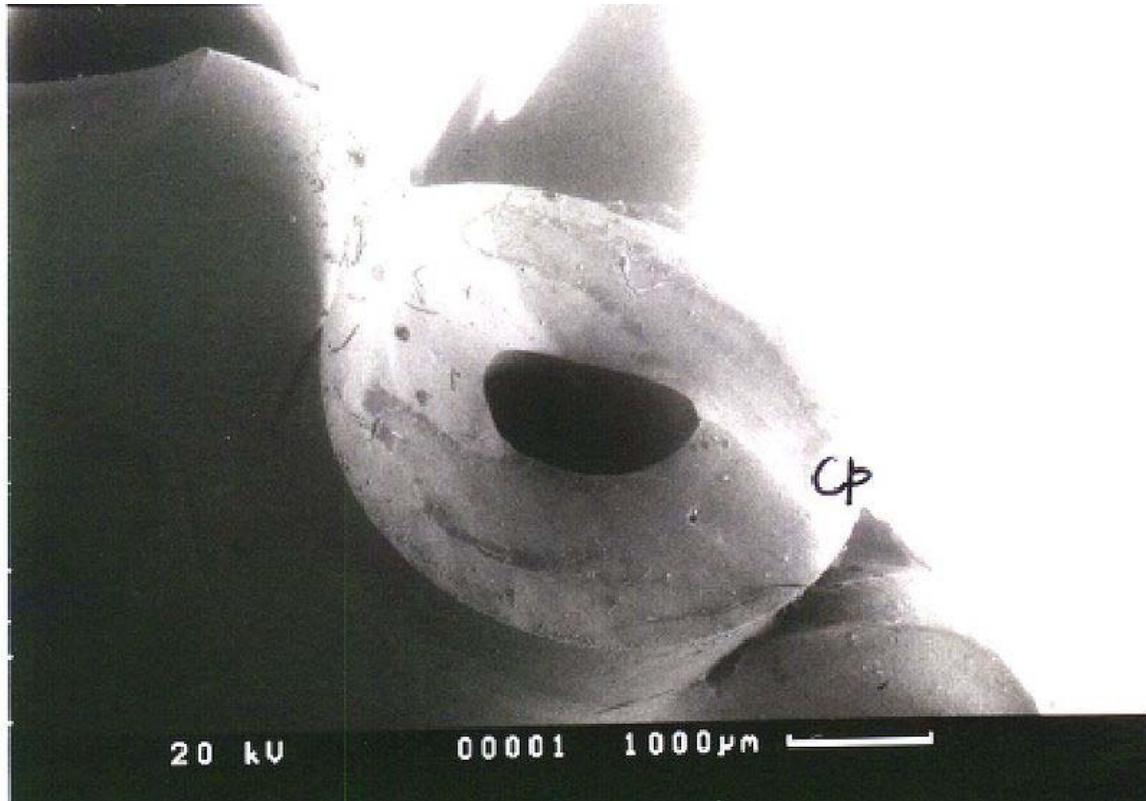
Methods



Crankshaft fatigue fracture

An important aim of fractography is to establish and examine the origin of cracking, as examination at the origin may reveal the cause of crack initiation. Initial fractographic examination is commonly carried out on a macro scale utilising low power optical microscopy and oblique lighting techniques to identify the extent of cracking, possible modes and likely origins. Optical microscopy or macrophotography are often enough to pinpoint the nature of the failure and the causes of crack initiation and growth if the loading pattern is known.

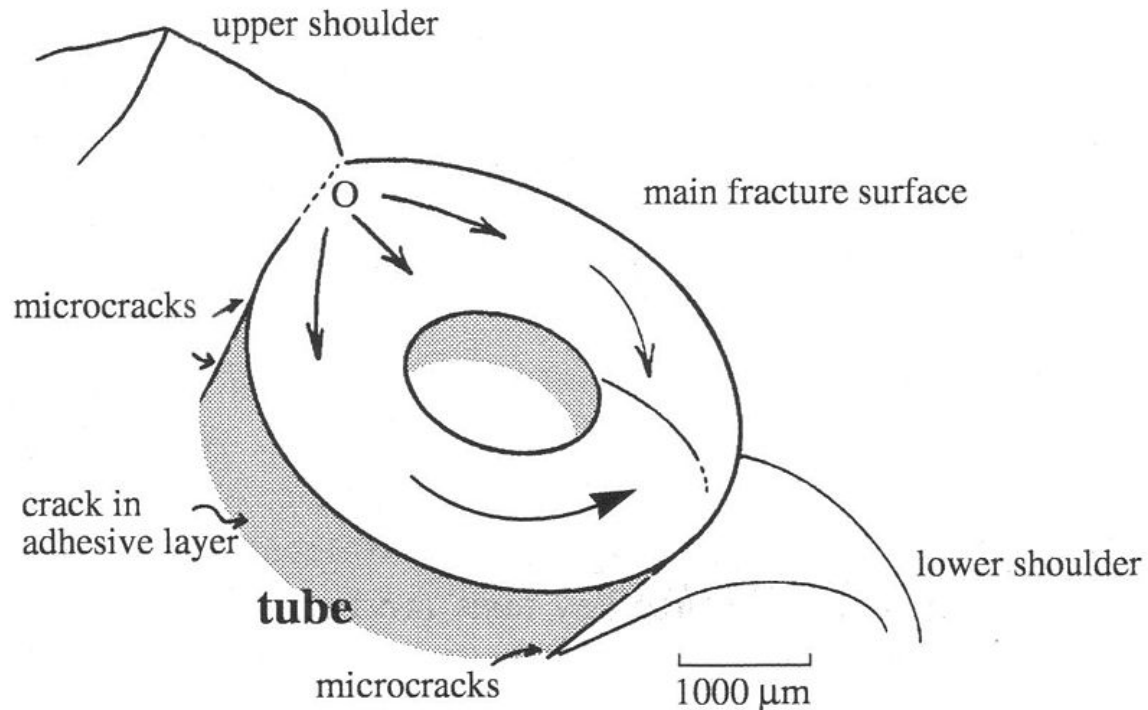
Common features that may be a cause for crack initiation are inclusions, voids or foreign material, points of stress concentration and "hachures", or the lines on fractures which show crack direction. The broken crankshaft shown at right failed from a surface defect near the bulb at lower centre, the single brittle crack growing up into the bulk material by small steps, a problem known as fatigue. The crankshaft also shows hachures which point back to the origin of the fracture. Some modes of crack growth can leave characteristic marks on the surface that identify the mode of crack growth and origin on a macro scale e.g. beachmarks or striations on fatigue cracks. The areas of the product can also be very revealing, especially if there are traces of sub-critical cracks, or cracks which have not grown to completion. They can indicate that the material was faulty when loaded, or alternatively, that the sample was overloaded at the time of failure.



Fractured breast implant catheter in SEM

A Cusp (singularity) is formed where brittle cracks meet, as shown on the picture of a failed catheter (Cp). The cusp was formed by brittle failure of the catheter on a breast implant in silicone rubber. The origin of the cracks is at the shoulder at the left-hand side. Identifying such features will allow a fracture surface map to be made of the surface being studied. The implant failed because of overload, all the imposed loads being concentrated at the connection between the catheter and the bag holding salt solution. As a result, the patient reported loss of fluid from the implant, and it was extracted surgically and replaced.

Fracture surface map



Fracture map of failed breast implant

A schematic fracture surface map is a valuable result of visual or microscopic examination. It seeks to isolate and identify the features on the surface which show how the product failed. Such a map can be a valuable way of presenting information which shows clearly how a crack was initiated and grew with time. In the case of the failed breast implant, the crack path was very simple, but the cause more subtle. Further scanning electron microscopy showed numerous microcracks between the bag and the catheter, indicating that the adhesive bond between the two components had failed prematurely, perhaps through faulty manufacture. The material of construction of both bag and catheter, silicone rubber is a physically weak elastomer, and product design must allow for the low tear or shear strength of the material.

Scanning electron microscopy

In many cases, fractography requires examination at a finer scale, which is usually carried out in a Scanning electron microscope or SEM. The resolution is much higher than the optical microscope, although samples are examined in a partial vacuum and colour is absent. Improved SEM's now allow examination at near atmospheric pressures, so allowing examination of sensitive materials such as those of biological origin. The atmosphere within the sample chamber can also be controlled using nitrogen or water vapour for example, a method known as environmental SEM or ESEM. The method is especially useful when combined with Energy dispersive X-ray spectroscopy or EDX,

which can be performed in the microscope, so very small areas of the sample can be analysed for their elemental distribution.



Fatigue fracture in rubber brake seal showing striations at left (SEM)

The fracture surface photograph shows a brittle fracture in a car brake seal. Crack growth can be seen from the fine lines or striations in the surface, indicative of fatigue. The problem led to an accident when the crack suddenly grew to completion, hydraulic fluid was lost, the driver lost braking power, and the vehicle crashed. The crack grew from cuts at the edge of the seal, probably caused by sharp particles trapped in the brake cylinder.

Applications

Fractography is a widely used technique in forensic engineering, forensic materials engineering and fracture mechanics to understand the causes of failures and also to verify theoretical failure predictions with real life failures. It is of use in forensic science for analysing broken products which have been used as weapons, such as broken bottles for example. Thus a defendant might claim that a bottle was faulty and broke accidentally when it impacted a victim of an assault. Fractography could show the allegation to be false, and that considerable force was needed to smash the bottle before using the broken end as a weapon to deliberately attack the victim. Bullet holes in glass windscreens or windows can also indicate the direction of impact and the energy of the projectile. In these cases, the overall pattern of cracking is vital to reconstructing the sequence of events, rather than the specific characteristics of a single crack.

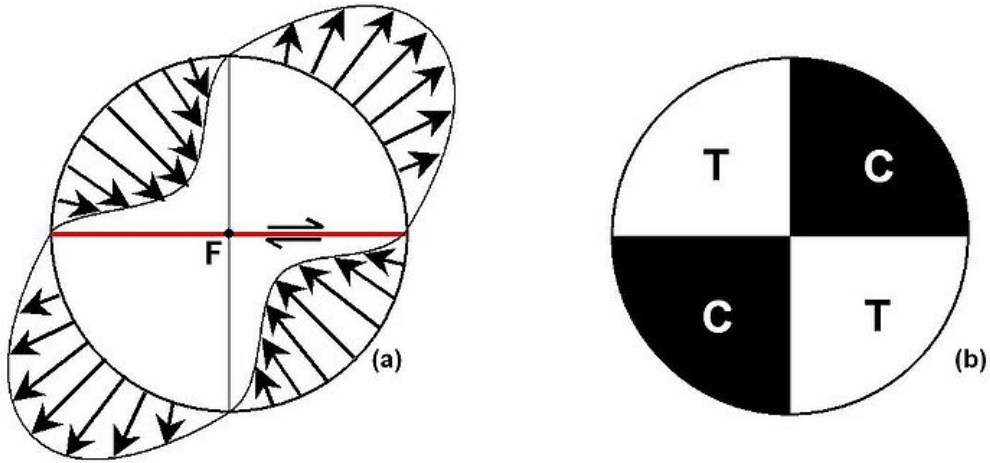
Optical fractography and Electron fractography are two more types of fractography. Electron fractography is microscopic and needs an SEM (Scanning Electron Microscope) to be conducted. Optical fractography needs much less equipment.

Chapter 4

Focal Mechanism

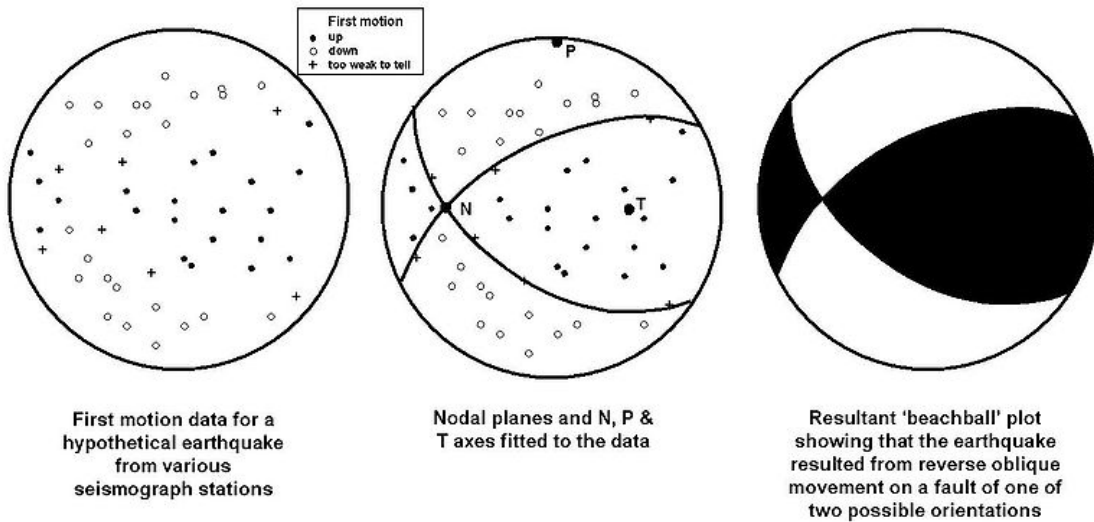
The **focal mechanism** of an earthquake describes the inelastic deformation in the source region that generates the seismic waves. In the case of a fault-related event it refers to the orientation of the fault plane that slipped and the slip vector and is also known as a **fault-plane solution**. Focal mechanisms are derived from a solution of the moment tensor for the earthquake, which itself is estimated by an analysis of observed seismic waveforms. The focal mechanism can be derived from observing the pattern of "first motions", that is, whether the first arriving P waves break up or down. This method was used before waveforms were recorded and analysed digitally and this method is still used for earthquakes too small for easy moment tensor solution. Focal mechanisms are now mainly derived using semi-automatic analysis of the recorded waveforms.

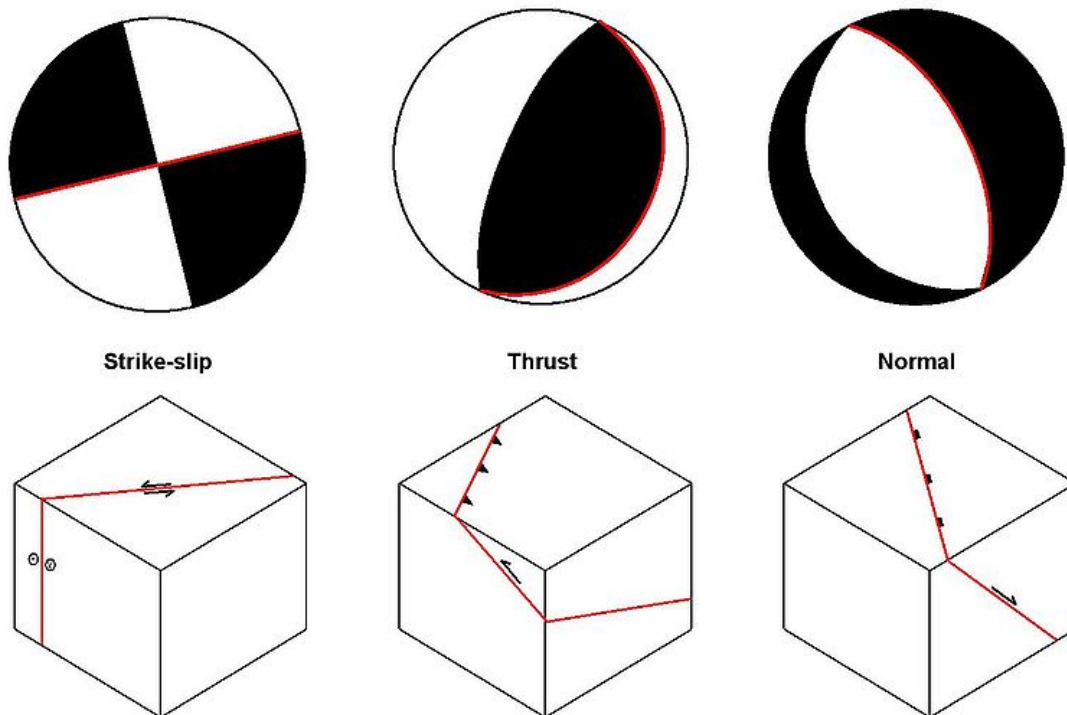
Moment tensor solutions



Schematic diagram showing the direction of initial movement of particles around the focus (F) of an earthquake on a W-E dextral strike-slip fault, viewed from above (a) and the equivalent zones of compressional (C) and tensional (T) sense first motion in the seismic waves radiating outward (b).

Note that due to the symmetry, an identical pattern would result from movement on an N-S sinistral strike-slip fault passing through the focus





Types of 'beachball plot' associated with different fault end-members
(nodal plane in red parallel to fault)

The moment tensor solution is typically displayed graphically using a so-called *beachball* diagram. The pattern of energy radiated during an earthquake with a single direction of motion on a single fault plane may be modelled as a *double couple*, which is described mathematically as a special case of a second order tensor (similar to those for stress and strain) known as the moment tensor.

Earthquakes not caused by fault movement have quite different patterns of energy radiation. In the case of an underground nuclear explosion, for instance, the seismic moment tensor is isotropic and this difference allows such explosions to be easily discriminated from their seismic response. This is an important part of monitoring to discriminate between earthquakes and explosions for the Comprehensive Test Ban Treaty.

Graphical representation ("beachball plot")

The data for an earthquake is plotted using a lower-hemisphere stereographic projection. The azimuth and take-off angle are used to plot the position of an individual seismic record. The take-off angle is the angle from the vertical of a seismic ray as it emerges from the earthquake focus. These angles are calculated from a standard set of tables that describe the relationship between the take-off angle and the distance between the focus and the observing station. By convention, filled symbols are used to plot data from

The fault plane responsible for the earthquake will be parallel to one of the nodal planes, the other being called the auxiliary plane. Unfortunately it is not possible to determine solely from a focal mechanism which of the nodal planes is in fact the fault plane. For this other geological or geophysical evidence is needed to remove the ambiguity. The slip vector, which is the direction of motion of one side of the fault relative to the other, lies within the fault plane, 90 deg from the N-axis.

To give an example, in the 2004 Indian Ocean earthquake, the moment tensor solution gives two nodal planes, one dipping northeast at 13 degrees and one dipping southwest at 79 degrees. In this case the earthquake can be confidently associated with the plane dipping shallowly to the northeast, as this is the orientation of the subducting slab as defined by historical earthquake locations and plate tectonic models.

Beach Ball Calculator

There are several programs available to prepare Focal Mechanism Solutions (FMS). BBC, a MATLAB based tool box, is available to prepare the beach ball diagrams. This software plots the first motion polarity data arrived at different stations. The compression and dilation are separated using mouse help. A final diagram is prepared automatically.

Chapter 5

Fracture Toughness

In materials science, **fracture toughness** is a property which describes the ability of a material containing a crack to resist fracture, and is one of the most important properties of any material for virtually all design applications. It is denoted K_{Ic} and has the units of $\text{Pa}\sqrt{\text{m}}$.

The subscript Ic denotes mode I crack opening under a normal tensile stress perpendicular to the crack, since the material can be made deep enough to stand shear (mode II) or tear (mode III).

Fracture toughness is a quantitative way of expressing a material's resistance to brittle fracture when a crack is present. If a material has much fracture toughness it will probably undergo ductile fracture. Brittle fracture is very characteristic of materials with less fracture toughness.

Fracture mechanics, which leads to the concept of fracture toughness, was broadly based on the work of A. A. Griffith who, among other things, studied the behavior of cracks in brittle materials.

A related concept is the *work of fracture* (γ_{wof}) which is directly proportional to K_{Ic}^2/E , where E is the Young's modulus of the material. Note that, in SI units, γ_{wof} is given in J/m^2 .

Table of values

Here are some typical values of fracture toughness for various materials:

Material	K_{Ic} ($\text{MPa}\cdot\text{m}^{1/2}$)
Metals	
Aluminum alloy (7075) 24	

Steel alloy (4340)	50
Titanium alloy	44–66
Aluminum	14–28

Ceramics

Aluminium oxide	3–5
Silicon carbide	3–5
Soda-lime-glass	0.7–0.8
Concrete	0.2–1.4

Polymers

Polymethyl methacrylate	0.7–1.6
Polystyrene	0.7–1.1

Composites

Mullite-fibre composite	1.8–3.3
Silica aerogels	0.0008–0.0048

Crack growth as a stability problem

Consider a body with flaws (cracks) that is subject to some loading; the stability of the crack can be assessed as follows. We can assume for simplicity that the loading is of constant displacement or displacement controlled type (such as loading with a screw jack); we can also simplify the discussion by characterizing the crack by its area, A . If we consider an adjacent state of the body as being one with a broader crack (area $A+dA$), we can then assess strain energy in the two states and evaluate strain energy release rate.

The rate is reckoned with respect to the change in crack area, so if we use U for strain energy, the strain energy release rate is numerically dU/dA . It may be noted that for a body loaded in constant displacement mode, the displacement is applied and the force level is dictated by stiffness (or compliance) of the body. If the crack grows in size, the stiffness decreases, so the force level will decrease. This decrease in force level under the same displacement (strain) level indicates that the elastic strain energy stored in the body is decreasing—is being released. Hence the term strain energy release rate which is usually denoted with symbol G .

The strain energy release rate is higher for higher loads and broader cracks. If the strain energy so released exceeds a critical value G_c , then the crack will grow spontaneously. For brittle materials, G_c can be equated to the surface energy of the (two) new crack surfaces; in other words, in brittle materials, a crack will grow spontaneously if the strain energy released is equal to or more than the energy required to grow the crack surface(s). The stability condition can be written as

$$\text{elastic energy released} = \text{surface energy created.}$$

If the elastic energy released is less than the critical value, then the crack will not grow; equality signifies neutral stability and if the strain energy release rate exceeds the critical value, the crack will start growing in an unstable manner. For ductile materials, energy associated with plastic deformation has to be taken into account. When there is plastic deformation at the crack tip (as occurs most often in metals) the energy to propagate the crack may increase by several orders of magnitude as the work related to plastic deformation may be much larger than the surface energy. In such cases, the stability criterion has to restated as

$$\text{elastic energy released} = \text{surface energy} + \text{plastic deformation energy}.$$

Practically, this means a higher value for the critical value G_c . From the definition of G , we can deduce that it has dimensions of work (or energy) /area or force/length. For ductile metals G_{Ic} is around 50–200 kJ/m², for brittle metals it is usually 1–5 and for glasses and brittle polymers it is almost always less than 0.5.

The problem can also be formulated in terms of stress instead of energy, leading to the terms stress intensity factor K (or K_I for mode I) and critical stress intensity factor K_c (and K_{Ic}). These K_c and K_{Ic} (etc.) quantities are commonly referred to as fracture toughness, though it is equivalent to use G_c . Typical values for K_{Ic} are 150 MN/m^{3/2} for ductile (very tough) metals, 25 for brittle ones and 1–10 for glasses and brittle polymers. Notice the different units used by G_{Ic} and K_{Ic} . Engineers tend to use the latter as an indication of toughness.

Transformation toughening

Composites exhibiting the highest level of fracture toughness are typically made of a pure alumina or some silica-alumina (SiO₂ /Al₂O₃) matrix with tiny inclusions of zirconia (ZrO₂) dispersed as uniformly as possible within the solid matrix. (*Note: a wet chemical approach is typically necessary in order to establish the compositional uniformity of the ceramic body before firing).

The process of "transformation toughening" is based on the assumption that zirconia undergoes several martensitic (displacive, diffusionless) phase transformations (cubic → tetragonal → monoclinic) between room temperature and practical sintering (or firing) temperatures. Thus, due to the volume restrictions induced by the solid matrix, metastable crystalline structures can become frozen in which impart an internal strain field surrounding each zirconia inclusion upon cooling. This enables a zirconia particle (or inclusion) to absorb the energy of an approaching crack tip front in its nearby vicinity.

Thus, the application of large shear stresses during fracture nucleates the transformation of a zirconia inclusion from the metastable phase. The subsequent volume expansion from the inclusion (via an increase in the height of the unit cell) introduces compressive stresses which therefore strengthen the matrix near the approaching crack tip front. Zirconia "whiskers" may be used expressly for this purpose.

Appropriately referred to by its first discoverers as "ceramic steel", the stress intensity factor values for window glass (silica), transformation toughened alumina, and a typical iron/carbon steel range from 1 to 20 to 50 respectively.

Conjoint action

There are number of instances where this picture of a critical crack is modified by corrosion. Thus, fretting corrosion occurs when a corrosive medium is present at the interface between two rubbing surfaces. Fretting (in the absence of corrosion) results from the disruption of very small areas that bond and break as the surfaces undergo friction, often under vibrating conditions. The bonding contact areas deform under the localised pressure and the two surfaces gradually wear away. Fracture mechanics dictates that each minute localised fracture has to satisfy the general rule that the elastic energy released as the bond fractures has to exceed the work done in plastically deforming it and in creating the (very tiny) fracture surfaces. This process is enhanced when corrosion is present, not least because the corrosion products act as an abrasive between the rubbing surfaces.

Fatigue is another instance where cyclical stressing, this time of a bulk lump of metal, causes small flaws to develop. Ultimately one such flaw exceeds the critical condition and fracture propagates across the whole structure. The fatigue life of a component is the time it takes for criticality to be reached, for a given regime of cyclical stress. **Corrosion fatigue** is what happens when a cyclically stressed structure is subjected to a corrosive environment at the same time. This not only serves to initiate surface cracks but actually modifies the crack growth process. As a result the fatigue life is shortened, often considerably.

Stress-corrosion cracking (SCC)

This phenomenon is the unexpected sudden failure of normally ductile metals subjected to a constant tensile stress in a corrosive environment. Certain austenitic stainless steels and aluminium alloys crack in the presence of chlorides, mild steel cracks in the presence of alkali (**boiler cracking**) and copper alloys crack in ammoniacal solutions (**season cracking**). Worse still, high-tensile structural steels crack in an unexpectedly brittle manner in a whole variety of aqueous environments, especially chloride. With the possible exception of the latter, which is a special example of *hydrogen cracking*, all the others display the phenomenon of subcritical crack growth; i.e. small surface flaws propagate (usually smoothly) under conditions where fracture mechanics predicts that failure should not occur. That is, in the presence of a corrodent, cracks develop and propagate well below K_{Ic} . In fact, the subcritical value of the stress intensity, designated as K_{Isc} , may be less than 1% of K_{Ic} , as the following table shows:

Alloy	$K_{Ic} (MN / m^{3/2})$	SCC environment	$K_{Isc} (MN / m^{3/2})$
13Cr steel	60	3% NaCl	12

18Cr-8Ni	200	42% MgCl ₂	10
Cu-30Zn	200	NH ₄ OH, pH7	1
Al-3Mg-7Zn	25	aqueous halides	5
Ti-6Al-1V	60	0.6M KCl	20

The subcritical nature of propagation may be attributed to the chemical energy released as the crack propagates. That is,

$$\text{elastic energy released} + \text{chemical energy} = \text{surface energy} + \text{deformation energy}.$$

The crack initiates at K_{Isc} and thereafter propagates at a rate governed by the slowest process, which most of the time is the rate at which corrosive ions can diffuse to the crack tip. As the crack advances so K rises (because crack size appears in the calculation of stress intensity). Finally it reaches K_{Ic} , whereupon swift fracture ensues and the component fails. One of the practical difficulties with SCC is its unexpected nature. Stainless steels, for example, are employed because under most conditions they are passive; i.e. effectively inert. Very often one finds a single crack has propagated while the rest of the metal surface stays apparently unaffected.

Chapter 6

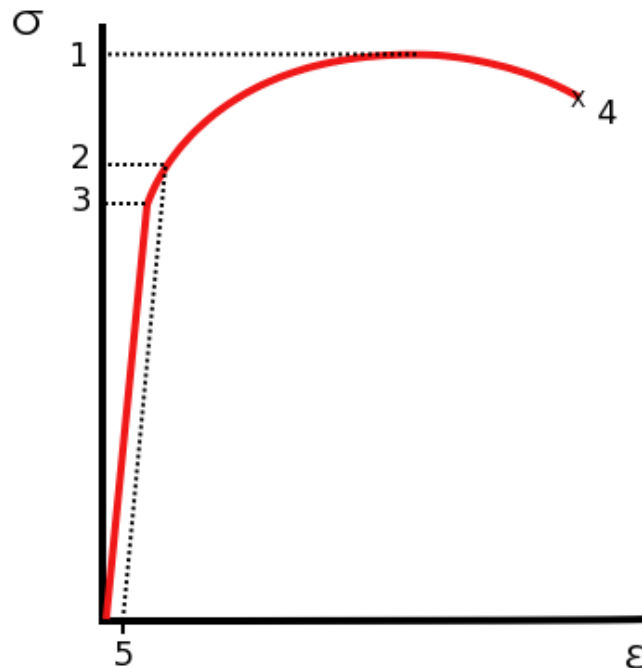
Fracture

A **fracture** is the (local) separation of an object or material into two, or more, pieces under the action of stress.

The word *fracture* is often applied to bones of living creatures (that is, a bone fracture), or to crystals or crystalline materials, such as gemstones or metal. Sometimes, in crystalline materials, individual crystals fracture without the body actually separating into two or more pieces. Depending on the substance which is fractured, a fracture reduces strength (most substances) or inhibits transmission of light (optical crystals).

A detailed understanding of how fracture occurs in materials may be assisted by the study of fracture mechanics.

Fracture strength



Stress vs. strain curve typical of aluminum

1. Ultimate tensile strength

2. Yield strength
3. Proportional limit stress
4. Fracture
5. Offset strain (typically 0.2%)

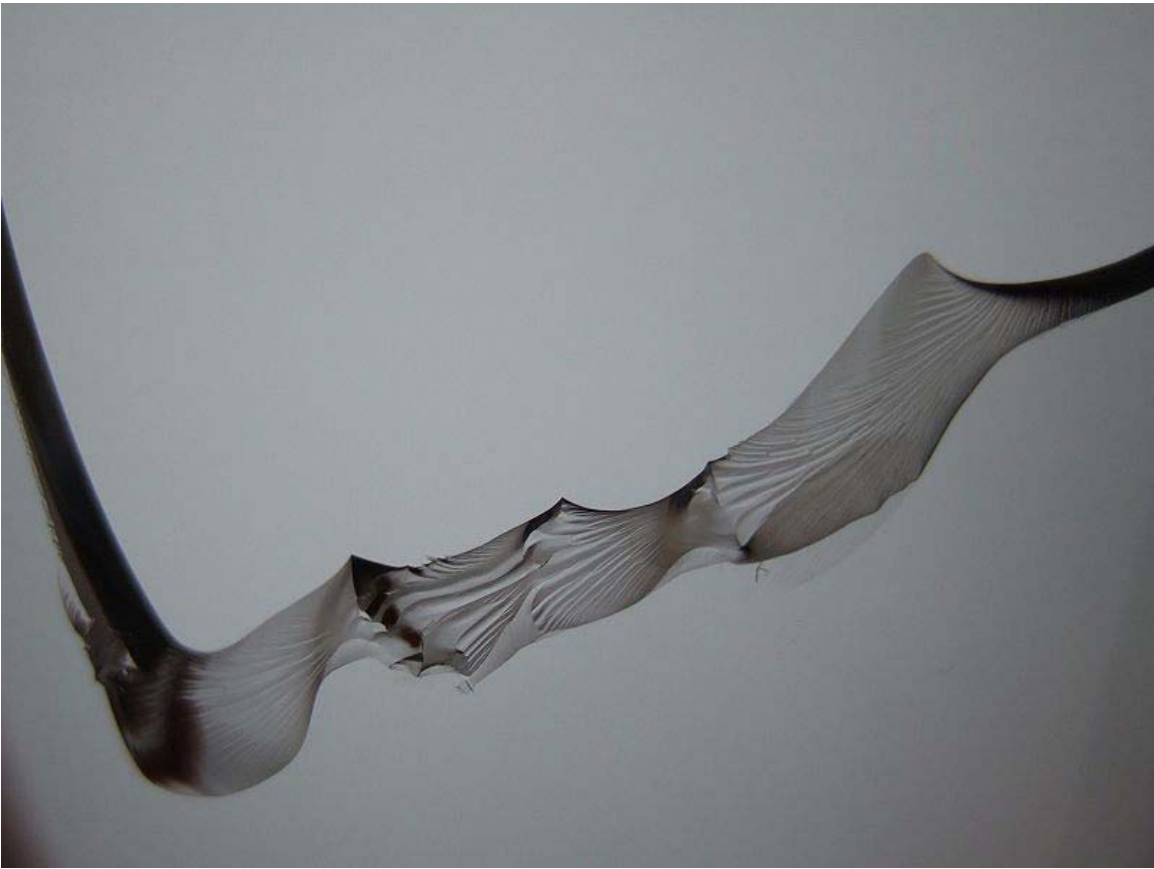
Fracture strength, also known as **breaking strength**, is the stress at which a specimen fails via fracture. This is usually determined for a given specimen by a tensile test, which charts the stress-strain curve. The final recorded point is the fracture strength.

Ductile materials have a fracture strength lower than the ultimate tensile strength (UTS), whereas in brittle materials the fracture strength is equivalent to the UTS. If a ductile material reaches its ultimate tensile strength in a load-controlled situation, it will continue to deform, with no additional load application, until it ruptures. However, if the loading is displacement-controlled, the deformation of the material may relieve the load, preventing rupture.

If the stress-strain curve is plotted in terms of *true stress* and *true strain* the curve will always slope upwards and never reverse, as true stress is corrected for the decrease in cross-sectional area. The true stress on the material at the time of rupture is known as the breaking strength. This is the maximum stress on the true stress-strain curve, given by point 3 on curve B.

Types

Brittle fracture



Brittle fracture in glass.



Fracture of an Aluminum Crank Arm. Bright: Brittle fracture. Dark: Fatigue fracture.

In *brittle fracture*, no apparent plastic deformation takes place before fracture. In brittle crystalline materials, fracture can occur by *cleavage* as the result of tensile stress acting normal to crystallographic planes with low bonding (cleavage planes). In amorphous solids, by contrast, the lack of a crystalline structure results in a conchoidal fracture, with cracks proceeding normal to the applied tension.

The theoretical strength of a crystalline material is (roughly)

$$\sigma_{\text{theoretical}} = \sqrt{\frac{E\gamma}{r_0}}$$

where: -

E is the Young's modulus of the material,

γ is the surface energy, and
 r_o is the equilibrium distance between atomic centers.

On the other hand, a crack introduces a stress concentration modeled by

$$\sigma_{\text{elliptical crack}} = \sigma_{\text{applied}} \left(1 + 2\sqrt{\frac{a}{\rho}}\right) = 2\sigma_{\text{applied}} \sqrt{\frac{a}{\rho}} \text{ (For sharp cracks)}$$

where: -

σ_{applied} is the loading stress,
 a is half the length of the crack, and
 ρ is the radius of curvature at the crack tip.

Putting these two equations together, we get

$$\sigma_{\text{fracture}} = \sqrt{\frac{E\gamma\rho}{4ar_o}}$$

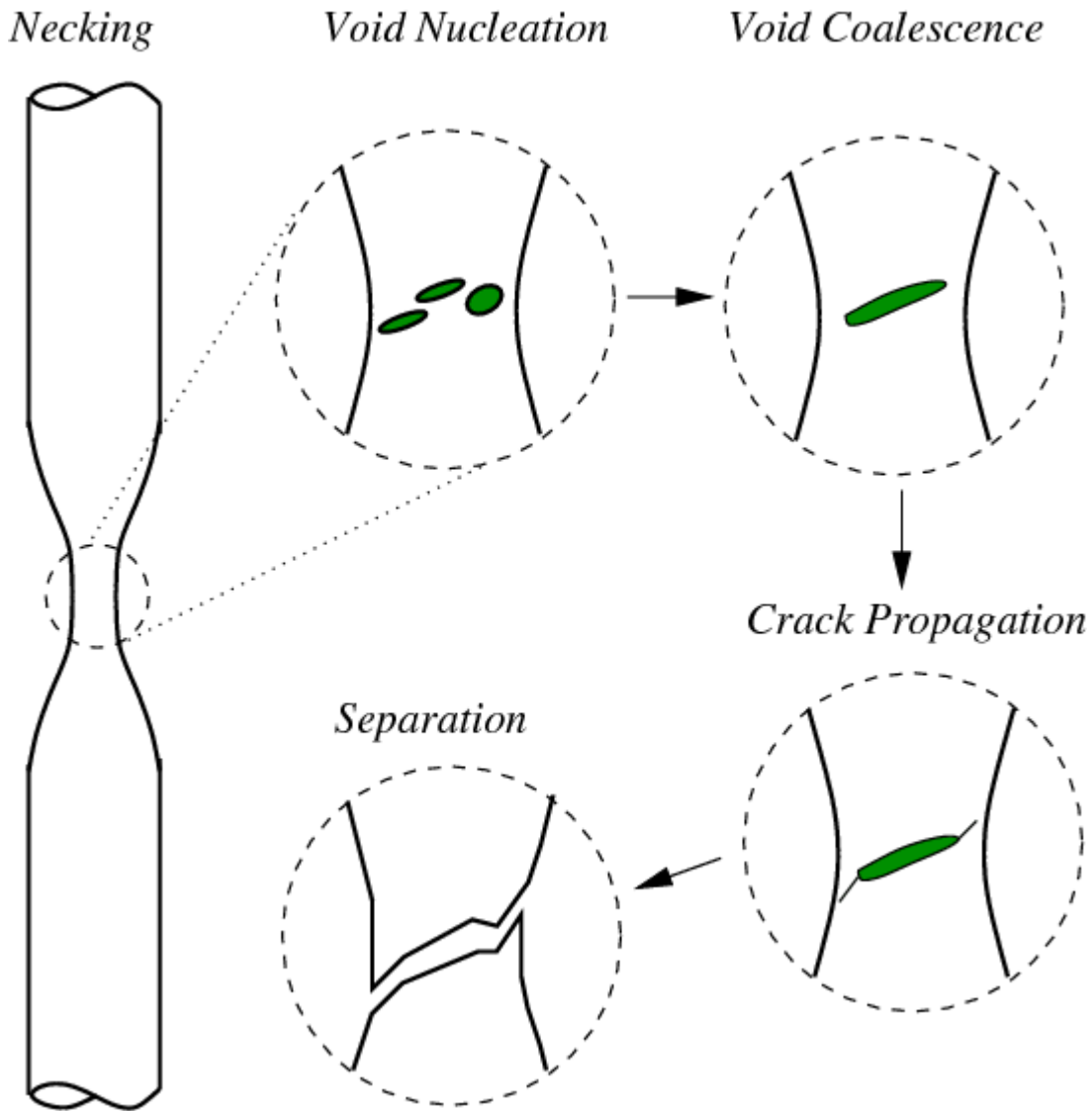
Looking closely, we can see that sharp cracks (small ρ) and large defects (large a) both lower the fracture strength of the material.

Recently, scientists have discovered supersonic fracture, the phenomenon of crack motion faster than the speed of sound in a material. This phenomenon was recently also verified by experiment of fracture in rubber-like materials.

Ductile fracture



Ductile failure of a specimen strained axially.



Schematic representation of the steps in ductile fracture (in pure tension).

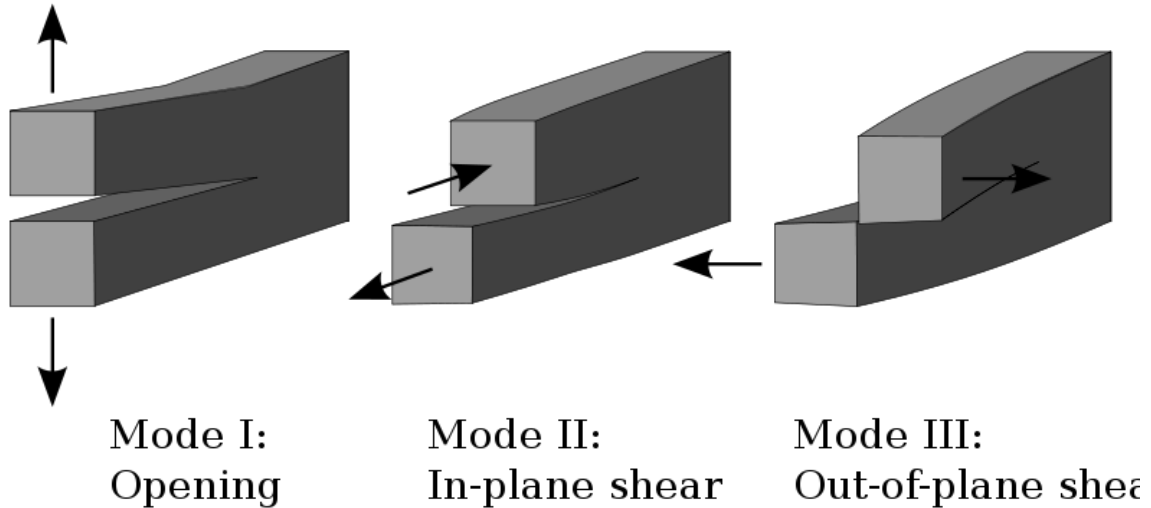
In *ductile fracture*, extensive plastic deformation takes place before fracture. The terms *rupture* or *ductile rupture* describe the ultimate failure of tough ductile materials loaded in tension. Rather than cracking, the material "pulls apart," generally leaving a rough surface. In this case there is slow propagation and an absorption of a large amount of energy before fracture.

Many ductile metals, especially materials with high purity, can sustain very large deformation of 50–100% or more strain before fracture under favorable loading conditions and environmental conditions. The strain at which the fracture happens is controlled by the purity of the materials. At room temperature, pure iron can undergo deformation up to 100% strain before breaking, while cast iron or high-carbon steels can barely sustain 3% of strain.

Because ductile rupture involves a high degree of plastic deformation, the fracture behavior of a propagating crack as modeled above changes fundamentally. Some of the energy from stress concentrations at the crack tips is dissipated by plastic deformation before the crack actually propagates.

The basic steps are: void formation, void coalescence (also known as crack formation), crack propagation, and failure, often resulting in a cup-and-cone shaped failure surface.

Crack separation modes



The three fracture modes.

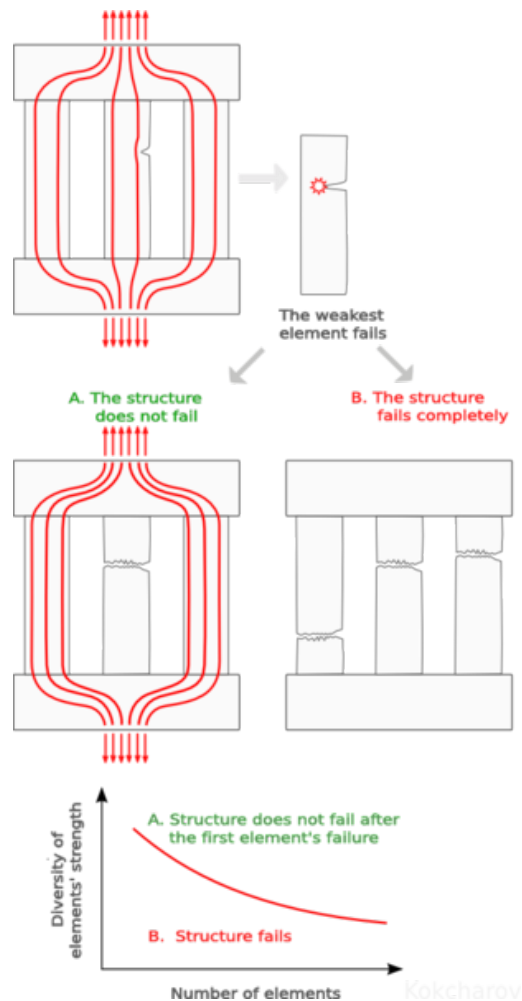
There are three ways of applying a force to enable a crack to propagate:

- **Mode I crack** – Opening mode (a tensile stress normal to the plane of the crack)
- **Mode II crack** – Sliding mode (a shear stress acting parallel to the plane of the crack and perpendicular to the crack front)
- **Mode III crack** – Tearing mode (a shear stress acting parallel to the plane of the crack and parallel to the crack front)

Chapter 7

Structural Fracture Mechanics

Structural Fracture Mechanics is the field of structural engineering concerned with the study of load-carrying structures that includes one or several failed or damaged components. It uses methods of analytical solid mechanics, structural engineering, safety engineering, probability theory, and catastrophe theory to calculate the load and stress in the structural components and analyze the safety of a damaged structure.



Model of Structural Fracture Mechanics.

There is a direct analogy between Fracture Mechanics of solid and Structural Fracture Mechanics:

Analogy between Fracture Mechanics of solid and Structural Fracture Mechanics		
	Fracture Mechanics	Structural Fracture Mechanics
Model	Solid with a crack	Multi-component structure with a failed component
Defect driving force	Stress intensity factor	Overload stress
System property	Fracture toughness	Reserve ability / Structural robustness

There are different causes of the first component failure: 1) mechanical overload, fatigue (material), unpredicted scenario, etc. 2) “human intervention” like unprofessional behavior or a terrorist attack.

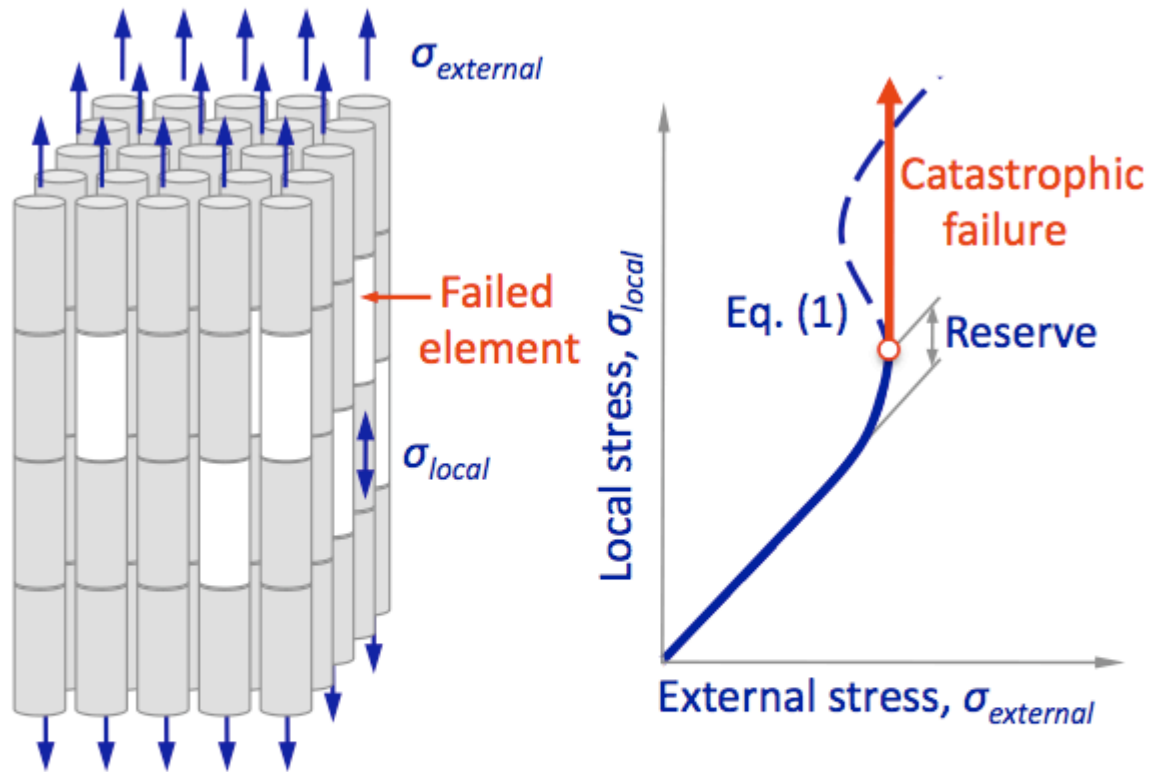
There are two typical scenarios:

- A. A localized failure does NOT cause immediate collapse of the entire structure.
- B. The entire structure fails immediately after one of its components fails.

If the structure does not collapse immediately there is a limited period of time until the catastrophic structural failure of the entire structure. There is a critical number of structural elements that defines whether the system has reserve ability or not.

Safety engineers use the failure of the first component as an indicator and try to intervene during the given period of time to avoid the catastrophe of the entire structure. For example, “Leak-Before-Break” methodology means that a leak will be discovered prior to a catastrophic failure of the entire piping system occurring in service. It has been applied to pressure vessels, nuclear piping, gas and oil pipelines, etc.

The methods of Structural Fracture Mechanics are used as checking calculations to estimate sensitivity of a structure to its component failure.



$$\sigma_{external} = \frac{\sigma_{local}}{1 + q [1 - e^{-(\sigma_{local} - 1)^b}]} \quad (1)$$

$q, b = \text{model's parameters}$

Catastrophe failure model and reserve ability of a complex system.

The failure of a complex system with parallel redundancy can be estimated based on probabilistic properties of the system elements. The model supposes that failure of several elements causes neighboring elements overloading. The model equation (1) shows the relationship between local and external stresses. The equation (1) is similar to the cusp catastrophe behavior. The theory predicts reserve ability of the complex system and the critical external stress.

Chapter 8

Peridynamics



A ductile fracture of an Al-Mg-Si alloy. A fracture is a mathematical singularity to which the classical equations of continuum mechanics cannot be applied directly - **Peridynamics** offers a numerical method.

Peridynamics is a formulation of continuum mechanics that is oriented toward deformations with discontinuities, especially fractures.

Purpose of peridynamics

The peridynamic theory is based on integral equations, in contrast with the classical theory of continuum mechanics, which is based on partial differential equations. Since partial derivatives do not exist on crack surfaces and other singularities, the classical equations of continuum mechanics cannot be applied directly when such features are present in a deformation. The integral equations of the peridynamic theory can be applied directly, because they do not require partial derivatives.

The ability to apply the same equations directly at all points in a mathematical model of a deforming structure helps the peridynamic approach avoid the need for the special techniques of fracture mechanics. For example, in peridynamics, there is no need for a separate crack growth law based on a stress intensity factor.

Definition and basic terminology

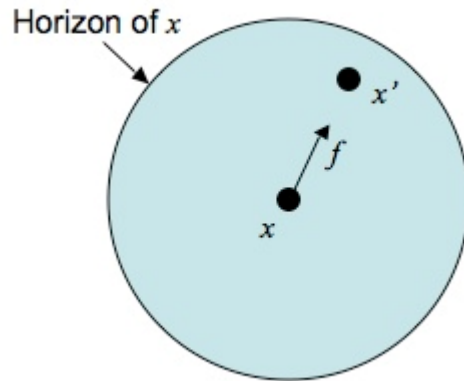
The basic equation of peridynamics is the following equation of motion:

$$\rho(x)\ddot{u}(x,t) = \int_R f(u(x',t) - u(x,t), x' - x, x) dV_{x'} + b(x,t)$$

where x is a point in a body R , t is time, u is the displacement vector field, and ρ is the mass density in the undeformed body. x' is a dummy variable of integration.

The vector valued function f is the force density that x' exerts on x . This force density depends on the relative displacement and relative position vectors between x' and x . The dimensions of f are force per volume squared. The function f is called the "pairwise force function" and contains all the constitutive (material-dependent) properties. It describes how the internal forces depend on the deformation.

The interaction between any x and x' is called a "bond." The physical mechanism in this interaction need not be specified. It is usually assumed that f vanishes whenever x' is outside a neighborhood of x (in the undeformed configuration) called the *horizon*.



The term "peridynamic," an adjective, was proposed in the year 2000 and comes from the prefix *peri*, which means *all around, near, or surrounding*; and the root *dyna*, which means *force or power*. The term "peridynamics," a noun, is a shortened form of the phrase *peridynamic model of solid mechanics*.

Pairwise force functions

Using the abbreviated notation $u = u(x,t)$ and $u' = u(x',t)$ Newton's third law places the following restriction on f :

$$f(u - u', x - x', x') = -f(u' - u, x' - x, x)$$

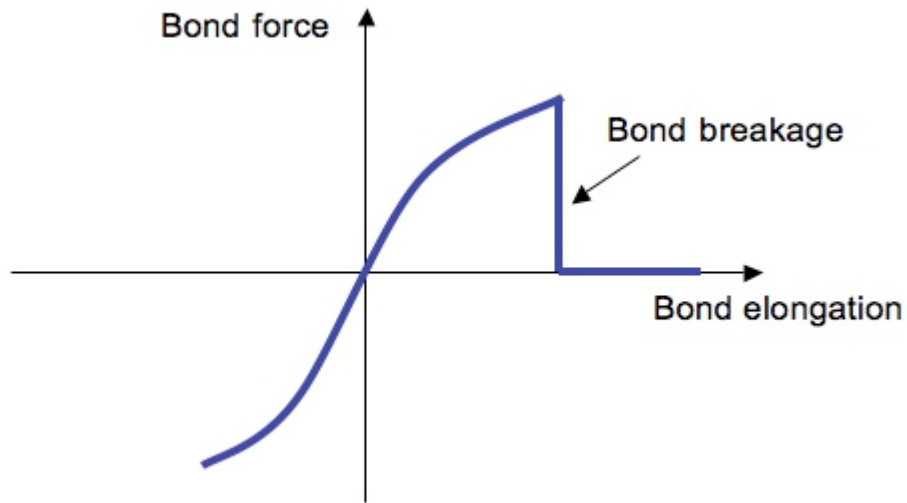
for any x, x', u, u' . This equation states that the force density vector that x exerts on x' equals minus the force density vector that x' exerts on x . Balance of angular momentum requires that f be parallel to the vector connecting the deformed position of x to the deformed position of x' :

$$((x' + u') - (x + u)) \times f(u' - u, x' - x, x) = 0.$$

A pairwise force function is specified by a graph of $|f|$ versus bond elongation e , defined by

$$e = |(x' + u') - (x + u)| - |x' - x|.$$

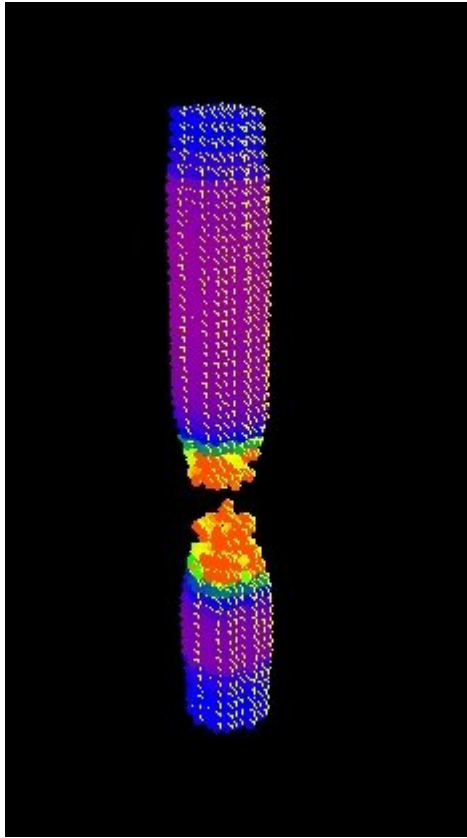
A schematic of a pairwise force function for the bond connecting two typical points is shown in the following figure:



Damage

Damage is incorporated in the pairwise force function by allowing bonds to break when their elongation exceeds some prescribed value. After a bond breaks, it no longer sustains any force, and the endpoints are effectively disconnected from each other. When a bond breaks, the force it was carrying is redistributed to other bonds that have not yet broken. This increased load makes it more likely that these other bonds will break. The process of bond breakage and load redistribution, leading to further breakage, is how cracks grow in the peridynamic model.

Peridynamic states



Computer model of the necking of an aluminum rod under tension. Colors indicate temperature increase due to plastic heating. Calculation performed with the Emu computer code using peridynamic states.

The theory described above assumes that each peridynamic bond responds independently of all the others. This is an oversimplification for most materials and leads to restrictions on the types of materials that can be modeled. In particular, this assumption implies that any isotropic linear elastic solid is restricted to a Poisson ratio of 1/4.

To address this lack of generality, the idea of "peridynamic states" was introduced. This allows the force density in each bond to depend on the stretches in all the bonds connected to its endpoints, in addition to its own stretch. For example, the force in a bond could depend on the net volume changes at the endpoints. The effect of this volume change, relative to the effect of the bond stretch, determines the Poisson ratio. With peridynamic states, any material that can be modeled within the standard theory of continuum mechanics can be modeled as a peridynamic material, while retaining the advantages of the peridynamic theory for fracture.

Chapter 9

Strength of Materials

In materials science, the **strength** of a material is its ability to withstand an applied stress without failure. The applied stress may be tensile, compressive, or shear. Strength of materials is a subject which deals with loads, deformations and the forces acting on the material. A load applied to a mechanical member will induce internal forces within the member called stresses. Those stresses acting on the material cause deformations of the material. Deformation of the material is called **strain**, while the intensity of the internal forces are called **stress**. The strength of any material relies on three different type of analytical method: strength, stiffness and stability, where strength refers to the load carrying capacity, stiffness refers to the deformation or elongation, and stability means refers to the ability to maintain its initial configuration. Material yield strength refers to the point on the engineering stress-strain curve (as opposed to true stress-strain curve) beyond which the material experiences deformations that will not be completely reversed upon removal of the loading. The ultimate strength refers to the point on the engineering stress-strain curve corresponding to the stress that produces fracture.

A material's strength is dependent on its microstructure. The engineering processes to which a material is subjected can alter this microstructure. The variety of strengthening mechanisms that alter the strength of a material includes work hardening, solid solution strengthening, precipitation hardening and grain boundary strengthening and can be quantified and qualitatively explained. However, strengthening mechanisms are accompanied by the caveat that some mechanical properties of the material may degenerate in an attempt to make the material stronger. For example, in grain boundary strengthening, although yield strength is maximized with decreasing grain size, ultimately, very small grain sizes make the material brittle. In general, the yield strength of a material is an adequate indicator of the material's mechanical strength. Considered in tandem with the fact that the yield strength is the parameter that predicts plastic deformation in the material, one can make informed decisions on how to increase the strength of a material depending its microstructural properties and the desired end effect. Strength is considered in terms of compressive strength, tensile strength, and shear strength, namely the limit states of compressive stress, tensile stress and shear stress, respectively. The effects of dynamic loading are probably the most important practical

part of the strength of materials, especially the problem of fatigue. Repeated loading often initiates brittle cracks, which grow slowly until failure occurs.

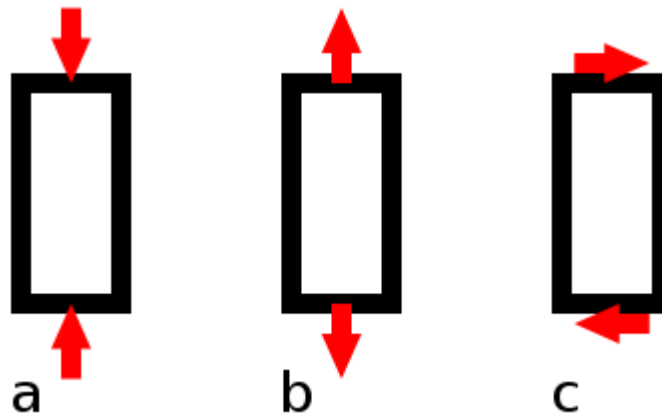
However, the term **strength of materials** most often refers to various methods of calculating stresses in structural members, such as beams, columns and shafts. The methods that can be employed to predict the response of a structure under loading and its susceptibility to various failure modes may take into account various properties of the materials other than material (yield or ultimate) strength. For example failure in buckling is dependent on material stiffness (Young's Modulus).

Types of loadings

- Transverse loading - Forces applied perpendicular to the longitudinal axis of a member. Transverse loading causes the member to bend and deflect from its original position, with internal tensile and compressive strains accompanying change in curvature. Transverse loading also induces shear forces that cause shear deformation of the material and increase the transverse deflection of the member.
- Axial loading - The applied forces are collinear with the longitudinal axes of the member. The forces cause the member to either stretch or shorten.
- Torsional loading - Twisting action caused by a pair of externally applied equal and oppositely directed couples acting on parallel planes or by a single external couple applied to a member that has one end fixed against rotation.

Definitions

Stress terms



A material being loaded in a) compression, b) tension, c) shear.

Uniaxial stress is expressed by

$$\sigma = \frac{F}{A},$$

where F is the force [N] acting on an area A [m²]. The area can be the undeformed area or the deformed area, depending on whether engineering stress or true stress is of interest.

- *Compressive stress* (or compression) is the stress state caused by an applied load that acts to reduce the length of the material (compression member) in the axis of the applied load, in other words the stress state caused by squeezing the material. A simple case of compression is the uniaxial compression induced by the action of opposite, pushing forces. Compressive strength for materials is generally higher than their tensile strength. However, structures loaded in compression are subject to additional failure modes dependent on geometry, such as Euler buckling.
- *Tensile stress* is the stress state caused by an applied load that tends to elongate the material in the axis of the applied load, in other words the stress caused by *pulling* the material. The strength of structures of equal cross sectional area loaded in tension is independent of shape of the cross section. Materials loaded in tension are susceptible to stress concentrations such as material defects or abrupt changes in geometry. However, materials exhibiting ductile behavior (most metals for example) can tolerate some defects while brittle materials (such as ceramics) can fail well below their ultimate material strength. For example; the stress of metal is 70Pa.
- *Shear stress* is the stress state caused by a pair of opposing forces acting along parallel lines of action through the material, in other words the stress caused by faces of the material *sliding* relative to one another. An example is cutting paper with scissors or stresses due to torsional loading.

Strength terms

- *Yield strength* is the lowest stress that produces a permanent deformation in a material. In some materials, like aluminium alloys, the point of yielding is hard to define, thus it is usually given as the stress required to cause 0.2% plastic strain. This is called a 0.2% proof stress.
- *Compressive strength* is a limit state of compressive stress that leads to failure in the manner of ductile failure (infinite theoretical yield) or in the manner of brittle failure (rupture as the result of crack propagation, or sliding along a weak plane).
- *Tensile strength* or *ultimate tensile strength* is a limit state of tensile stress that leads to tensile failure in the manner of ductile failure (yield as the first stage of failure, some hardening in the second stage and breakage after a possible "neck" formation) or in the manner of brittle failure (sudden breaking in two or more pieces with a low stress state). Tensile strength can be quoted as either true stress or engineering stress.

- *Fatigue strength* is a measure of the strength of a material or a component under cyclic loading, and is usually more difficult to assess than the static strength measures. Fatigue strength is given as stress amplitude or stress range ($\Delta\sigma = \sigma_{\max} - \sigma_{\min}$), usually at zero mean stress, along with the number of cycles to failure.
- *Impact strength*, is the capability of the material to withstand a suddenly applied load and is expressed in terms of energy. Often measured with the Izod impact strength test or Charpy impact test, both of which measure the impact energy required to fracture a sample. Volume, modulus of elasticity, distribution of forces, and yield strength effect the impact strength of a material. In order for a material or object to have a higher impact strength the stresses must be distributed evenly throughout the object. It also must have a large volume with a low modulus of elasticity and a high material yield strength.

Strain (deformation) terms

- *Deformation* of the material is the change in geometry when stress is applied (in the form of force loading, gravitational field, acceleration, thermal expansion, etc.). Deformation is expressed by the displacement field of the material.
- *Strain* or *reduced deformation* is a mathematical term to express the trend of the deformation change among the material field. Strain is the deformation per unit length. For uniaxial loading - displacements of a specimen (for example a bar element) it is expressed as the quotient of the displacement and the length of the specimen. For 3D displacement fields it is expressed as derivatives of displacement functions in terms of a second order tensor (with 6 independent elements).
- *Deflection* is a term to describe the magnitude to which a structural element bends under a load.

Stress-strain relations

- *Elasticity* is the ability of a material to return to its previous shape after stress is released. In many materials, the relation between applied stress and the resulting strain is directly proportional (up to a certain limit), and a graph representing those two quantities is a straight line.

The slope of this line is known as Young's Modulus, or the "Modulus of Elasticity." The Modulus of Elasticity can be used to determine stress-strain relationships in the linear-elastic portion of the stress-strain curve. The linear-elastic region is either below the yield point, or if a yield point is not well defined for the material, taken to be between 0 and 0.2% strain, and is defined as the region of strain in which no yielding (permanent deformation) occurs.

- *Plasticity* or plastic deformation is the opposite of elastic deformation and is accepted as unrecoverable strain. Plastic deformation is retained even after the relaxation of the applied stress. Most materials in the linear-elastic category are

usually capable of plastic deformation. Brittle materials, like ceramics, do not experience any plastic deformation and will fracture under relatively low stress. Materials such as metals usually experience a small amount of plastic deformation before failure while ductile metals such as copper and lead or polymers will plasticly deform much more.

Consider the difference between a carrot and chewed bubble gum. The carrot will stretch very little before breaking, but nevertheless will still stretch. The chewed bubble gum, on the other hand, will plastically deform enormously before finally breaking.

Design terms

Ultimate strength is an attribute directly related to a material, rather than just specific specimen of the material, and as such is quoted force per unit of cross section area (N/m^2). The ultimate strength is the maximum stress that a material can withstand before it breaks or weakens. For example, the ultimate tensile strength (UTS) of AISI 1018 Steel is $440 \text{ MN}/\text{m}^2$. In general, the SI unit of stress is the pascal, where $1 \text{ Pa} = 1 \text{ N}/\text{m}^2$. In Imperial units, the unit of stress is given as lbf/in^2 or pounds-force per square inch. This unit is often abbreviated as **psi**. One thousand psi is abbreviated **ksi**.

A Factor of safety is a design criteria that an engineered component or structure must achieve. $FS = UTS / R$, where FS: the factor of safety, R: The applied stress, and UTS: ultimate stress (psi or N/m^2)

Margin of Safety is also sometimes used to as design criteria. It is defined $MS = \text{Factor of safety} - 1$

For example to achieve a factor of safety of 4, the allowable stress in an AISI 1018 steel component can be calculated to be $R = UTS / FS = 440/4 = 110 \text{ MPa}$, or $R = 110 \times 10^6 \text{ N}/\text{m}^2$. Such allowable stresses are also known as "design stresses" or "working stresses."

Design stresses that have been determined from the ultimate or yield point values of the materials give safe and reliable results only for static loading. Many machine parts fail when subjected to a non steady and continuously varying loadings that develop stresses that are below the yield point. Such failures are called fatigue failure. The failure is by a fracture that appears to be brittle with little or no visible evidence of yielding. However, when the stress is kept below "fatigue stress" or "endurance limit stress", the part will endure indefinitely. A purely reversing or cyclic stress means when the stress alternates between equal positive and negative peak stresses during each cycle of operation. In purely cyclic stress, the average stress is zero. When a part is subjected to a cyclic stress, also known as stress range (S_r), it has been observed that the failure of the part occurs after a number of stress reversals (N) even if the magnitude of the stress range is below the material's yield strength. Generally, higher the range stress, lesser number of reversals is needed for failure.

Failure theories

We are interested in learning how static mechanical stress can cause failure in machine parts. Static stress means that the stress has been applied slowly and is maintained at a steady level. Failure from cyclic (or dynamic) stress and impact stress will be treated later. There are many other factors such as, surface wear damage from friction, overheating, chemical corrosion, metallurgical fault or a combination of these and others that may also cause failure. There are four important failure theories, namely (1) maximum shear stress theory, (2) maximum normal stress theory, (3) maximum strain energy theory, and (4) maximum distortion energy theory. Out of these four theories of failure, the maximum normal stress theory is only applicable for brittle materials, and the remaining three theories are applicable for ductile materials.

- Maximum Shear stress Theory- This theory postulates that failure will occur in a machine part if the magnitude of the maximum shear stress (τ_{max}) in the part exceeds the shear strength (τ_{yp}) of the material determined from uniaxial testing.

This theory postulates, that failure will occur when, $\tau_{max} = \tau_{yp}$ or \max of $[|S1-S2|/2, |S2-S3|/2, \text{ and } |S3-S1|/2] = \tau_{yp}/2$ Dividing both side by 2, \max of $[|S1-S2|, |S2-S3|, \text{ and } |S3-S1|] = S_{yp}$ Using a design factor of safety N_{fs} , the theory formulates the design equation as, \max of $[|S1-S2|, |S2-S3|, \text{ and } |S3-S1|]$ should be less than or equal to S_{yp}/N_{fs}

- Maximum normal stress theory- this theory postulates, that failure will occur in machine part if the maximum normal stress in the part exceeds the ultimate tensile stress of the material as determined from uniaxial testing. This theory deals with brittle materials only. The maximum tensile stress should be less than or equal to ultimate tensile stress divided by factor of safety. The magnitude of the maximum compressive stress should be less than ultimate compressive stress divided by factor of safety.

As the three principal stresses at a point in the part $S1, S2, \text{ or } S3$ may be both tensile and compressive stresses, when this theory is applied, we need to check for failures both from tension and compression. The method of application of this theory is to find the maximum tensile stress, and the maximum compressive stress from the given values of $S1, S2, \text{ and } S3$. The largest positive value among $S1, S2, \text{ and } S3$ is the maximum tensile stress and the smallest negative value is the maximum compressive stress. For example if $S1 = 80 \text{ MPa}$, $S2 = -100 \text{ MPa}$, and $S3 = -150 \text{ MPa}$, then the maximum tensile stress = 80 MPa , and the maximum compressive stress = -150 MPa (smallest negative value!). Thus according to this theory, the safe design condition for brittle material can be given by: The maximum tensile stress should be less than or equal to S_{ut}/N_{fs} and The magnitude of the maximum compressive stress should less than S_{uc}/N_{fs}

- Maximum strain energy theory-this theory postulates that failure will occur when the strain energy per unit volume due to the applied stresses in a part equals the strain energy per unit volume at the yield point in uniaxial testing.

Strain energy is the energy stored in a material due elastic deformation, which is, work done during elastic deformation. Work done per unit volume = strain x average stress. During tensile test, stress increases from zero to S_{yp} , that is average stress = $S_{yp}/2$. Elastic strain at yield point = S_{yp}/E , where E is the elastic modulus of elasticity. Strain energy per unit volume during uniaxial tension = average stress x strain = $S_{yp}^2/2E$

- Maximum distortion energy theory- this theory is also known as shear energy theory or von Mises-Hencky theory. This theory postulates that failure will occur when the distortion energy per unit volume due to the applied stresses in a part equals the distortion energy per unit volume at the yield point in uniaxial testing. The total elastic energy due to strain can be divided into two parts. One part causes change in volume, and the other part causes change in shape. Distortion energy is the amount of energy that is needed to change the shape.

Application of failure theory

Out of the four theories, only the maximum normal stress theory predicts failure for brittle materials. The rest of the three theories are applicable for ductile materials. Out of these three, the distortion energy theory provides most accurate results in majority of the stress conditions. The strain energy theory needs the value of Poisson's ratio of the part material, which is often not readily available. The maximum shear stress theory is conservative. For simple unidirectional normal stresses all theories are equivalent, which means all theories will give the same result.

Chapter 10

Stress (Mechanics)

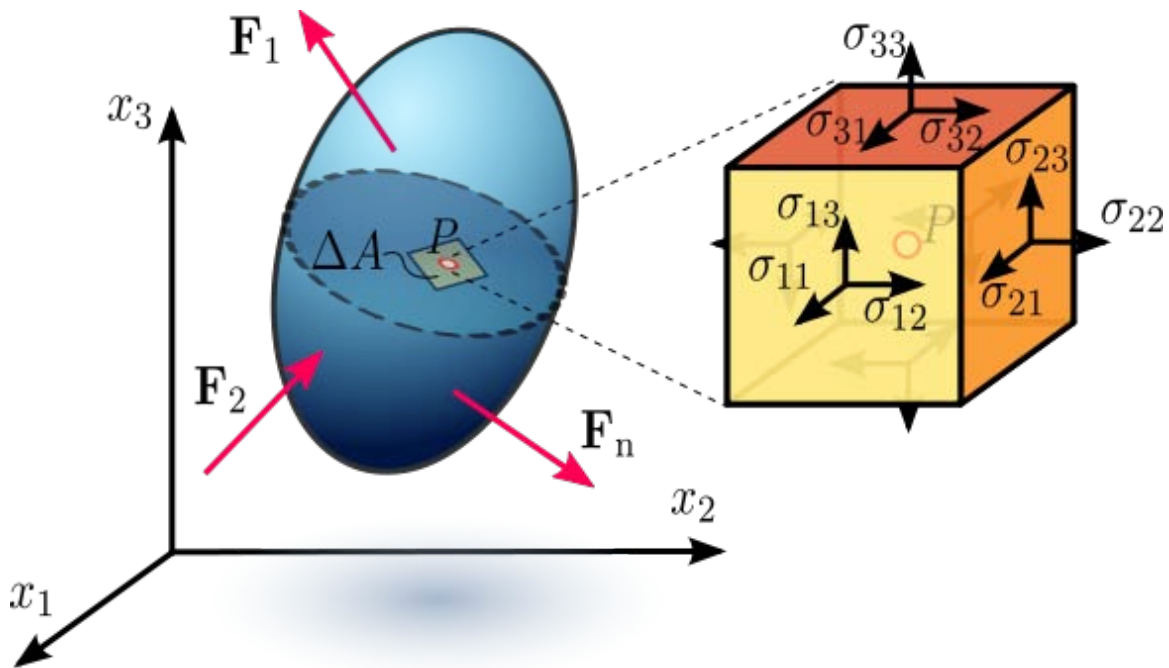


Figure 1.1 Stress in a loaded deformable material body assumed as a continuum.

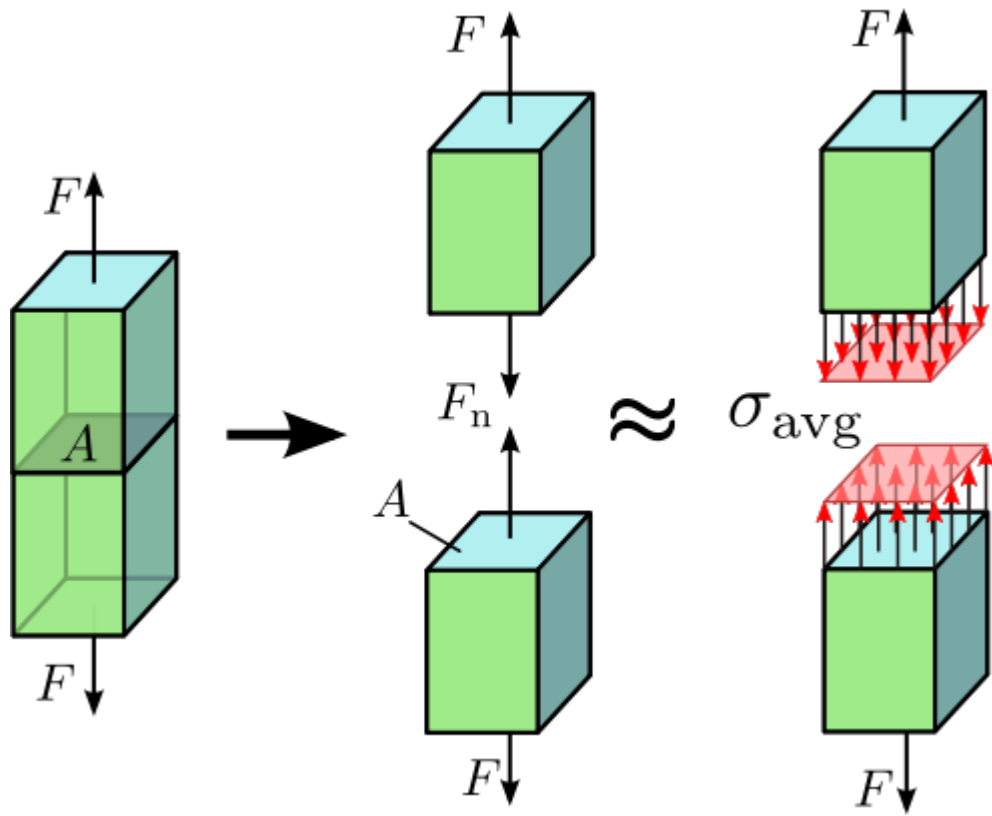


Figure 1.2 Axial stress in a prismatic bar axially loaded

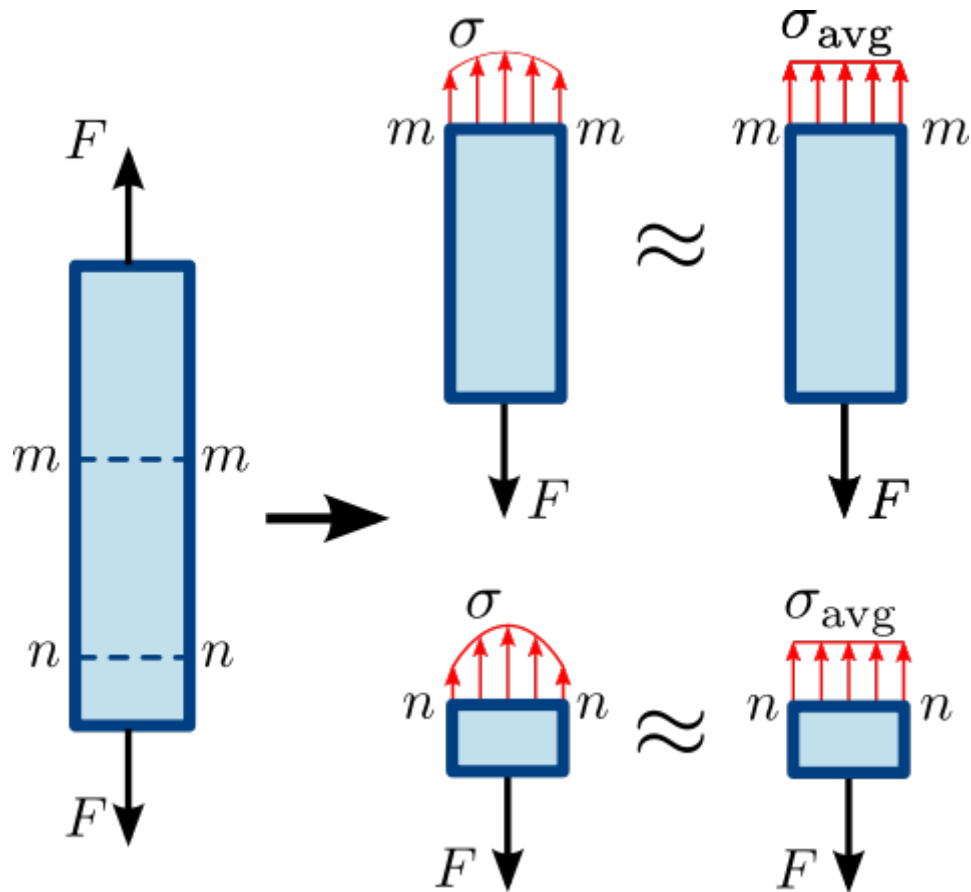


Figure 1.3 Normal stress in a prismatic (straight member of uniform cross-sectional area) bar. The stress or force distribution in the cross section of the bar is not necessarily uniform. However, an average normal stress σ_{avg} can be used

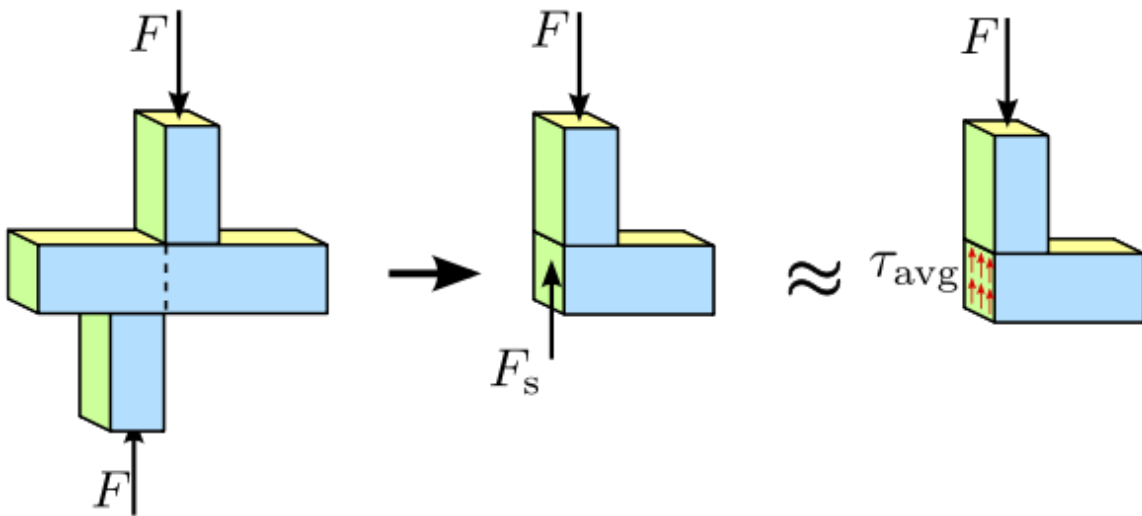


Figure 1.4 Shear stress in a prismatic bar. The stress or force distribution in the cross section of the bar is not necessarily uniform. Nevertheless, an average shear stress τ_{avg} is a reasonable approximation.

In continuum mechanics, **stress** is a measure of the internal forces acting within a deformable body. Quantitatively, it is a measure of the average force per unit area of a surface within the body on which internal forces act. These internal forces are produced between the particles in the body as a reaction to external forces applied on the body. Because the loaded deformable body is assumed to behave as a continuum, these internal forces are distributed continuously within the volume of the material body, and result in deformation of the body's shape. Beyond certain limits of material strength, this can lead to a permanent change of shape or physical failure.

However, treating physical force as a "one dimensional entity", as it is often done in mechanics, creates a few problems. Any model of continuum mechanics which explicitly expresses force as a variable generally fails to merge and describe deformation of matter and solid bodies, because the attributes of matter and solids are three dimensional. Classical models of continuum mechanics assume an average force and fail to properly incorporate "geometrical factors", which are important to describe stress distribution and accumulation of energy during the continuum.

The dimension of stress is that of pressure, and therefore the SI unit for stress is the pascal (symbol Pa), which is equivalent to one newton (force) per square meter (unit area), that is N/m^2 . In Imperial units, stress is measured in pound-force per square inch, which is abbreviated as psi.

Introduction

Stress is a measure of the average force per unit area of a surface within a deformable body on which internal forces act. It is a measure of the intensity of the internal forces acting between particles of a deformable body across imaginary internal surfaces. These internal forces are produced between the particles in the body as a reaction to external forces applied on the body. External forces are either surface forces or body forces. Because the loaded deformable body is assumed to behave as a continuum, these internal forces are distributed continuously within the volume of the material body, *i.e.* the stress distribution in the body is expressed as a piecewise continuous function of space coordinates and time.

Normal , shear stresses and virial stresses

For the simple case of a body axially loaded, e.g., a prismatic bar subjected to tension or compression by a force passing through its centroid (Figures 1.2 and 1.3) the stress σ , or intensity of internal forces, can be obtained by dividing the total *normal force* F_n , determined from the equilibrium of forces, by the cross-sectional area A of the prism it is acting upon. The normal force can be a *tensile force* if acting outward from the plane, or *compressive force* if acting inward to the plane. In the case of a prismatic bar axially loaded, the stress σ is represented by a scalar called *engineering stress* or *nominal stress* that represents an average stress (σ_{avg}) over the area, meaning that the stress in the cross section is uniformly distributed. Thus, we have

$$\sigma_{\text{avg}} = \frac{F_n}{A} \approx \sigma$$

A different type of stress is obtained when transverse forces F are applied to the prismatic bar as shown in Figure 1.4. Considering the same cross-section as before, from static equilibrium the internal force has a magnitude equal to F_s and in opposite direction parallel to the cross-section. F_s is called the *shear force*. Dividing the shear force F_s by the area A of the cross section we obtain the *shear stress*. In this case the shear stress τ is a scalar quantity representing an average shear stress (τ_{avg}) in the section, *i.e.* the stress in the cross-section is uniformly distributed. In materials science and in engineering aspects the average of the "scalar" shear force (τ_{avg}) are true for crystallized materials during brittle fracture and operates through the fractured cross-section or stress plane.

$$\tau_{\text{avg}} = \frac{F_s}{A} \approx \tau$$

In Figure 1.3, the normal stress is observed in two planes $m - m$ and $n - n$ of the axially loaded prismatic bar. The stress on plane $n - n$, which is closer to the point of application of the load F , varies more across the cross-section than that of plane $m - m$. However, if the cross-sectional area of the bar is very small, *i.e.* the bar is slender, the variation of stress across the area is small and the normal stress can be approximated by σ_{avg} . On the other hand, the variation of shear stress across the section of a prismatic bar cannot be assumed to be uniform.

Virial stress is a measure of stress on an atomic scale. It is given by

$$\tau_{ij} = \frac{1}{\Omega} \sum_{k \in \Omega} \left(-m^{(k)} (u_i^{(k)} - \bar{u}_i) (u_j^{(k)} - \bar{u}_j) + \frac{1}{2} \sum_{\ell \in \Omega} (x_i^{(\ell)} - x_i^{(k)}) f_j^{(k\ell)} \right)$$

where

- k and ℓ are atoms in the domain,
- Ω is the volume of the domain,
- $m^{(k)}$ is the mass of atom k ,
- $u_i^{(k)}$ is the i^{th} component of the velocity of atom k ,
- \bar{u}_j is the j^{th} component of the average velocity of atoms in the volume,
- $x_i^{(k)}$ is the i^{th} component of the position of atom k , and
- $f_i^{(k\ell)}$ is the i^{th} component of the force between atom k and ℓ .

At zero kelvin, all velocities are zero so we have

$$\tau_{ij} = \frac{1}{2\Omega} \sum_{k,\ell \in \Omega} (x_i^{(\ell)} - x_i^{(k)}) f_j^{(k\ell)}$$

This can be thought of as follows. The τ_{11} component of stress is the force in the 1 direction divided by the area of a plane perpendicular to that direction. Consider two adjacent volumes separated by such a plane. The 11-component of stress on that interface is the sum of all pairwise forces between atoms on the two sides....

Stress modeling (Cauchy)

In general, stress is not uniformly distributed over the cross-section of a material body, and consequently the stress at a point in a given region is different from the average stress over the entire area. Therefore, it is necessary to define the stress not over a given area but at a specific point in the body (Figure 1.1). According to Cauchy, the *stress at any point* in an object, assumed to behave as a continuum, is completely defined by the nine components σ_{ij} of a second-order tensor of type (0,2) known as the Cauchy stress tensor, $\boldsymbol{\sigma}$:

$$\boldsymbol{\sigma} = \begin{bmatrix} \sigma_{11} & \sigma_{12} & \sigma_{13} \\ \sigma_{21} & \sigma_{22} & \sigma_{23} \\ \sigma_{31} & \sigma_{32} & \sigma_{33} \end{bmatrix} \equiv \begin{bmatrix} \sigma_{xx} & \sigma_{xy} & \sigma_{xz} \\ \sigma_{yx} & \sigma_{yy} & \sigma_{yz} \\ \sigma_{zx} & \sigma_{zy} & \sigma_{zz} \end{bmatrix} \equiv \begin{bmatrix} \sigma_x & \tau_{xy} & \tau_{xz} \\ \tau_{yx} & \sigma_y & \tau_{yz} \\ \tau_{zx} & \tau_{zy} & \sigma_z \end{bmatrix}$$

The Cauchy stress tensor obeys the tensor transformation law under a change in the system of coordinates. A graphical representation of this transformation law is the Mohr's circle of stress distribution.

The Cauchy stress tensor is used for stress analysis of material bodies experiencing small deformations where the differences in stress distribution in most cases can be neglected. For large deformations, also called finite deformations, other measures of stress, such as the first and second Piola-Kirchhoff stress tensors, the Biot stress tensor, and the Kirchhoff stress tensor, are required.

According to the principle of conservation of linear momentum, if a continuous body is in static equilibrium it can be demonstrated that the components of the Cauchy stress tensor in every material point in the body satisfy the equilibrium equations (Cauchy's equations of motion for zero acceleration). At the same time, according to the principle of conservation of angular momentum, equilibrium requires that the summation of moments with respect to an arbitrary point is zero, which leads to the conclusion that the stress tensor is symmetric, thus having only six independent stress components instead of the original nine.

There are certain invariants associated with the stress tensor, whose values do not depend upon the coordinate system chosen or the area element upon which the stress tensor operates. These are the three eigenvalues of the stress tensor, which are called the principal stresses. Solids, liquids, and gases have stress fields. Static fluids support normal stress but will flow under shear stress. Moving viscous fluids can support shear stress (dynamic pressure). Solids can support both shear and normal stress, with ductile materials failing under shear and brittle materials failing under normal stress. All materials have temperature dependent variations in stress-related properties, and non-Newtonian materials have rate-dependent variations.

Stress analysis

Stress analysis means the determination of the internal distribution of stresses in a structure. It is needed in engineering for the study and design of structures such as tunnels, dams, mechanical parts, and structural frames, under prescribed or expected loads. To determine the distribution of stress in a structure, the engineer needs to solve a boundary-value problem by specifying the boundary conditions. These are displacements and forces on the boundary of the structure.

Constitutive equations, such as Hooke's Law for linear elastic materials, describe the stress-strain relationship in these calculations.

When a structure is expected to deform elastically (and resume its original shape), a boundary-value problem based on the theory of elasticity is applied, with infinitesimal strains, under design loads.

When the applied loads permanently deform the structure, the theory of plasticity is used.

The stress analysis can be simplified when the physical dimensions and the distribution of loads allow the structure to be treated as one-dimensional or two-dimensional. For a two-dimensional analysis a plane stress or a plane strain condition can be assumed. Alternatively, experimental determination of stresses can be carried out.

Approximate computer-based solutions for boundary-value problems can be obtained through numerical methods such as the Finite Element Method, the Finite Difference Method, and the Boundary Element Method. Analytical or closed-form solutions can be obtained for simple geometries, constitutive relations, and boundary conditions.

Theoretical background

Continuum mechanics deals with deformable bodies, as opposed to rigid bodies. The stresses considered in continuum mechanics are only those produced by deformation of the body, *sc.* only relative changes in stress are considered, not the absolute values. A body is considered stress-free if the only forces present are those inter-atomic forces (ionic, metallic, and van der Waals forces) required to hold the body together and to keep its shape in the absence of all external influences, including gravitational attraction.

Stresses generated during manufacture of the body to a specific configuration are also excluded.

Following the classical dynamics of Newton and Euler, the motion of a material body is produced by the action of externally applied forces which are assumed to be of two kinds: surface forces and body forces.

Surface forces, or contact forces, can act either on the bounding surface of the body, as a result of mechanical contact with other bodies, or on imaginary internal surfaces that bound portions of the body, as a result of the mechanical interaction between the parts of the body to either side of the surface (Euler-Cauchy's stress principle). When a body is acted upon by external contact forces, internal contact forces are then transmitted from point to point inside the body to balance their action, according to Newton's second law of motion of conservation of linear momentum and angular momentum (for continuous bodies these laws are called the Euler's equations of motion). The internal contact forces are related to the body's deformation through constitutive equations.

The concept of stress can then be thought as a measure of the intensity of the internal contact forces acting between particles of the body across imaginary internal surfaces. In other words, stress is a measure of the average quantity of force exerted per unit area of the surface on which these internal forces act. The intensity of contact forces is related, specifically in an inverse proportion, to the area of contact. For example, if a force applied to a small area is compared to a distributed load of the same resultant magnitude applied to a larger area, one finds that the effects or intensities of these two forces are locally different because the stresses are not the same.

Body forces are forces originating from sources outside of the body that act on the volume (or mass) of the body. Saying that body forces are due to outside sources implies that the *internal forces* are manifested through the contact forces alone. These forces arise from the presence of the body in force fields, (e.g., a gravitational field). As the mass of a continuous body is assumed to be continuously distributed, any force originating from the mass is also continuously distributed. Thus, body forces are assumed to be continuous over the entire volume of the body.

The density of internal forces at every point in a deformable body are not necessarily equal, *i.e.* there is a distribution of stresses throughout the body. This variation of internal forces throughout the body is governed by Newton's second law of motion of conservation of linear momentum and angular momentum, which normally are applied to a mass particle but are extended in continuum mechanics to a body of continuously distributed mass. For continuous bodies these laws are called Euler's equations of motion. If a body is represented as an assemblage of discrete particles, each governed by Newton's laws of motion, then Euler's equations can be derived from Newton's laws. Euler's equations can, however, be taken as axioms describing the laws of motion for extended bodies, independently of any particle structure.

Euler–Cauchy stress principle

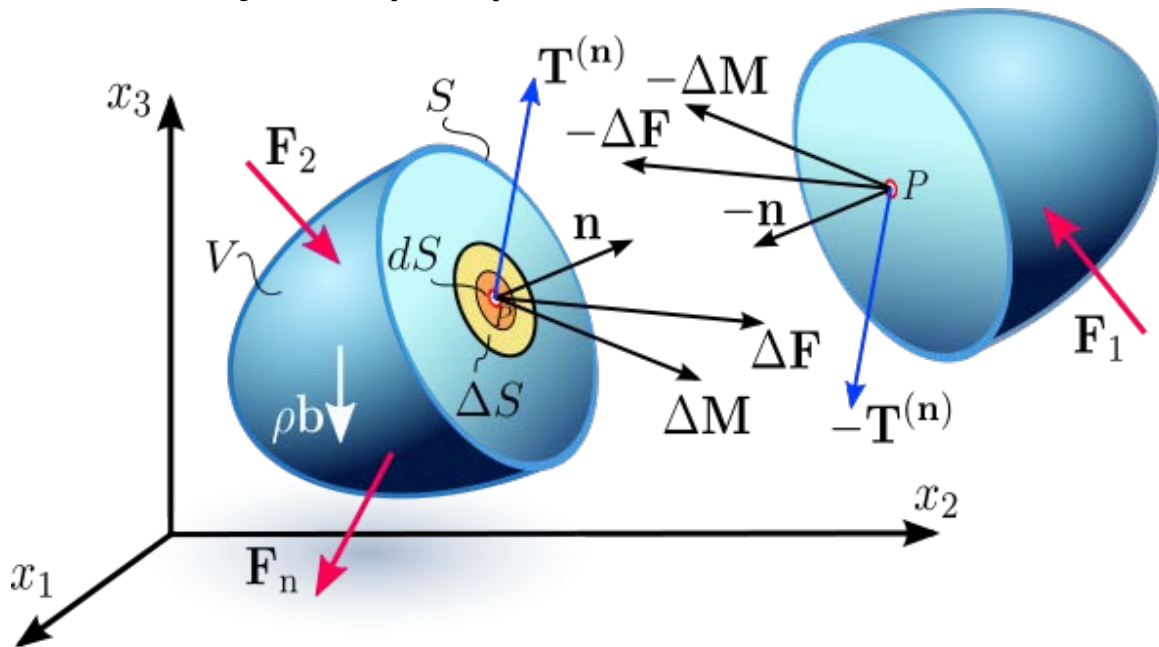


Figure 2.1a Internal distribution of contact forces and couple stresses on a differential dS of the internal surface S in a continuum, as a result of the interaction between the two portions of the continuum separated by the surface

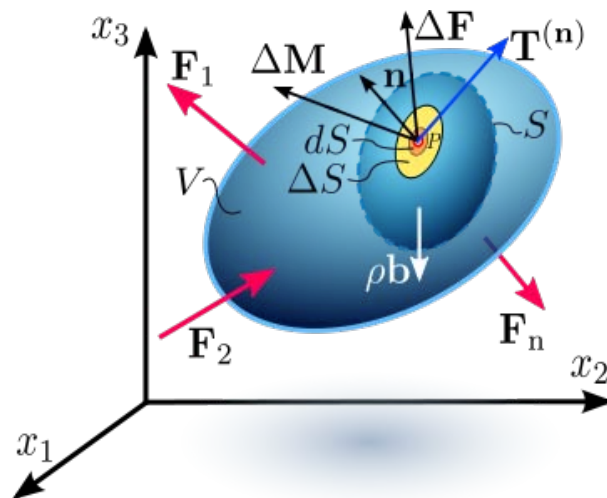


Figure 2.1b Internal distribution of contact forces and couple stresses on a differential dS of the internal surface S in a continuum, as a result of the interaction between the two portions of the continuum separated by the surface

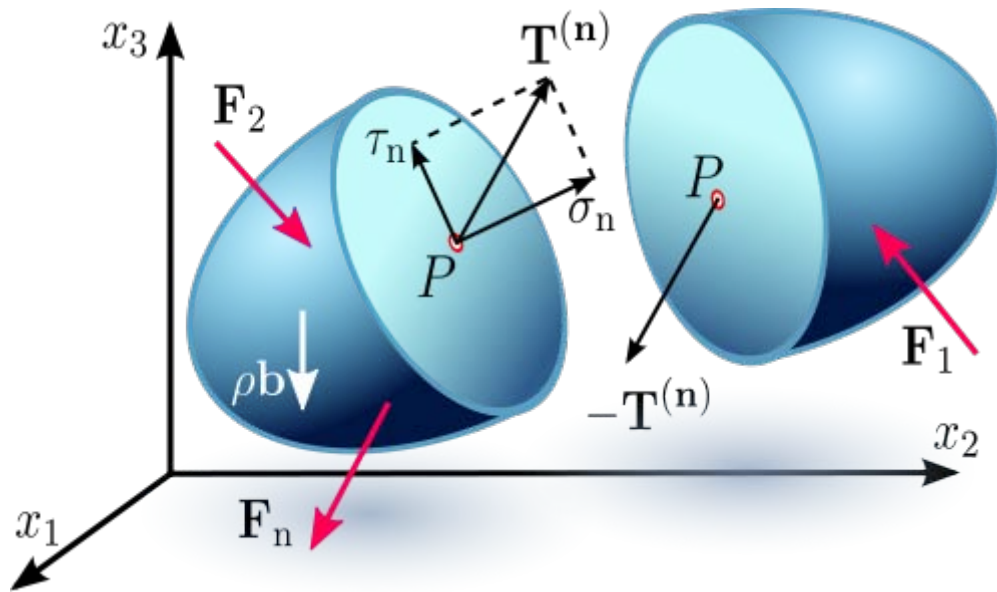


Figure 2.1c Stress vector on an internal surface S with normal vector \mathbf{n} . Depending on the orientation of the plane under consideration, the stress vector may not necessarily be perpendicular to that plane, *i.e.* parallel to \mathbf{n} , and can be resolved into two components: one component normal to the plane, called *normal stress* σ_n , and another component parallel to this plane, called the *shearing stress* τ .

The Euler–Cauchy stress principle states that *upon any surface (real or imaginary) that divides the body, the action of one part of the body on the other is equivalent (equipollent) to the system of distributed forces and couples on the surface dividing the body*, and it is represented by a vector field $\mathbf{T}^{(\mathbf{n})}$, called the stress vector, defined on the surface S and assumed to depend continuously on the surface's unit vector \mathbf{n} .

To explain this principle, we consider an imaginary surface S passing through an internal material point P dividing the continuous body into two segments, as seen in Figure 2.1a or 2.1b (some authors use the cutting plane diagram and others use the diagram with the arbitrary volume inside the continuum enclosed by the surface S). The body is subjected to external surface forces \mathbf{F} and body forces \mathbf{b} . The internal contact forces being transmitted from one segment to the other through the dividing plane, due to the action of one portion of the continuum onto the other, generate a force distribution on a small area ΔS , with a normal unit vector \mathbf{n} , on the dividing plane S . The force distribution is equipollent to a contact force $\Delta \mathbf{F}$ and a couple stress $\Delta \mathbf{M}$, as shown in Figure 2.1a and 2.1b. Cauchy's stress principle asserts that as ΔS becomes very small and tends to zero the ratio $\Delta \mathbf{F}/\Delta S$ becomes $d\mathbf{F}/dS$ and the couple stress vector $\Delta \mathbf{M}$ vanishes. In specific fields of continuum mechanics the couple stress is assumed not to vanish; however, as stated previously, in classical branches of continuum mechanics we deal with non-polar materials which do not consider couple stresses and body moments. The resultant vector $d\mathbf{F}/dS$ is defined as the *stress vector* or *traction vector* given by $\mathbf{T}^{(\mathbf{n})} = T_i^{(\mathbf{n})} \mathbf{e}_i$ at the point P associated with a plane with a normal vector \mathbf{n} :

$$T_i^{(\mathbf{n})} = \lim_{\Delta S \rightarrow 0} \frac{\Delta F_i}{\Delta S} = \frac{dF_i}{dS}.$$

This equation means that the stress vector depends on its location in the body and the orientation of the plane on which it is acting.

Depending on the orientation of the plane under consideration, the stress vector may not necessarily be perpendicular to that plane, *i.e.* parallel to \mathbf{n} , and can be resolved into two components:

- one normal to the plane, called *normal stress*

$$\sigma_n = \lim_{\Delta S \rightarrow 0} \frac{\Delta F_n}{\Delta S} = \frac{dF_n}{dS},$$

where dF_n is the normal component of the force $d\mathbf{F}$ to the differential area dS

- and the other parallel to this plane, called the *shear stress*

$$\tau = \lim_{\Delta S \rightarrow 0} \frac{\Delta F_s}{\Delta S} = \frac{dF_s}{dS},$$

where dF_s is the tangential component of the force $d\mathbf{F}$ to the differential surface area dS . The shear stress can be further decomposed into two mutually perpendicular vectors.

Cauchy's postulate

According to the *Cauchy Postulate*, the stress vector $\mathbf{T}^{(\mathbf{n})}$ remains unchanged for all surfaces passing through the point P and having the same normal vector \mathbf{n} at P , *i.e.* having a common tangent at P . This means that the stress vector is a function of the normal vector \mathbf{n} only, and it is not influenced by the curvature of the internal surfaces.

Cauchy's fundamental lemma

A consequence of Cauchy's postulate is *Cauchy's Fundamental Lemma*, also called the *Cauchy reciprocal theorem*, which states that the stress vectors acting on opposite sides of the same surface are equal in magnitude and opposite in direction. Cauchy's fundamental lemma is equivalent to Newton's third law of motion of action and reaction, and it is expressed as

$$-\mathbf{T}^{(\mathbf{n})} = \mathbf{T}^{(-\mathbf{n})}.$$

Cauchy's stress theorem – stress tensor

The state of stress at a point in the body is then defined by all the stress vectors $\mathbf{T}^{(\mathbf{n})}$ associated with all planes (infinite in number) that pass through that point. However,

according to *Cauchy's fundamental theorem*, also called *Cauchy's stress theorem*, merely by knowing the stress vectors on three mutually perpendicular planes, the stress vector on any other plane passing through that point can be found through coordinate transformation equations.

Cauchy's stress theorem states that there exists a second-order tensor field $\boldsymbol{\sigma}(\mathbf{x}, t)$, called the *Cauchy stress tensor*, independent of \mathbf{n} , such that \mathbf{T} is a linear function of \mathbf{n} :

$$\mathbf{T}^{(\mathbf{n})} = \boldsymbol{\sigma} \cdot \mathbf{n} \quad \text{or} \quad T_j^{(n)} = \sigma_{ij} n_i.$$

This equation implies that the stress vector $\mathbf{T}^{(\mathbf{n})}$ at any point P in a continuum associated with a plane with normal vector \mathbf{n} can be expressed as a function of the stress vectors on the planes perpendicular to the coordinate axes, *i.e.* in terms of the components σ_{ij} of the stress tensor $\boldsymbol{\sigma}$.

To prove this expression, consider a tetrahedron with three faces oriented in the coordinate planes, and with an infinitesimal area dA oriented in an arbitrary direction specified by a normal vector \mathbf{n} (Figure 2.2). The tetrahedron is formed by slicing the infinitesimal element along an arbitrary plane \mathbf{n} . The stress vector on this plane is denoted by $\mathbf{T}^{(\mathbf{n})}$. The stress vectors acting on the faces of the tetrahedron are denoted as $\mathbf{T}^{(\mathbf{e}_1)}$, $\mathbf{T}^{(\mathbf{e}_2)}$, and $\mathbf{T}^{(\mathbf{e}_3)}$, and are by definition the components σ_{ij} of the stress tensor $\boldsymbol{\sigma}$. This tetrahedron is sometimes called the *Cauchy tetrahedron*. From equilibrium of forces, *i.e.* Euler's first law of motion (Newton's second law of motion), we have

$$\mathbf{T}^{(\mathbf{n})} dA - \mathbf{T}^{(\mathbf{e}_1)} dA_1 - \mathbf{T}^{(\mathbf{e}_2)} dA_2 - \mathbf{T}^{(\mathbf{e}_3)} dA_3 = \rho \left(\frac{h}{3} dA \right) \mathbf{a},$$

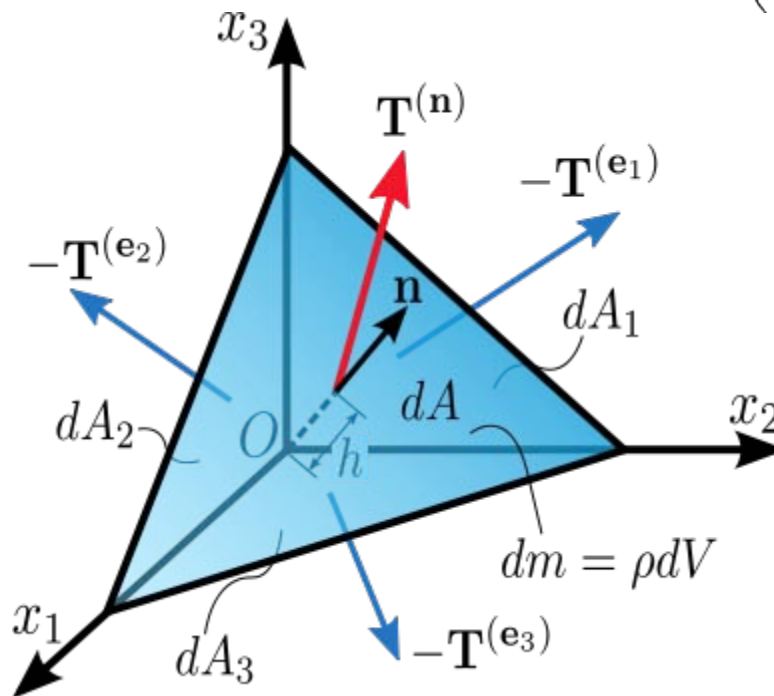


Figure 2.2. Stress vector acting on a plane with normal vector \mathbf{n} .

A note on the sign convention: The tetrahedron is formed by slicing a parallelepiped along an arbitrary plane \mathbf{n} . So, the force acting on the plane \mathbf{n} is the reaction exerted by the other half of the parallelepiped and has an opposite sign.

where the right-hand-side of the equation represents the product of the mass enclosed by the tetrahedron and its acceleration: ρ is the density, \mathbf{a} is the acceleration, and h is the height of the tetrahedron, considering the plane \mathbf{n} as the base. The area of the faces of the tetrahedron perpendicular to the axes can be found by projecting dA into each face (using the dot product):

$$\begin{aligned} dA_1 &= (\mathbf{n} \cdot \mathbf{e}_1) dA = n_1 dA, \\ dA_2 &= (\mathbf{n} \cdot \mathbf{e}_2) dA = n_2 dA, \\ dA_3 &= (\mathbf{n} \cdot \mathbf{e}_3) dA = n_3 dA, \end{aligned}$$

and then substituting into the equation to cancel out dA :

$$\mathbf{T}^{(\mathbf{n})} - \mathbf{T}^{(\mathbf{e}_1)} n_1 - \mathbf{T}^{(\mathbf{e}_2)} n_2 - \mathbf{T}^{(\mathbf{e}_3)} n_3 = \rho \left(\frac{h}{3} \right) \mathbf{a}.$$

To consider the limiting case as the tetrahedron shrinks to a point, h must go to 0 (intuitively, the plane \mathbf{n} is translated along \mathbf{n} toward O). As a result, the right-hand-side of the equation approaches 0, so

$$\mathbf{T}^{(\mathbf{n})} = \mathbf{T}^{(\mathbf{e}_1)} n_1 + \mathbf{T}^{(\mathbf{e}_2)} n_2 + \mathbf{T}^{(\mathbf{e}_3)} n_3.$$

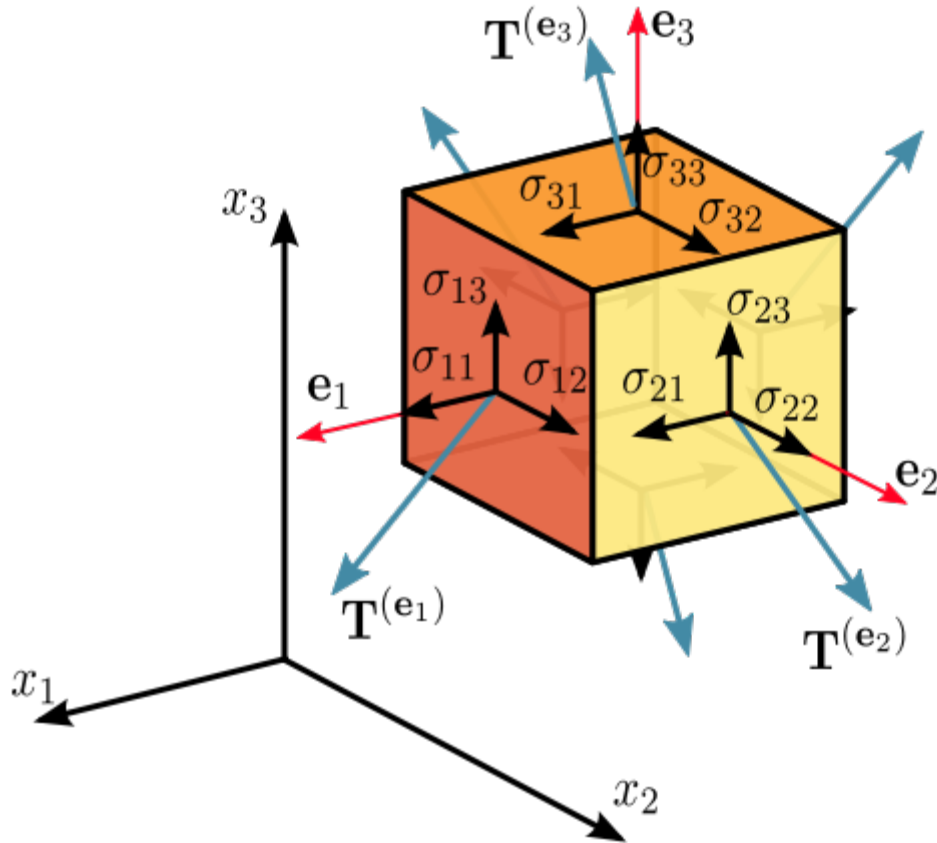


Figure 2.3 Components of stress in three dimensions

Assuming a material element (Figure 2.3) with planes perpendicular to the coordinate axes of a Cartesian coordinate system, the stress vectors associated with each of the element planes, *i.e.* $\mathbf{T}^{(\mathbf{e}_1)}$, $\mathbf{T}^{(\mathbf{e}_2)}$, and $\mathbf{T}^{(\mathbf{e}_3)}$ can be decomposed into a normal component and two shear components, *i.e.* components in the direction of the three coordinate axes. For the particular case of a surface with normal unit vector oriented in the direction of the x_1 -axis, the normal stress is denoted by σ_{11} , and the two shear stresses are denoted as σ_{12} and σ_{13} :

$$\begin{aligned}\mathbf{T}^{(\mathbf{e}_1)} &= T_1^{(\mathbf{e}_1)} \mathbf{e}_1 + T_2^{(\mathbf{e}_1)} \mathbf{e}_2 + T_3^{(\mathbf{e}_1)} \mathbf{e}_3 = \sigma_{11} \mathbf{e}_1 + \sigma_{12} \mathbf{e}_2 + \sigma_{13} \mathbf{e}_3, \\ \mathbf{T}^{(\mathbf{e}_2)} &= T_1^{(\mathbf{e}_2)} \mathbf{e}_1 + T_2^{(\mathbf{e}_2)} \mathbf{e}_2 + T_3^{(\mathbf{e}_2)} \mathbf{e}_3 = \sigma_{21} \mathbf{e}_1 + \sigma_{22} \mathbf{e}_2 + \sigma_{23} \mathbf{e}_3, \\ \mathbf{T}^{(\mathbf{e}_3)} &= T_1^{(\mathbf{e}_3)} \mathbf{e}_1 + T_2^{(\mathbf{e}_3)} \mathbf{e}_2 + T_3^{(\mathbf{e}_3)} \mathbf{e}_3 = \sigma_{31} \mathbf{e}_1 + \sigma_{32} \mathbf{e}_2 + \sigma_{33} \mathbf{e}_3,\end{aligned}$$

In index notation this is

$$\mathbf{T}^{(\mathbf{e}_i)} = T_j^{(\mathbf{e}_i)} \mathbf{e}_j = \sigma_{ij} \mathbf{e}_j.$$

The nine components σ_{ij} of the stress vectors are the components of a second-order Cartesian tensor called the *Cauchy stress tensor*, which completely defines the state of stress at a point and is given by

$$\boldsymbol{\sigma} = \sigma_{ij} = \begin{bmatrix} \mathbf{T}^{(\mathbf{e}_1)} \\ \mathbf{T}^{(\mathbf{e}_2)} \\ \mathbf{T}^{(\mathbf{e}_3)} \end{bmatrix} = \begin{bmatrix} \sigma_{11} & \sigma_{12} & \sigma_{13} \\ \sigma_{21} & \sigma_{22} & \sigma_{23} \\ \sigma_{31} & \sigma_{32} & \sigma_{33} \end{bmatrix} \equiv \begin{bmatrix} \sigma_{xx} & \sigma_{xy} & \sigma_{xz} \\ \sigma_{yx} & \sigma_{yy} & \sigma_{yz} \\ \sigma_{zx} & \sigma_{zy} & \sigma_{zz} \end{bmatrix} \equiv \begin{bmatrix} \sigma_x & \tau_{xy} & \tau_{xz} \\ \tau_{yx} & \sigma_y & \tau_{yz} \\ \tau_{zx} & \tau_{zy} & \sigma_z \end{bmatrix},$$

where σ_{11} , σ_{22} , and σ_{33} are normal stresses, and σ_{12} , σ_{13} , σ_{21} , σ_{23} , σ_{31} , and σ_{32} are shear stresses. The first index i indicates that the stress acts on a plane normal to the x_i -axis, and the second index j denotes the direction in which the stress acts. A stress component is positive if it acts in the positive direction of the coordinate axes, and if the plane where it acts has an outward normal vector pointing in the positive coordinate direction.

Thus, using the components of the stress tensor

$$\begin{aligned} \mathbf{T}^{(\mathbf{n})} &= \mathbf{T}^{(\mathbf{e}_1)}n_1 + \mathbf{T}^{(\mathbf{e}_2)}n_2 + \mathbf{T}^{(\mathbf{e}_3)}n_3 \\ &= \sum_{i=1}^3 \mathbf{T}^{(\mathbf{e}_i)}n_i \\ &= (\sigma_{ij}\mathbf{e}_j)n_i \\ &= \sigma_{ij}n_i\mathbf{e}_j \end{aligned}$$

or, equivalently,

$$T_j^{(\mathbf{n})} = \sigma_{ij}n_i.$$

Alternatively, in matrix form we have

$$\begin{bmatrix} T_1^{(\mathbf{n})} & T_2^{(\mathbf{n})} & T_3^{(\mathbf{n})} \end{bmatrix} = \begin{bmatrix} n_1 & n_2 & n_3 \end{bmatrix} \cdot \begin{bmatrix} \sigma_{11} & \sigma_{12} & \sigma_{13} \\ \sigma_{21} & \sigma_{22} & \sigma_{23} \\ \sigma_{31} & \sigma_{32} & \sigma_{33} \end{bmatrix}.$$

The Voigt notation representation of the Cauchy stress tensor takes advantage of the symmetry of the stress tensor to express the stress as a six-dimensional vector of the form:

$$\boldsymbol{\sigma} = [\sigma_1 \quad \sigma_2 \quad \sigma_3 \quad \sigma_4 \quad \sigma_5 \quad \sigma_6]^T \equiv [\sigma_{11} \quad \sigma_{22} \quad \sigma_{33} \quad \sigma_{23} \quad \sigma_{31} \quad \sigma_{12}]^T.$$

The Voigt notation is used extensively in representing stress-strain relations in solid mechanics and for computational efficiency in numerical structural mechanics software.

Transformation rule of the stress tensor

It can be shown that the stress tensor is a contravariant second order tensor, which is a statement of how it transforms under a change of the coordinate system. From an x_i -system to an x'_i -system, the components σ_{ij} in the initial system are transformed into the components σ'_{ij} in the new system according to the tensor transformation rule (Figure 2.4):

$$\sigma'_{ij} = a_{im} a_{jn} \sigma_{mn} \quad \text{OR} \quad \boldsymbol{\sigma}' = \mathbf{A} \boldsymbol{\sigma} \mathbf{A}^T,$$

where \mathbf{A} is a rotation matrix with components a_{ij} . In matrix form this

$$\begin{bmatrix} \sigma'_{11} & \sigma'_{12} & \sigma'_{13} \\ \sigma'_{21} & \sigma'_{22} & \sigma'_{23} \\ \sigma'_{31} & \sigma'_{32} & \sigma'_{33} \end{bmatrix} = \begin{bmatrix} a_{11} & a_{12} & a_{13} \\ a_{21} & a_{22} & a_{23} \\ a_{31} & a_{32} & a_{33} \end{bmatrix} \begin{bmatrix} \sigma_{11} & \sigma_{12} & \sigma_{13} \\ \sigma_{21} & \sigma_{22} & \sigma_{23} \\ \sigma_{31} & \sigma_{32} & \sigma_{33} \end{bmatrix} \begin{bmatrix} a_{11} & a_{21} & a_{31} \\ a_{12} & a_{22} & a_{32} \\ a_{13} & a_{23} & a_{33} \end{bmatrix}.$$

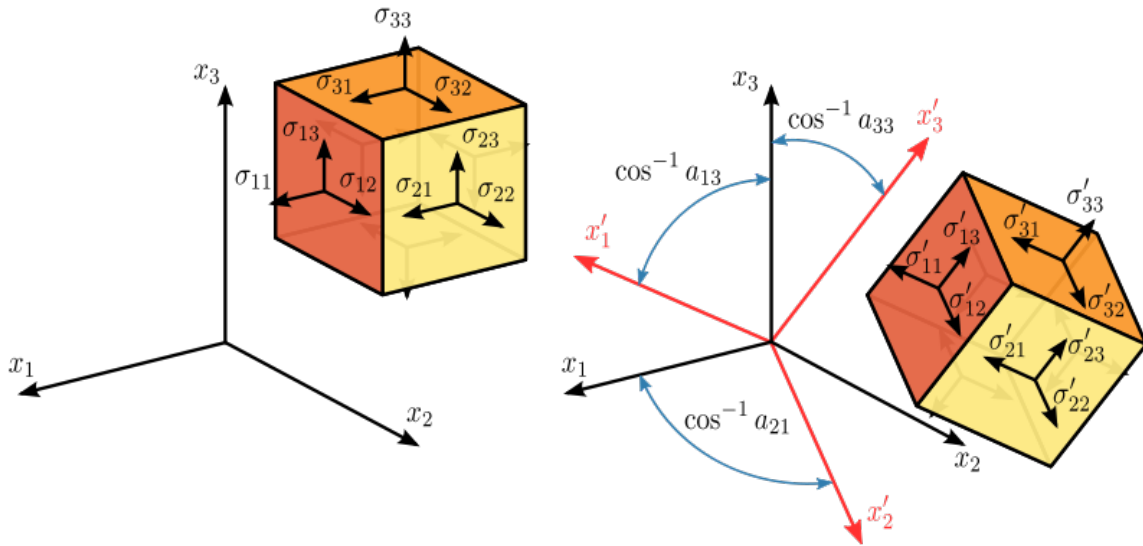


Figure 2.4 Transformation of the stress tensor

Expanding the matrix operation, and simplifying some terms by taking advantage of the symmetry of the stress tensor, gives

$$\begin{aligned} \sigma'_{11} &= a_{11}^2 \sigma_{11} + a_{12}^2 \sigma_{22} + a_{13}^2 \sigma_{33} + 2a_{11}a_{12}\sigma_{12} + 2a_{11}a_{13}\sigma_{13} + 2a_{12}a_{13}\sigma_{23}, \\ \sigma'_{22} &= a_{21}^2 \sigma_{11} + a_{22}^2 \sigma_{22} + a_{23}^2 \sigma_{33} + 2a_{21}a_{22}\sigma_{12} + 2a_{21}a_{23}\sigma_{13} + 2a_{22}a_{23}\sigma_{23}, \\ \sigma'_{33} &= a_{31}^2 \sigma_{11} + a_{32}^2 \sigma_{22} + a_{33}^2 \sigma_{33} + 2a_{31}a_{32}\sigma_{12} + 2a_{31}a_{33}\sigma_{13} + 2a_{32}a_{33}\sigma_{23}, \\ \sigma'_{12} &= a_{11}a_{21}\sigma_{11} + a_{12}a_{22}\sigma_{22} + a_{13}a_{23}\sigma_{33} \\ &\quad + (a_{11}a_{22} + a_{12}a_{21})\sigma_{12} + (a_{12}a_{23} + a_{13}a_{22})\sigma_{23} + (a_{11}a_{23} + a_{13}a_{21})\sigma_{13}, \\ \sigma'_{23} &= a_{21}a_{31}\sigma_{11} + a_{22}a_{32}\sigma_{22} + a_{23}a_{33}\sigma_{33} \\ &\quad + (a_{21}a_{32} + a_{22}a_{31})\sigma_{12} + (a_{22}a_{33} + a_{23}a_{32})\sigma_{23} + (a_{21}a_{33} + a_{23}a_{31})\sigma_{13}, \end{aligned}$$

$$\begin{aligned}\sigma'_{13} = & a_{11}a_{31}\sigma_{11} + a_{12}a_{32}\sigma_{22} + a_{13}a_{33}\sigma_{33} \\ & + (a_{11}a_{32} + a_{12}a_{31})\sigma_{12} + (a_{12}a_{33} + a_{13}a_{32})\sigma_{23} + (a_{11}a_{33} + a_{13}a_{31})\sigma_{13}.\end{aligned}$$

The Mohr circle for stress is a graphical representation of this transformation of stresses.

Normal and shear stresses

The magnitude of the normal stress component σ_n of any stress vector $\mathbf{T}^{(\mathbf{n})}$ acting on an arbitrary plane with normal vector \mathbf{n} at a given point, in terms of the components σ_{ij} of the stress tensor $\boldsymbol{\sigma}$, is the dot product of the stress vector and the normal vector:

$$\begin{aligned}\sigma_n &= \mathbf{T}^{(\mathbf{n})} \cdot \mathbf{n} \\ &= T_i^{(\mathbf{n})} n_i \\ &= \sigma_{ij} n_i n_j.\end{aligned}$$

The magnitude of the shear stress component τ_n , acting in the plane spanned by the two vectors $\mathbf{T}^{(\mathbf{n})}$ and \mathbf{n} , can then be found using the Pythagorean theorem:

$$\begin{aligned}\tau_n &= \sqrt{(T^{(\mathbf{n})})^2 - \sigma_n^2} \\ &= \sqrt{T_i^{(\mathbf{n})} T_i^{(\mathbf{n})} - \sigma_n^2},\end{aligned}$$

where

$$(T^{(\mathbf{n})})^2 = T_i^{(\mathbf{n})} T_i^{(\mathbf{n})} = (\sigma_{ij} n_j) (\sigma_{ik} n_k) = \sigma_{ij} \sigma_{ik} n_j n_k.$$

Equilibrium equations and symmetry of the stress tensor

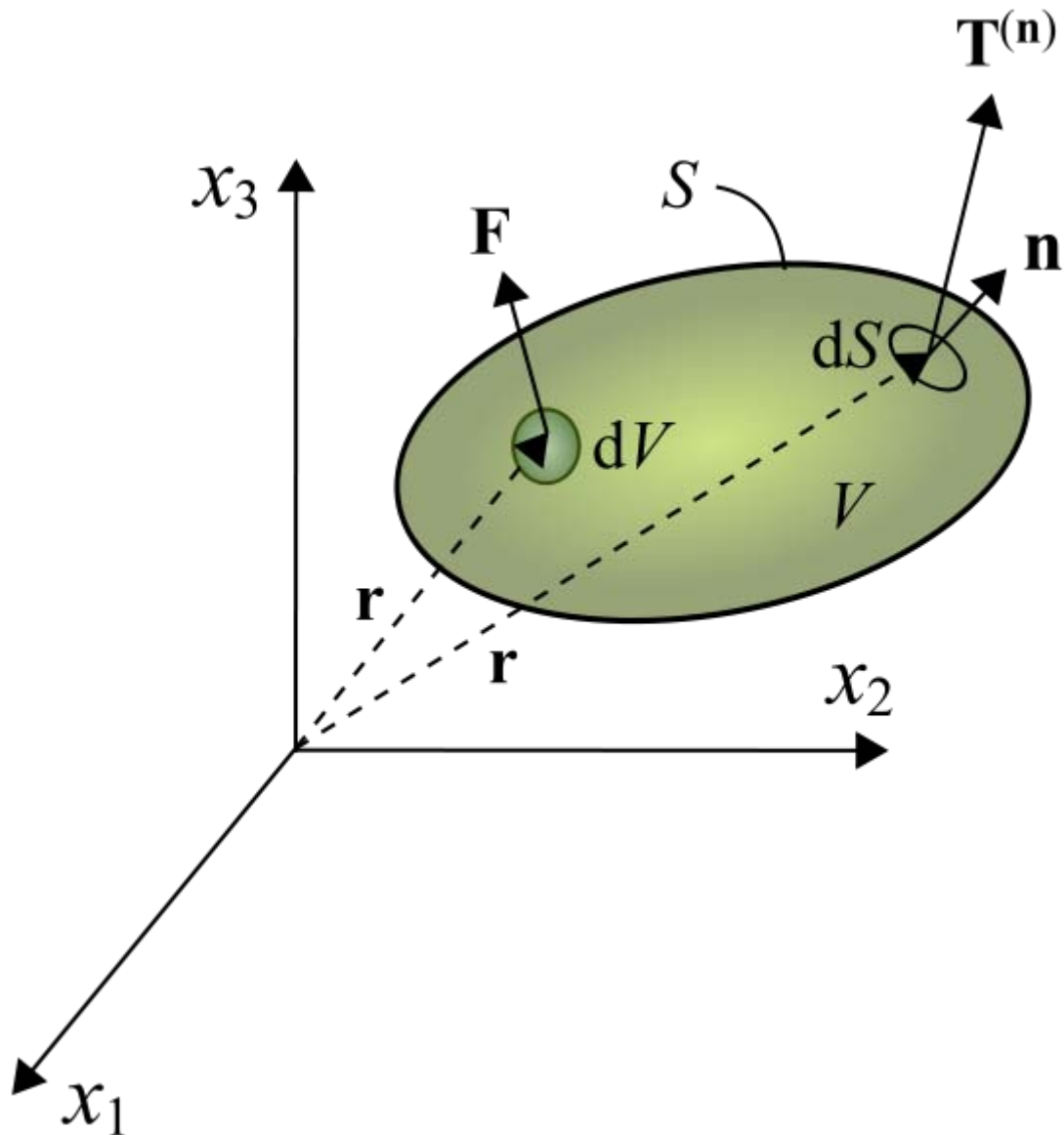


Figure 4. Continuum body in equilibrium

When a body is in equilibrium the components of the stress tensor in every point of the body satisfy the equilibrium equations,

$$\sigma_{ji,j} + F_i = 0$$

For example, for a hydrostatic fluid in equilibrium conditions, the stress tensor takes on the form:

$$\sigma_{ij} = -p\delta_{ij},$$

where p is the hydrostatic pressure, and δ_{ij} is the Kronecker delta.

At the same time, equilibrium requires that the summation of moments with respect to an arbitrary point is zero, which leads to the conclusion that the stress tensor is symmetric, i.e.

$$\sigma_{ij} = \sigma_{ji}$$

However, in the presence of couple-stresses, i.e. moments per unit volume, the stress tensor is non-symmetric. This also is the case when the Knudsen number is close to one, $K_n \rightarrow 1$, or the continuum is a non-Newtonian fluid, which can lead to rotationally non-invariant fluids, such as polymers.

Principal stresses and stress invariants

At every point in a stressed body there are at least three planes, called *principal planes*, with normal vectors \mathbf{n} , called *principal directions*, where the corresponding stress vector is perpendicular to the plane, i.e., parallel or in the same direction as the normal vector \mathbf{n} , and where there are no normal shear stresses $\tau_{\mathbf{n}}$. The three stresses normal to these principal planes are called *principal stresses*.

The components σ_{ij} of the stress tensor depend on the orientation of the coordinate system at the point under consideration. However, the stress tensor itself is a physical quantity and as such, it is independent of the coordinate system chosen to represent it. There are certain invariants associated with every tensor which are also independent of the coordinate system. For example, a vector is a simple tensor of rank one. In three dimensions, it has three components. The value of these components will depend on the coordinate system chosen to represent the vector, but the length of the vector is a physical quantity (a scalar) and is independent of the coordinate system chosen to represent the vector. Similarly, every second rank tensor (such as the stress and the strain tensors) has three independent invariant quantities associated with it. One set of such invariants are the principal stresses of the stress tensor, which are just the eigenvalues of the stress tensor. Their direction vectors are the principal directions or eigenvectors.

A stress vector parallel to the normal vector \mathbf{n} is given by:

$$\mathbf{T}^{(\mathbf{n})} = \lambda \mathbf{n} = \sigma_{\mathbf{n}} \mathbf{n}$$

where λ is a constant of proportionality, and in this particular case corresponds to the magnitudes $\sigma_{\mathbf{n}}$ of the normal stress vectors or principal stresses.

Knowing that $T_i^{(n)} = \sigma_{ij} n_j$ and $n_i = \delta_{ij} n_j$, we have

$$\begin{aligned}
T_i^{(n)} &= \lambda n_i \\
\sigma_{ij} n_j &= \lambda n_i \\
\sigma_{ij} n_j - \lambda n_i &= 0 \\
(\sigma_{ij} - \lambda \delta_{ij}) n_j &= 0
\end{aligned}$$

This is a homogeneous system, i.e. equal to zero, of three linear equations where n_j are the unknowns. To obtain a nontrivial (non-zero) solution for n_j , the determinant matrix of the coefficients must be equal to zero, i.e. the system is singular. Thus,

$$|\sigma_{ij} - \lambda \delta_{ij}| = \begin{vmatrix} \sigma_{11} - \lambda & \sigma_{12} & \sigma_{13} \\ \sigma_{21} & \sigma_{22} - \lambda & \sigma_{23} \\ \sigma_{31} & \sigma_{32} & \sigma_{33} - \lambda \end{vmatrix} = 0$$

Expanding the determinant leads to the *characteristic equation*

$$|\sigma_{ij} - \lambda \delta_{ij}| = -\lambda^3 + I_1 \lambda^2 - I_2 \lambda + I_3 = 0$$

where

$$\begin{aligned}
I_1 &= \sigma_{11} + \sigma_{22} + \sigma_{33} \\
&= \sigma_{kk} \\
I_2 &= \begin{vmatrix} \sigma_{22} & \sigma_{23} \\ \sigma_{32} & \sigma_{33} \end{vmatrix} + \begin{vmatrix} \sigma_{11} & \sigma_{13} \\ \sigma_{31} & \sigma_{33} \end{vmatrix} + \begin{vmatrix} \sigma_{11} & \sigma_{12} \\ \sigma_{21} & \sigma_{22} \end{vmatrix} \\
&= \sigma_{11} \sigma_{22} + \sigma_{22} \sigma_{33} + \sigma_{11} \sigma_{33} - \sigma_{12}^2 - \sigma_{23}^2 - \sigma_{13}^2 \\
&= \frac{1}{2} (\sigma_{ii} \sigma_{jj} - \sigma_{ij} \sigma_{ji}) \\
I_3 &= \det(\sigma_{ij}) \\
&= \sigma_{11} \sigma_{22} \sigma_{33} + 2 \sigma_{12} \sigma_{23} \sigma_{31} - \sigma_{12}^2 \sigma_{33} - \sigma_{23}^2 \sigma_{11} - \sigma_{13}^2 \sigma_{22}
\end{aligned}$$

The characteristic equation has three real roots λ , i.e. not imaginary due to the symmetry of the stress tensor. The three roots $\lambda_1 = \sigma_1$, $\lambda_2 = \sigma_2$, and $\lambda_3 = \sigma_3$ are the eigenvalues or principal stresses, and they are the roots of the Cayley–Hamilton theorem. The principal stresses are unique for a given stress tensor. Therefore, from the characteristic equation it is seen that the coefficients I_1 , I_2 and I_3 , called the first, second, and third *stress invariants*, respectively, have always the same value regardless of the orientation of the coordinate system chosen.

For each eigenvalue, there is a non-trivial solution for n_j in the equation $(\sigma_{ij} - \lambda\delta_{ij}) n_j = 0$. These solutions are the principal directions or eigenvectors defining the plane where the principal stresses act. The principal stresses and principal directions characterize the stress at a point and are independent of the orientation of the coordinate system.

If we choose a coordinate system with axes oriented to the principal directions, then the normal stresses will be the principal stresses and the stress tensor is represented by a diagonal matrix:

$$\sigma_{ij} = \begin{bmatrix} \sigma_1 & 0 & 0 \\ 0 & \sigma_2 & 0 \\ 0 & 0 & \sigma_3 \end{bmatrix}$$

The principal stresses may be combined to form the stress invariants, I_1 , I_2 , and I_3 . The first and third invariant are the trace and determinant respectively, of the stress tensor. Thus,

$$\begin{aligned} I_1 &= \sigma_1 + \sigma_2 + \sigma_3 \\ I_2 &= \sigma_1\sigma_2 + \sigma_2\sigma_3 + \sigma_3\sigma_1 \\ I_3 &= \sigma_1\sigma_2\sigma_3 \end{aligned}$$

Because of its simplicity, working and thinking in the principal coordinate system is often very useful when considering the state of the elastic medium at a particular point.

Principal stresses are often expressed in the following equation for evaluating stresses in the x and y directions or axial and bending stresses on a part. The principal normal stresses can then be used to calculate the Von Mises stress and ultimately the safety factor and margin of safety.

$$\sigma_1, \sigma_2 = \frac{\sigma_x + \sigma_y}{2} \pm \sqrt{\left(\frac{\sigma_x - \sigma_y}{2}\right)^2 + \tau_{xy}^2}$$

Using just the part of the equation under the square root is equal to the maximum and minimum shear stress for plus and minus. This is shown as:

$$\tau_{max}, \tau_{min} = \pm \sqrt{\left(\frac{\sigma_x - \sigma_y}{2}\right)^2 + \tau_{xy}^2}$$

Maximum and minimum shear stresses

The maximum shear stress or maximum principal shear stress is equal to one-half the difference between the largest and smallest principal stresses, and acts on the plane that bisects the angle between the directions of the largest and smallest principal stresses, i.e. the plane of the maximum shear stress is oriented 45° from the principal stress planes. The maximum shear stress is expressed as

$$\tau_{\max} = \frac{1}{2} |\sigma_{\max} - \sigma_{\min}|$$

Assuming $\sigma_1 \geq \sigma_2 \geq \sigma_3$ then

$$\tau_{\max} = \frac{1}{2} |\sigma_1 - \sigma_3|$$

The normal stress component acting on the plane for the maximum shear stress is non-zero and it is equal to

$$\sigma_n = \frac{1}{2} (\sigma_1 + \sigma_3)$$

Stress deviator tensor

The stress tensor σ_{ij} can be expressed as the sum of two other stress tensors:

1. a *mean hydrostatic stress tensor* or *volumetric stress tensor* or *mean normal stress tensor*, $p\delta_{ij}$, which tends to change the volume of the stressed body; and
2. a deviatoric component called the *stress deviator tensor*, s_{ij} , which tends to distort it.

So:

$$\sigma_{ij} = s_{ij} + p\delta_{ij},$$

where P is the mean stress given by

$$p = \frac{\sigma_{kk}}{3} = \frac{\sigma_{11} + \sigma_{22} + \sigma_{33}}{3} = \frac{1}{3} I_1.$$

Note that convention in solid mechanics differs slightly from what is listed above. In solid mechanics, pressure is generally defined as negative one-third the trace of the stress tensor.

The deviatoric stress tensor can be obtained by subtracting the hydrostatic stress tensor from the stress tensor:

$$s_{ij} = \sigma_{ij} - \frac{\sigma_{kk}}{3}\delta_{ij},$$

$$\begin{bmatrix} s_{11} & s_{12} & s_{13} \\ s_{21} & s_{22} & s_{23} \\ s_{31} & s_{32} & s_{33} \end{bmatrix} = \begin{bmatrix} \sigma_{11} & \sigma_{12} & \sigma_{13} \\ \sigma_{21} & \sigma_{22} & \sigma_{23} \\ \sigma_{31} & \sigma_{32} & \sigma_{33} \end{bmatrix} - \begin{bmatrix} p & 0 & 0 \\ 0 & p & 0 \\ 0 & 0 & p \end{bmatrix}$$

$$= \begin{bmatrix} \sigma_{11} - p & \sigma_{12} & \sigma_{13} \\ \sigma_{21} & \sigma_{22} - p & \sigma_{23} \\ \sigma_{31} & \sigma_{32} & \sigma_{33} - p \end{bmatrix}.$$

Invariants of the stress deviator tensor

As it is a second order tensor, the stress deviator tensor also has a set of invariants, which can be obtained using the same procedure used to calculate the invariants of the stress tensor. It can be shown that the principal directions of the stress deviator tensor s_{ij} are the same as the principal directions of the stress tensor σ_{ij} . Thus, the characteristic equation is

$$|s_{ij} - \lambda\delta_{ij}| = \lambda^3 - J_1\lambda^2 - J_2\lambda - J_3 = 0,$$

where J_1 , J_2 and J_3 are the first, second, and third *deviatoric stress invariants*, respectively. Their values are the same (invariant) regardless of the orientation of the coordinate system chosen. These deviatoric stress invariants can be expressed as a function of the components of s_{ij} or its principal values s_1 , s_2 , and s_3 , or alternatively, as a function of σ_{ij} or its principal values σ_1 , σ_2 , and σ_3 . Thus,

$$J_1 = s_{kk} = 0,$$

$$J_2 = \frac{1}{2}s_{ij}s_{ji}$$

$$= -s_1s_2 - s_2s_3 - s_3s_1$$

$$= \frac{1}{6} [(\sigma_{11} - \sigma_{22})^2 + (\sigma_{22} - \sigma_{33})^2 + (\sigma_{33} - \sigma_{11})^2] + \sigma_{12}^2 + \sigma_{23}^2 + \sigma_{31}^2$$

$$= \frac{1}{6} [(\sigma_1 - \sigma_2)^2 + (\sigma_2 - \sigma_3)^2 + (\sigma_3 - \sigma_1)^2]$$

$$= \frac{1}{3}I_1^2 - I_2,$$

$$J_3 = \det(s_{ij})$$

$$= \frac{1}{3}s_{ij}s_{jk}s_{ki}$$

$$= s_1s_2s_3$$

$$= \frac{2}{27}I_1^3 - \frac{1}{3}I_1I_2 + I_3.$$

Because $s_{kk} = 0$, the stress deviator tensor is in a state of pure shear.

A quantity called the equivalent stress or von Mises stress is commonly used in solid mechanics. The equivalent stress is defined as

$$\sigma_e = \sqrt{3 J_2} = \sqrt{\frac{1}{2} [(\sigma_1 - \sigma_2)^2 + (\sigma_2 - \sigma_3)^2 + (\sigma_3 - \sigma_1)^2]}.$$

Octahedral stresses

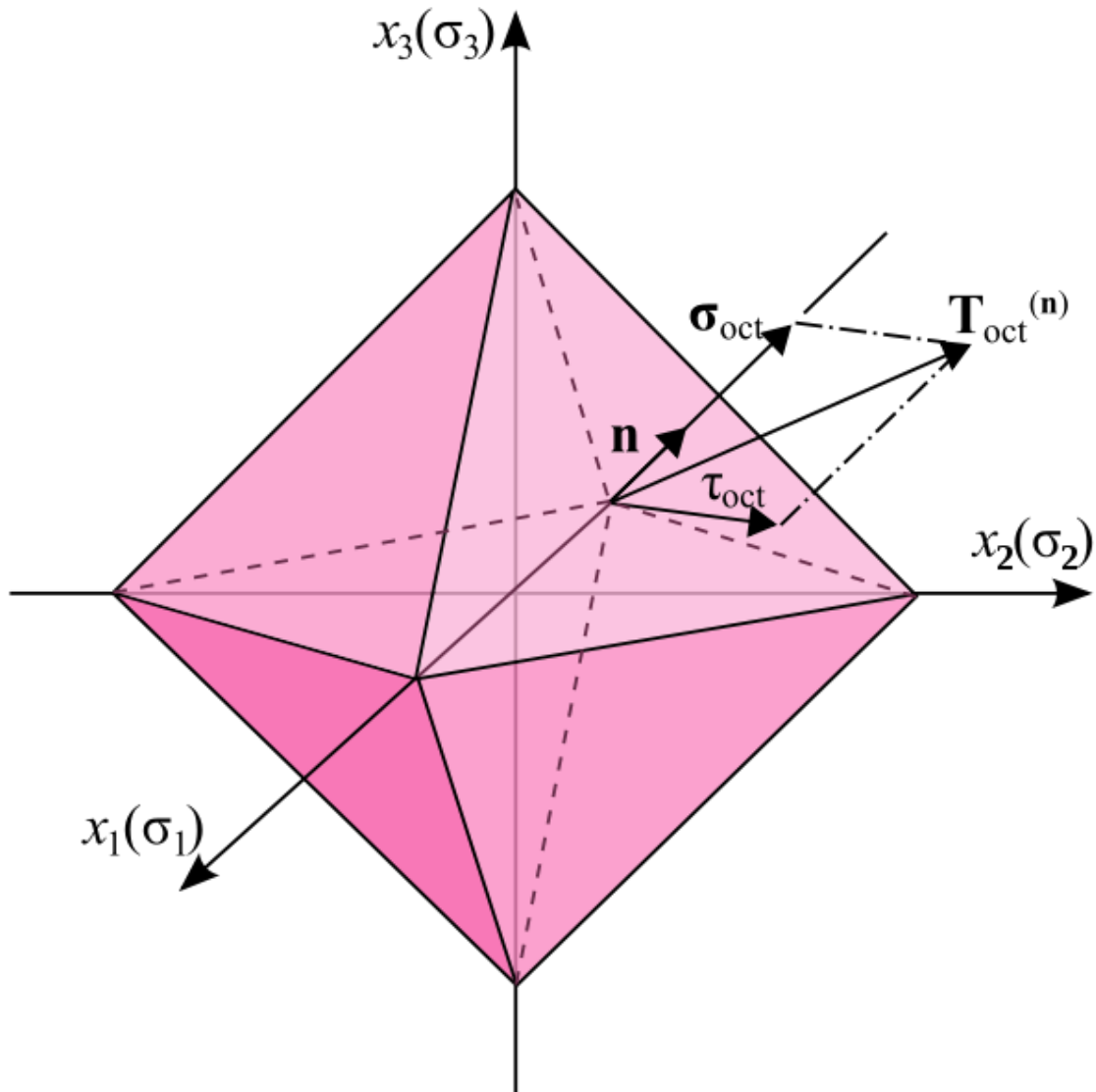


Figure 6. Octahedral stress planes

Considering the principal directions as the coordinate axes, a plane whose normal vector makes equal angles with each of the principal axes (i.e. having direction cosines equal to $|1/\sqrt{3}|$) is called an *octahedral plane*. There are a total of eight octahedral planes

(Figure 6). The normal and shear components of the stress tensor on these planes are called *octahedral normal stress* σ_{oct} and *octahedral shear stress* τ_{oct} , respectively.

Knowing that the stress tensor of point O (Figure 6) in the principal axes is

$$\sigma_{ij} = \begin{bmatrix} \sigma_1 & 0 & 0 \\ 0 & \sigma_2 & 0 \\ 0 & 0 & \sigma_3 \end{bmatrix}$$

the stress vector on an octahedral plane is then given by:

$$\begin{aligned} \mathbf{T}_{\text{oct}}^{(\mathbf{n})} &= \sigma_{ij} n_i \mathbf{e}_j \\ &= \sigma_1 n_1 \mathbf{e}_1 + \sigma_2 n_2 \mathbf{e}_2 + \sigma_3 n_3 \mathbf{e}_3 \\ &= \frac{1}{\sqrt{3}} (\sigma_1 \mathbf{e}_1 + \sigma_2 \mathbf{e}_2 + \sigma_3 \mathbf{e}_3) \end{aligned}$$

The normal component of the stress vector at point O associated with the octahedral plane is

$$\begin{aligned} \sigma_{\text{oct}} &= T_i^{(n)} n_i \\ &= \sigma_{ij} n_i n_j \\ &= \sigma_1 n_1 n_1 + \sigma_2 n_2 n_2 + \sigma_3 n_3 n_3 \\ &= \frac{1}{3} (\sigma_1 + \sigma_2 + \sigma_3) = \frac{1}{3} I_1 \end{aligned}$$

which is the mean normal stress or hydrostatic stress. This value is the same in all eight octahedral planes. The shear stress on the octahedral plane is then

$$\begin{aligned} \tau_{\text{oct}} &= \sqrt{T_i^{(n)} T_i^{(n)} - \sigma_{\text{oct}}^2} \\ &= \left[\frac{1}{3} (\sigma_1^2 + \sigma_2^2 + \sigma_3^2) - \frac{1}{9} (\sigma_1 + \sigma_2 + \sigma_3)^2 \right]^{1/2} \\ &= \frac{1}{3} \left[(\sigma_1 - \sigma_2)^2 + (\sigma_2 - \sigma_3)^2 + (\sigma_3 - \sigma_1)^2 \right]^{1/2} = \frac{1}{3} \sqrt{2I_1^2 - 6I_2} = \sqrt{\frac{2}{3} J_2} \end{aligned}$$

Alternative measures of stress

The Cauchy stress tensor is not the only measure of stress that is used in practice. Other measures of stress include the first and second Piola–Kirchhoff stress tensors, the Biot stress tensor, and the Kirchhoff stress tensor.

Piola–Kirchhoff stress tensor

In the case of finite deformations, the *Piola–Kirchhoff stress tensors* are used to express the stress relative to the reference configuration. This is in contrast to the Cauchy stress tensor which expresses the stress relative to the present configuration. For infinitesimal deformations or rotations, the Cauchy and Piola–Kirchhoff tensors are identical. These tensors take their names from Gabrio Piola and Gustav Kirchhoff.

Whereas the Cauchy stress tensor, $\boldsymbol{\sigma}$ relates stresses in the current configuration, the deformation gradient and strain tensors are described by relating the motion to the reference configuration; thus not all tensors describing the state of the material are in either the reference or current configuration. Having the stress, strain and deformation all described either in the reference or current configuration would make it easier to define constitutive models (for example, the Cauchy Stress tensor is variant to a pure rotation, while the deformation strain tensor is invariant; thus creating problems in defining a constitutive model that relates a varying tensor, in terms of an invariant one during pure rotation; as by definition constitutive models have to be invariant to pure rotations). The 1st Piola–Kirchhoff stress tensor, \mathbf{P} is one possible solution to this problem. It defines a family of tensors, which describe the configuration of the body in either the current or the reference state.

The 1st Piola–Kirchhoff stress tensor, \mathbf{P} relates forces in the *present* configuration with areas in the *reference* ("material") configuration.

$$\mathbf{P} = J \boldsymbol{\sigma} \cdot \mathbf{F}^{-T}$$

where \mathbf{F} is the deformation gradient and $J = \det \mathbf{F}$ is the Jacobian determinant.

In terms of components with respect to an orthonormal basis, the first Piola–Kirchhoff stress is given by

$$P_{iL} = J \sigma_{ik} F_{Lk}^{-1} = J \sigma_{ik} \frac{\partial X_L}{\partial x_k}$$

Because it relates different coordinate systems, the 1st Piola–Kirchhoff stress is a two-point tensor. In general, it is not symmetric. The 1st Piola–Kirchhoff stress is the 3D generalization of the 1D concept of engineering stress.

If the material rotates without a change in stress state (rigid rotation), the components of the 1st Piola–Kirchhoff stress tensor will vary with material orientation.

The 1st Piola–Kirchhoff stress is energy conjugate to the deformation gradient.

2nd Piola–Kirchhoff stress tensor

Whereas the 1st Piola–Kirchhoff stress relates forces in the current configuration to areas in the reference configuration, the 2nd Piola–Kirchhoff stress tensor \mathbf{S} relates forces in the reference configuration to areas in the reference configuration. The force in the reference configuration is obtained via a mapping that preserves the relative relationship between the force direction and the area normal in the current configuration.

$$\mathbf{S} = J \mathbf{F}^{-1} \cdot \boldsymbol{\sigma} \cdot \mathbf{F}^{-T} .$$

In index notation with respect to an orthonormal basis,

$$S_{IL} = J F_{Ik}^{-1} F_{Lm}^{-1} \sigma_{km} = J \frac{\partial X_I}{\partial x_k} \frac{\partial X_L}{\partial x_m} \sigma_{km}$$

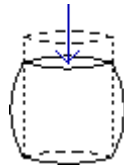
This tensor is symmetric.

If the material rotates without a change in stress state (rigid rotation), the components of the 2nd Piola–Kirchhoff stress tensor will remain constant, irrespective of material orientation.

The 2nd Piola–Kirchhoff stress tensor is energy conjugate to the Green–Lagrange finite strain tensor.

Chapter 11

Deformation (Engineering)



Compressive stress results in deformation which shortens the object but also expands it outwards.

In materials science, **deformation** is a change in the shape or size of an object due to an applied force (the deformation energy in this case is transferred through work) or a change in temperature (the deformation energy in this case is transferred through heat). The first case can be a result of tensile (pulling) forces, compressive (pushing) forces, shear, bending or torsion (twisting). In the second case, the most significant factor, which is determined by the temperature, is the mobility of the structural defects such as grain boundaries, point vacancies, line and screw dislocations, stacking faults and twins in both crystalline and non-crystalline solids. The movement or displacement of such mobile defects is thermally activated, and thus limited by the rate of atomic diffusion. Deformation is often described as strain.

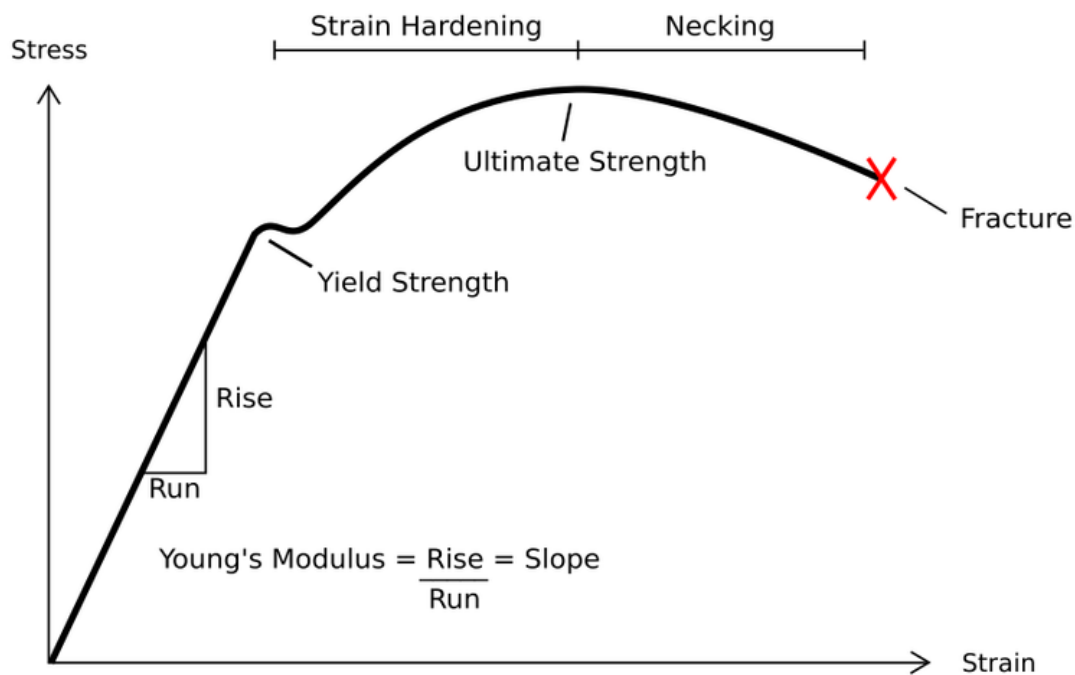
As deformation occurs, internal inter-molecular forces arise that oppose the applied force. If the applied force is not too large these forces may be sufficient to completely resist the applied force, allowing the object to assume a new equilibrium state and to return to its original state when the load is removed. A larger applied force may lead to a permanent deformation of the object or even to its structural failure.

In the figure it can be seen that the compressive loading (indicated by the arrow) has caused deformation in the cylinder so that the original shape (dashed lines) has changed (deformed) into one with bulging sides. The sides bulge because the material, although strong enough to not crack or otherwise fail, is not strong enough to support the load without change, thus the material is forced out laterally. Internal forces (in this case at right angles to the deformation) resist the applied load.

The concept of a rigid body can be applied if the deformation is negligible.

Types of deformation

Depending on the type of material, size and geometry of the object, and the forces applied, various types of deformation may result. The image to the right shows the engineering stress vs. strain diagram for a typical ductile material such as steel. Different deformation modes may occur under different conditions, as can be depicted using a deformation mechanism map.



Typical stress vs. strain diagram with the various stages of deformation.

Elastic deformation

This type of deformation is reversible. Once the forces are no longer applied, the object returns to its original shape. Elastomers and shape memory metals such as Nitinol exhibit large elastic deformation ranges, as does rubber. Soft thermoplastics and conventional metals have moderate elastic deformation ranges, while ceramics, crystals, and hard thermosetting plastics undergo almost no elastic deformation.

Linear elastic deformation is governed by Hooke's law, which states:

$$\sigma = E\varepsilon$$

Where σ is the applied stress, E is a material constant called Young's modulus, and ϵ is the resulting strain. This relationship only applies in the elastic range and indicates that the slope of the stress vs. strain curve can be used to find Young's modulus. Engineers often use this calculation in tensile tests. The elastic range ends when the material reaches its yield strength. At this point plastic deformation begins.

Note that not all elastic materials undergo linear elastic deformation; some, such as concrete, gray cast iron, and many polymers, respond nonlinearly. For these materials Hooke's law is inapplicable.

Plastic deformation

This type of deformation is irreversible. However, an object in the plastic deformation range will first have undergone elastic deformation, which is reversible, so the object will return part way to its original shape. Soft thermoplastics have a rather large plastic deformation range as do ductile metals such as copper, silver, and gold. Steel does, too, but not cast iron. Hard thermosetting plastics, rubber, crystals, and ceramics have minimal plastic deformation ranges. One material with a large plastic deformation range is wet chewing gum, which can be stretched dozens of times its original length.

Under tensile stress plastic deformation is characterized by a strain hardening region and a necking region and finally, fracture (also called rupture). During strain hardening the material becomes stronger through the movement of atomic dislocations. The necking phase is indicated by a reduction in cross-sectional area of the specimen. Necking begins after the ultimate strength is reached. During necking, the material can no longer withstand the maximum stress and the strain in the specimen rapidly increases. Plastic deformation ends with the fracture of the material.

Metal fatigue

Another deformation mechanism is metal fatigue, which occurs primarily in ductile metals. It was originally thought that a material deformed only within the elastic range returned completely to its original state once the forces were removed. However, faults are introduced at the molecular level with each deformation. After many deformations, cracks will begin to appear, followed soon after by a fracture, with no apparent plastic deformation in between. Depending on the material, shape, and how close to the elastic limit it is deformed, failure may require thousands, millions, billions, or trillions of deformations.

Metal fatigue has been a major cause of aircraft failure, such as the De Havilland Comet, especially before the process was well understood. There are two ways to determine when a part is in danger of metal fatigue; either predict when failure will occur due to the material/force/shape/iteration combination, and replace the vulnerable materials before this occurs, or perform inspections to detect the microscopic cracks and perform replacement once they occur. Selection of materials not likely to suffer from metal fatigue during the life of the product is the best solution, but not always possible.

Avoiding shapes with sharp corners limits metal fatigue by reducing stress concentrations, but does not eliminate it.

Compressive failure

Usually, compressive stress applied to bars, columns, etc. leads to shortening.

Loading a structural element or a specimen will increase the compressive stress until the reach of compressive strength. According to the properties of the material, failure will occur as yield for materials with ductile behaviour (most metals, some soils and plastics) or as rupture for brittle behaviour (geomaterials, cast iron, glass, etc).

In long, slender structural elements — such as columns or truss bars — an increase of compressive force F leads to structural failure due to buckling at lower stress than the compressive strength.

Fracture

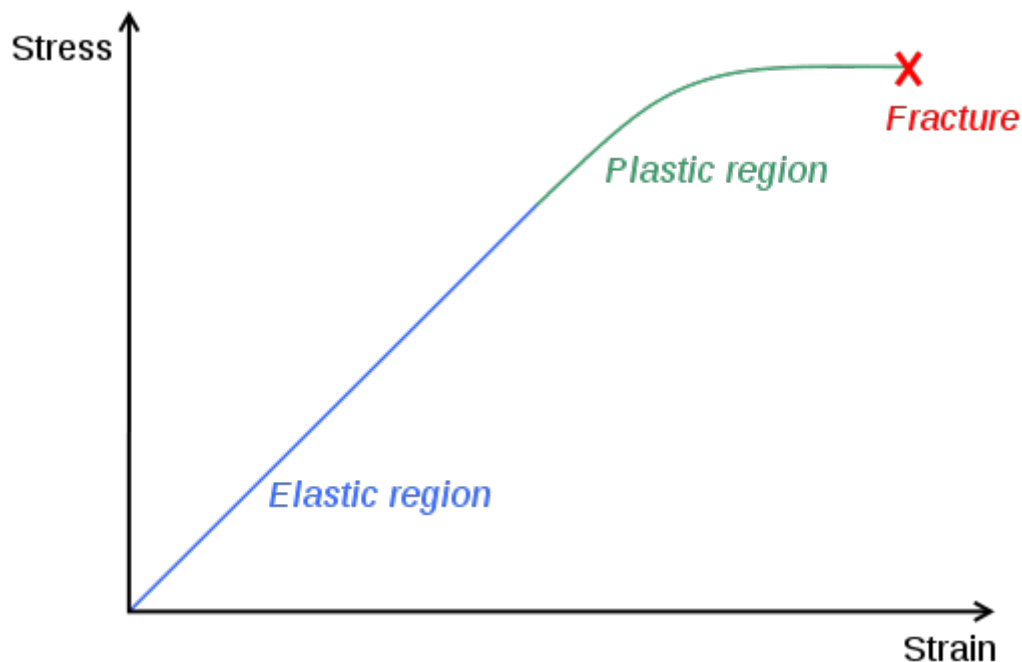


Diagram of a stress-strain curve, showing the relationship between stress (force applied) and strain (deformation) of a ductile metal.

This type of deformation is also irreversible. A break occurs after the material has reached the end of the elastic, and then plastic, deformation ranges. At this point forces accumulate until they are sufficient to cause a fracture. All materials will eventually fracture, if sufficient forces are applied.

Misconceptions

A popular misconception is that all materials that bend are "weak" and those that don't are "strong." In reality, many materials that undergo large elastic and plastic deformations, such as steel, are able to absorb stresses that would cause brittle materials, such as glass, with minimal elastic and plastic deformation ranges, to break.